



Vitrimers: Current research trends and their emerging applications

Jie Zheng¹, Zhuang Mao Png¹, Shi Hoe Ng¹, Guo Xiong Tham¹, Enyi Ye¹, Shermin S. Goh^{1,*}, Xian Jun Loh^{1,*}, Zibiao Li^{1,2,*}

¹ Institute of Materials Research and Engineering, A*STAR (Agency for Science, Technology and Research), 2 Fusionopolis Way, Innovis #08-03, Singapore 138634, Singapore

² Department of Materials Science and Engineering, National University of Singapore, Singapore 117574, Singapore

The development of recyclable plastics is a key research focus in today's world due to their environmental issues, and non-renewability concerns. Recently, vitrimeric materials have attracted great attention as an exciting class of renewable plastic due to their potential to exhibit strength, durability, and chemical resistance approaching that of traditional thermosets, while exhibiting end of life recyclability. This is due to their chemical structure, as vitrimers possess dynamic covalent crosslinks, which imparts stability while being reprocessable. This review summarizes the latest progress and developing prospects of vitrimeric materials. Special emphasis is given to vitrimer design strategies which paves the way for development of next-generation circular materials. The emerging applications of vitrimers in terms of their properties, including self-healing, malleability, orthogonal processability, and multiple shape memory, will also be discussed.

Keywords: Vitrimer; Covalent adaptable network; Polymers; Structural activity relationship; Circular material

Introduction

Plastics can be considered one of the key enabling materials in the last 100 years [1]. Their adaptability is unparalleled among materials, being pliable to mass-processing methods such as molding, extruding, and hot-pressing [2]. Plastics are also durable materials, often being resistant to moisture, oxidation, and biodegradation. There are two main classes of plastics, namely thermoplastics and thermosets. Thermoplastics such as poly(styrene), poly(ethylene), poly(ethylene terephthalate), and poly(vinyl chloride), can be readily melted and reprocessed at elevated temperature. On the other hand, thermosets such as melamine resins, epoxy resins, silicone resins, and urea-formaldehydes, cannot be readily recycled after their initial processing. However, they have significantly higher mechanical strength, thermal, and chemical stability as compared to thermo-

plastics. This difference can be understood by considering their chemical structures. Thermoplastics comprise linear polymeric chains which associate mainly by intermolecular forces. At higher temperatures, these forces are overcome, and the plastic turns from a solid into a viscoelastic liquid. In contrast, thermosets comprise three-dimensional (3D) networks with covalent crosslinks, which are formed during the curing step, such that the entire polymeric can be considered a single molecular unit [3]. These covalent crosslinks cannot be easily broken even at high temperatures, and the polymer usually decomposes before melting. While most plastics cannot be readily degraded into their corresponding monomers in a cost effective manner, thermoplastics can be recycled to some degree by mechanical processing [4,5]. The same cannot be said for thermosets, which are usually suitable only for reuse as filler materials, or as fuel [6]. There is thus motivation to develop new types of plastics with thermoset-like strength and durability, yet having end of life reprocessability. This would be a key enabler in the development of a circular economy, whereby products at the end of their

* Corresponding authors.

E-mail addresses: Goh, S.S. (gohsms@imre.a-star.edu.sg), Loh, X.J. (lohxj@imre.a-star.edu.sg), Li, Z. (lizb@imre.a-star.edu.sg).

lifespan may become the feedstock for other materials or reused in other ways.

A significant step towards such materials is the development of Covalent Adaptable Networks (CANs) [7–11]. CANs are polymeric materials with covalent crosslinks which become reversibly dynamic when a specific stimuli such as heat, catalyst, light, or pH is applied. In the absence of the corresponding stimuli, their cross-linked structure can impart to them thermoset-like properties such as increased strength and durability. Unlike traditional thermosets, which are essentially non-recyclable, CANs are in principal recyclable due to the dynamic nature of their crosslinks. In addition, CANs are also able to exhibit properties such as malleability, shape memory, and self-healing. In the last two decades, the field of CANs have seen great progress, with a dazzling array of crosslinks, polymers, and applications being reported [12–16].

In 2011, Leibler's group reported a new class of CANs, which he named vitrimers as their viscosity-temperature relationship resembles that of vitreous silica, following an Arrhenius-like dependence [17]. This can be attributed to the nature of their dynamic crosslinks. Traditionally, the crosslinks of CANs are dissociative in nature, being broken before reforming in the network. In contrast, the crosslinks of these vitrimers are associative in nature, with their crosslinks being broken only when new bonds are formed. As a result, the crosslink density of associative CANs can be considered almost constant regardless of external stimuli [18–22]. This has two main effects. Firstly, an extended rubbery phase can be observed when heated, as compared to dissociative CANs which transforms from a solid-like state to a liquid-like state more abruptly [23]. Secondly, some groups have also noted a greater creep/solvent resistance for associative CANs [21,24,25]. However, classification simply by the type of chemical bonds may be misleading, as certain chemical bonds may operate *via* either mechanism depending on the specific condition. For example, the carbamate bond undergoes associative transcarbomylation in the presence of excess hydroxyl groups [26], while the dissociative urethane reversion mechanism is predominant in the absence of those groups [27]. In addition, the mechanism of these materials may also not be easily elucidated simply by observing their physical properties; in some cases, materials operating *via* the dissociative mechanism may have rheological properties indistinguishable from vitrimers [23,28]. This happens when the rate constant of bond formation is significantly greater than that of bond cleavage, such that the proportion of dissociated bonds is small. As a result, the viscosity-temperature dependence of these materials still follow Arrhenius' law, and these materials can still be considered vitrimer-like materials (Fig. 1.1) [24]. Moreover, in real materials, polymer networks are crosslinked *via* not only covalent bonds, but also intramolecular interactions, such as van der Waals interactions, hydrogen bonding interactions, and metal-ligand coordination. These physical interactions support the mechanical properties of the materials along with the chemical bonds in the network. In this review, our focus will be on both vitrimers and materials with vitrimeric properties.

Since Leibler's seminal report, the number of vitrimeric polymers in the literature have increased tremendously. Numerous reversible chemical bonds such as those based on addition-elim-

ination reactions, conjugate addition-elimination reactions, transalkylation, and even heteroatom exchanges such as boronates and siloxanes have been shown to be effective as crosslinks in vitrimeric materials (see Section 3). Within each type of chemical bonds, different catalytic systems and polymeric backbones have also been explored. More recently, strategies such as the use of covalently bonded catalysts [29], neighboring group catalysis [30–33], and even catalyst free reactions [34,35] have been developed to make these materials more reprocessable. Vitrimeric materials have also been explored in numerous applications (see Section 4 and 5). To meet the environmental challenges, the re-processibility and recyclability of vitrimers have been demonstrated. In addition, various groups have also reported applications such as self-healing materials, re-usable adhesives, shape memory materials, and even in 3D printing. Vitrimers have also been combined with nano-materials to form composites with synergistic properties.

In this review, we aim to comprehensive summarize the recent developments in vitrimeric materials, giving special consideration towards the design principles behind them, as well as their emerging applications in various fields (Fig. 1.2). In Section 2, we will discuss the chemical and material fundamentals of CANs, with particular focus on vitrimeric properties. Next, we will give a review of vitrimers and vitrimer-like materials which have been developed, classifying them according to their key crosslinking chemical bond. Unique strategies used in these materials will also be highlighted (Section 3). In Sections 4 and 5, we will give an overview of the emerging applications of these next-generation materials and their composites.

Characteristics and chemical roots of CANs and vitrimers

Transition temperatures

In thermally activated vitrimers, distinct physical properties are observable at different temperatures. Two important transition temperatures describes the different behaviours. The first is the glass transition temperature (T_g), corresponding to the temperature at which polymer chain segmental movement happens, resulting in a change from a rigid state to a moldable state. This is usually measured by dynamic mechanical analysis (DMA) or differential scanning calorimetry (DSC). The second is the topology freezing transition temperature (T_v), corresponding to the temperature where rapid bond exchange occurs, resulting in polymer flow, and the material changes from a viscoelastic solid to a viscoelastic liquid. The temperature whereby a viscosity of 10^{12} Pa s is reached, is typically chosen to denote this point.

As T_g and T_v arise from different interactions, both temperatures are independent of each other. In most cases, T_g is lower than T_v , and the vitrimer transits from a rigid solid below to T_g , to an elastic solid between T_g and T_v , to a viscoelastic liquid above T_v (Fig. 2.1a(i)). At temperatures above T_v , the decrease in viscosity can be modelled by the Arrhenius equation, as the rate of flow is essentially controlled by the rate of chemical exchanges. On the other hand, in some cases, the T_v can be potentially below that of T_g (Fig. 2.1a(ii)). In such cases, below T_g , no extensive segmental motion occurs, and thus no exchange reactions occur. As a result, the network can be considered to be

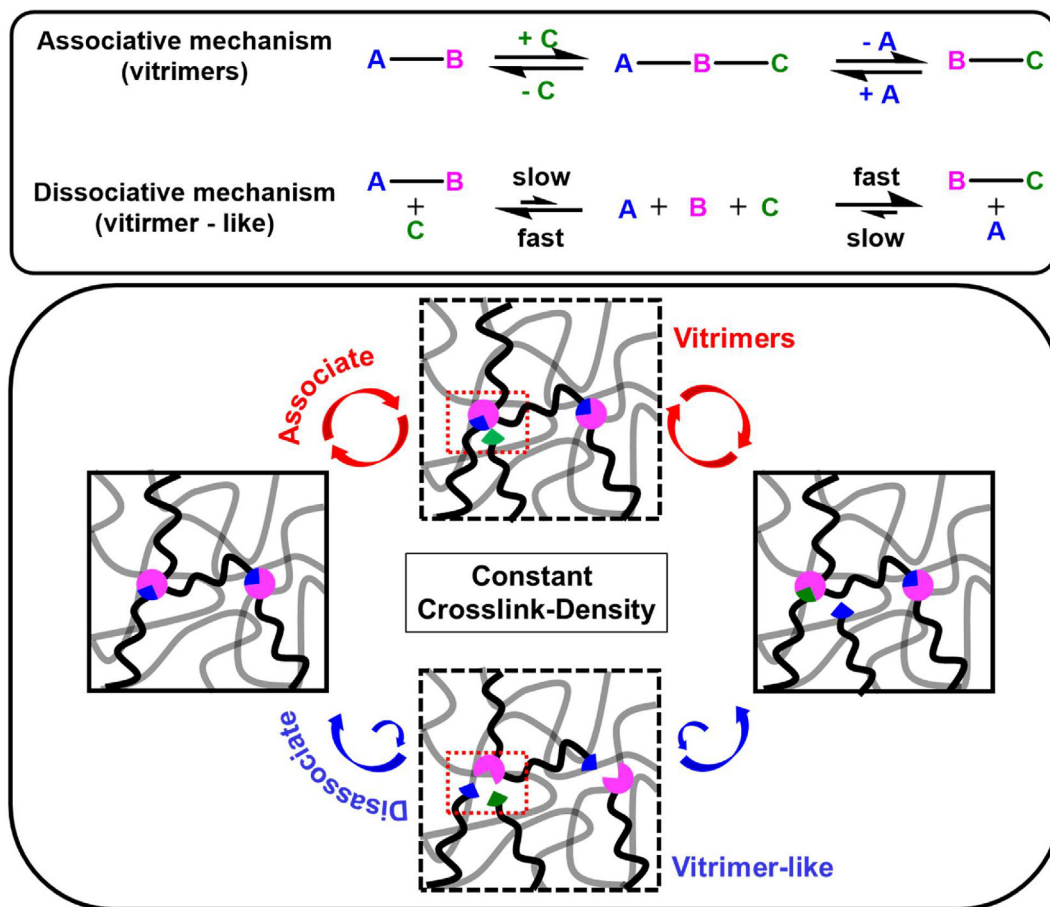


FIGURE 1.1

Scheme and image illustration of vitrimers and vitrimer-like materials. The crosslink density of these materials is almost constant at different temperatures.

fixed. When the temperature rises above T_g , the viscosity sharply decreases over a small temperature range as predicted by the

Williams–Landel–Ferry equation [36]. Further heating results in chemical kinetics controlling the rate of exchanges again, and the slope follows Arrhenius equation again. This type of behavior is relatively less common, and was first reported by Guan's group in 2017 [37].

Arrhenius equation

The Arrhenius equation, $k = Ae^{-\frac{E_a}{RT}}$ (k = rate constant, A = pre-exponential factor, E_a = activation energy, R = universal gas constant, and T = temperature), is an empirical equation which has been used to describe the viscosity dependence of vitrimers on its temperature. At temperatures above T_v , the rate of reaction k rises sharply, resulting in rapidly decreasing viscosity (Fig. 2.1B). A feature of this relation is that while the use of catalysts can sometimes decrease the T_v due to the lowered activation energy, changes in catalytic loading has no effect on T_v , as it does not affect the activation energy, although increasing the catalytic loading does increase the overall rate of exchange due to increasing the pre-exponential term. This has been verified experimentally by Ji's group in 2019, where the T_v of an transesterification based vitrimer with different catalytic loadings of triazabicyclodecene (TBD) was found to be constant at 85 °C [38]. In the context of vitrimers, the Arrhenius equation can also be written in the form $\ln \eta = \ln A + \frac{E_a}{RT}$, where η represents the vis-

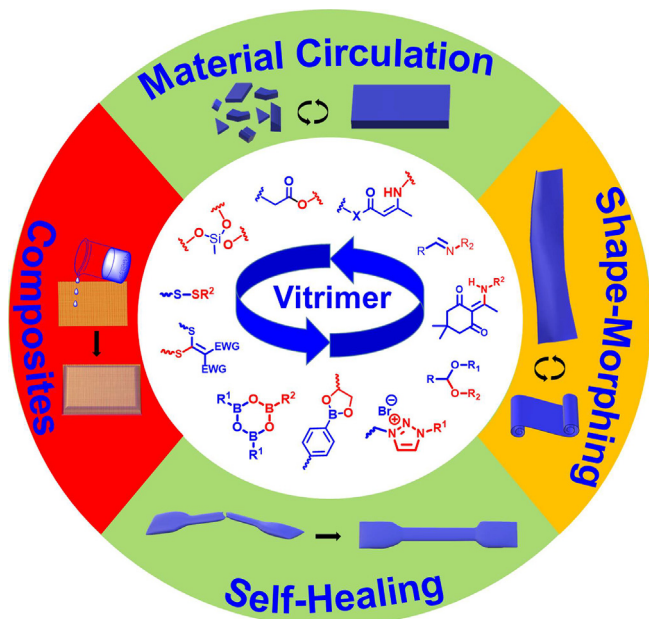


FIGURE 1.2

Schematic illustration of dynamic covalent bonds used in vitrimeric materials and their applications.

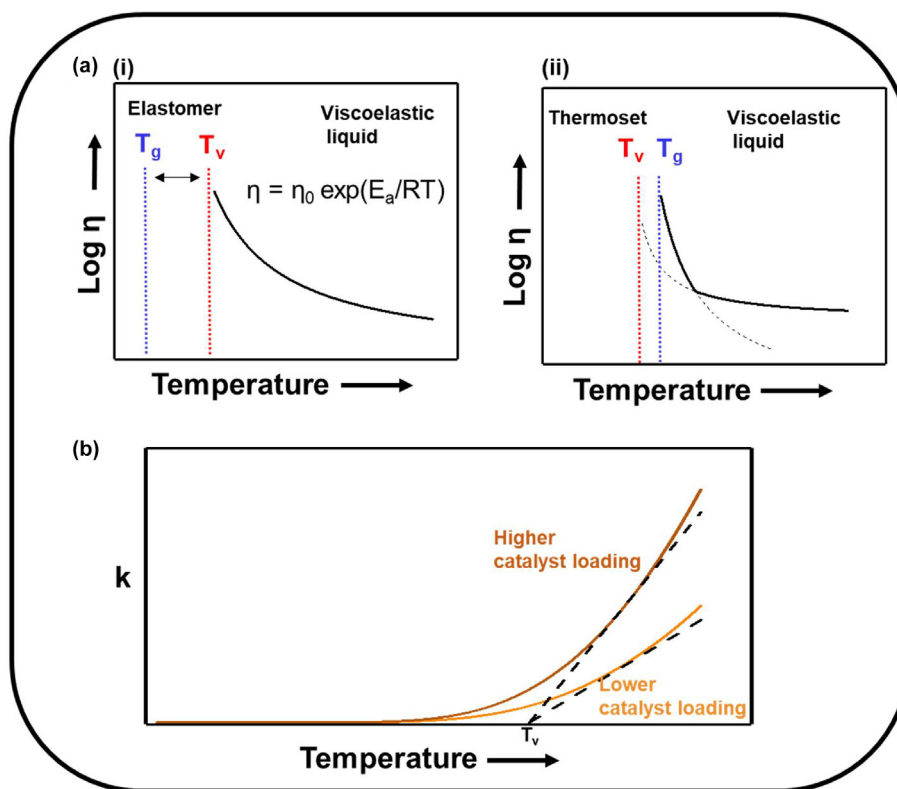


FIGURE 2.1

(a) Idealised viscosity-temperature relationship of vitrimers with (i) T_g lower than T_v , and (ii) T_v lower than T_g . (b) Plot of rate of reaction against temperature showing reaction with different catalyst loading with arbitrary units. The T_v is independent of the catalyst loading.

cosity, and a plot of $\ln \eta$ against $\frac{1}{T}$ gives the apparent $\frac{E_a}{R}$ as the slope.

Eyring's equation

Another equation which has been used to describe the rate of reactions is the Eyring's equation, $k = \frac{k_B T}{h} e^{-\frac{\Delta \ddagger G^0}{RT}}$ (k = rate constant, k_B = Boltzmann's constant, h = plank's constant, $\Delta \ddagger G^0$ = Gibbs energy of activation, R = universal gas constant, and T = temperature) [39,40]. Unlike the Arrhenius equation, Eyring's equation takes into account the activation entropy, which becomes particularly significant for some vitrimers, such as those employing neighbouring group participants. The proper orientation of molecules' design increases the statistical probability of these reactions occurring.

Dynamic equilibrium

In associative CANs, as bond formation and bond dissociation occurs in a single step, the enthalpy change (ΔH) of the reaction is typically close to zero, and the equilibrium between the cross-linked state and the dissociated state shows only a small dependence on temperature. On the other hand, in dissociative CANs, there can be significant enthalpy difference between these two states. As a result, the density of crosslinks is a function of temperature. As breaking of the crosslinks is usually an endothermic reaction, increasing the temperature shifts the equilibrium towards the dissociated state. This property can be exploited to form polymers with temperature controlled properties. One example is found in the work of Pei's group, where the density

of Diels–Alder crosslinks were tuned by subjecting the polymer to temperatures between 90 °C and 160 °C, followed by rapid cooling to room temperature, which prevents the crosslinks from reforming completely [41]. This enabled the tuning of the material's elastic modulus from between 35% and 85% of the original fully cross-linked polymer.

Cross-link density

The density of crosslinks in a polymer can be experimentally obtained by the equation $d = \frac{E'_r}{3R(T_g + 40)}$, where d = crosslinking density per unit volume (mol m^{-3}), E'_r represents the storage modulus in the rubbery plateau (MPa), R is the universal gas constant, and T_g is the glass transition temperature [42,43]. For incompressible materials (Poisson's ration ~ 0.5), the equation $M_c = \frac{2(1+\nu)\rho RT}{E}$ may also be used to calculate the crosslink density (M_c = the average molecular weight between crosslinks, ν = Poisson's ratio, ρ = density, R = universal gas constant, and E' = storage modulus (above T_g)) [24,37]. Related to the crosslink density is the gel point, which refers to the point whereby the crosslink density is high enough such that an essentially infinite molecular weight network is formed. The properties of the polymer with relation to its gel point is closely related to the Semenov-Rubinstein model [44]. This model predicts that the crosslinks has little effect on the viscoelastic properties of the material when the crosslink density is significantly below the gel point. Approaching the gel point, the chains associate in larger groups, and above the gel point, the network is fixed, and can only be

deformed by dissociation of the crosslink. This results have later been experimentally verified by Sheridan's group in a Diels-Alder based cross-linked network [45]. In dissociative CANs, the gel-point is also closely related to the gel-point temperature, as the crosslink density at equilibrium is closely related to its temperature.

Stimuli response

Fundamentally, CANs function on the basis of reversible stimuli response (Fig. 2.2). In the absence of stimuli, the covalent bonds should ideally be static, and the material acts as normal thermosets to meet the requirement. However, when the appropriate stimulus is applied, the exchanging between linkages (*i.e.* repeat breaking and reforming of chemical bonds) allows the possibility of the movement between polymer chains and the rearrangement of network topology, and overall resulting in the macrostructure change, such as stress relaxation, reprocessing, reshaping, damage healing as well as mechanical strength recovering. Ideally, the material returns to a dormant state when the stimulus is removed and serves as thermosets again.

The most commonly used stimulus is temperature. As predicted by Arrhenius's equation, the kinetics of chemical reactions are almost universally dependent on their temperature, due to the input of kinetic energy, leading to greater frequency of productive collisions, increasing the rate of reaction. In addition, the equilibrium of many reactions also depends on the temperature, especially in cases dissociative CANs. However, due to the universality of thermal activation, the activation temperature cannot be raised indefinitely, as the polymeric backbone may also begin to decompose, and other undesirable side reactions may occur. As a result, many thermally activated vitrimers also make use of some catalysts to selectively promote the dynamic covalent reaction at a lower temperature without affecting other parts of the polymer backbone.

Another attractive stimuli which could be used in vitrimeric materials is light. Three main classes of these reactions have been reported in CANs [12,46,47]. The first class are the photo-induced cyclisation, such as [2+2] or [4+4] cycloadditions [48,49]. These reactions can be controlled by the wavelength of

the incident light, as the wavelength promoting cleavage and cycloadditions tend to be different [50]. For instance, anthracene [4+4] dimerization occurs upon exposure to UV in the 360 nm region, while the cleavage occurs at 250 nm [51]. Another class of these reactions are photoreversible radical cleavages, such as in allyl sulphides [52,53], disulfides [54], and dimethacrylates [55]. More recently, a third class of non-radical photo-cleavage has also been developed in thioester-based thiol-ene elastomers, whereby an anionic exchange was promoted by exposure of UV in the presence of photo-bases [56]. Temperature and light are two complementary techniques to activate dynamic covalent bonds, with some recent reports combining both methods to achieve orthogonal activation [57].

A third stimuli seen in the literature is pH, which can be considered a special type of catalyst. Some crosslinks which pH has been used as an activator include imines [58,59], and acylhydrazones [60,61]. For instance, imine formation is usually catalysed at a pH of about 4, balancing between acid activation of the carbonyl without over-protonation of the amine. Some of these types of activation have been used in hydrogels with self-healing properties as well as in drug delivery applications. Apart from the stimuli mentioned above, other external stimuli, such as solvent, humidity, and redox agent, have also been studied to trigger the reversible bonds in vitrimeric materials (Fig. 2.2).

Vitrimer design

In this Section, vitrimer(-like) CANs are discussed based on their type of dynamic covalent bonds. Previously, in the seminal mini-review by Du Prez et al. (2016) [62], these materials were classified broadly by their reaction mechanisms – associative or dissociative. However, as the same type of chemical bond can undergo different mechanism, we have classified the materials by the type of dynamic bonds (Table 3.1). The most common type of dynamic covalent exchange is addition–elimination at a carbon-center, which can be found in esters and related functional groups such as carbamates, carbonates, and carbamides (Section 3.1), as well as acetals and imines (Section 3.2). An alternative related exchange is the conjugate addition–elimination, which is exhibited by vinylogous urethanes and thioethers (Section 3.3). In polyionic vitrimers, transalkylation occurs at Nitrogen and Sulfur-centers (Section 3.4), while in cross-linkers such as boronic esters, silyl ethers, and disulfide bonds (Section 3.5), bond formation and cleavage occurs between heteroatoms. By detailing this classification, we hope to enable the judicious choice of chemistry and cross-linkers in the design of vitrimers. We also endeavour to highlight important considerations in the design strategies of vitrimer(-like) materials.

Dynamic transesterification and related exchanges

Ester bond exchange

The first example of a vitrimer was reported by Leibler and co-workers in 2011 [17]. The authors prepared epoxy-acid and epoxy-anhydride networks with pendant hydroxyl groups (Figs. 3.1 and 3.2a), which could perform dynamic transesterification reactions catalysed by $Zn(OAc)_2$ or $Zn(acac)_2$ at elevated temperatures. While at room temperature the rate of reaction is insignificant and the polymers behaved as conventional thermosets, at high temperatures (*ca.* 200 °C) these exchange reac-

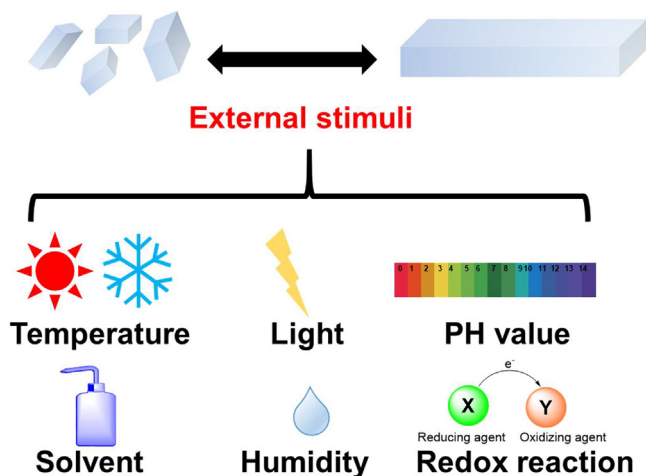


FIGURE 2.2

Illustration of external stimuli used to trigger the reversible bonds in CANs.

TABLE 3.1

Overview of dynamic covalent bonds found in vitrimers(-like) materials.

Dynamic bond	Scheme	Mechanism [†]	E_a /kJ mol ⁻¹	Catalyst [#]	T_g /°C	Mechanical Properties	Ref. ^d
Ester (3.1.1)		A	60–150	Uncat.; Zn(II); base	80	1.8 GPa ^a	[17]
Carbamate (3.1.2)		A/D	90–140	Sn(II)	54	72 ± 11 MPa ^a 2.2 ± 0.4 GPa ^b	[26]
Carbonate (3.1.2)		A	80–120	Ti(IV)	15–35	0.1–1.2 GPa ^b	[63]
Carbamide (3.1.3)		A/D/M	70–80	Uncat.	–70	>20 MPa ^a	[64]
Acetal (3.2.1)		A/D/M	55–140	Uncat.; acid	66–71	27.2–33.3 MPa ^a 0.8–1.1 GPa ^b	[65]
Imine (3.2.2)		A/M	10–130	Uncat.	55–135	10–64 MPa ^a 0.13–1.0 GPa ^b	[66]
Vinylogous Urethane (3.3.1)		A	30–80	Uncat.; acid; Sn(II)	87	90 MPa ^a 2.4 GPa ^b	[67]
Diketo-enamine (3.3.1)		A	30–50	Uncat.	125	38 MPa ^a 1.8 GPa ^b	[68]
Thioether (3.3.2)		A	55–70	Uncat.	–110	0.4–1.5 MPa ^c	[69]
Triazolium (3.4.1)		D	140–150	Uncat.	–8 to 23	15 MPa ^c	[28]
Pyridinium (3.4.1)		D	45	Uncat.	–22	1.3–3.4 MPa ^b	[70]
Anilinium (3.4.1)		D	50–60	Uncat.	11–15	225–380 kPa ^b	[71]
Sulfonium (3.4.2)		A	113	Uncat.	30–60 [†]	40–60 MPa ^b	[72]
Dioxaborolane (3.5.1)		A/M	40–80	Uncat.	98	28 MPa ^a 1.8 GPa ^b	[73]
Boroxine (3.5.1)		A	80	Uncat.	68	32.9 MPa ^a 0.7 GPa ^b	[74]
Silyl Ether (3.5.2)		A/M	80–180	Uncat.; acid	125	1.8 GPa ^b	[37]
Disulfide (3.5.3)		D	50–60	Uncat.	127	2.5 GPa ^b	[75]

[†] Mechanisms: A = associative; D = dissociative; M = metathesis. [#] Uncat. = uncatalyzed. [†] Temperature of malleability. ^a Tensile strength. ^b Young's modulus. ^c Storage modulus.

^d T_g and mechanical properties values mentioned in the table are only for the specific polymer examples.

tions ($E_a \sim 88$ kJ mol⁻¹) enabled the polymer network to exhibit viscoelastic properties such as stress relaxation and malleability. The group later showed that different catalysts and catalyst loadings could be used for these exchange reactions, resulting in different E_a , T_v and stress relaxation properties [76,77].

Until recently, transesterification vitrimers were typically catalysed by Lewis acids or strong organic bases. More recently, catalyst-free vitrimers based on internal activation [30] have been reported. In 2019, Du Prez developed catalyst-free vitrimers based on phthalate monoester transesterification with relaxation

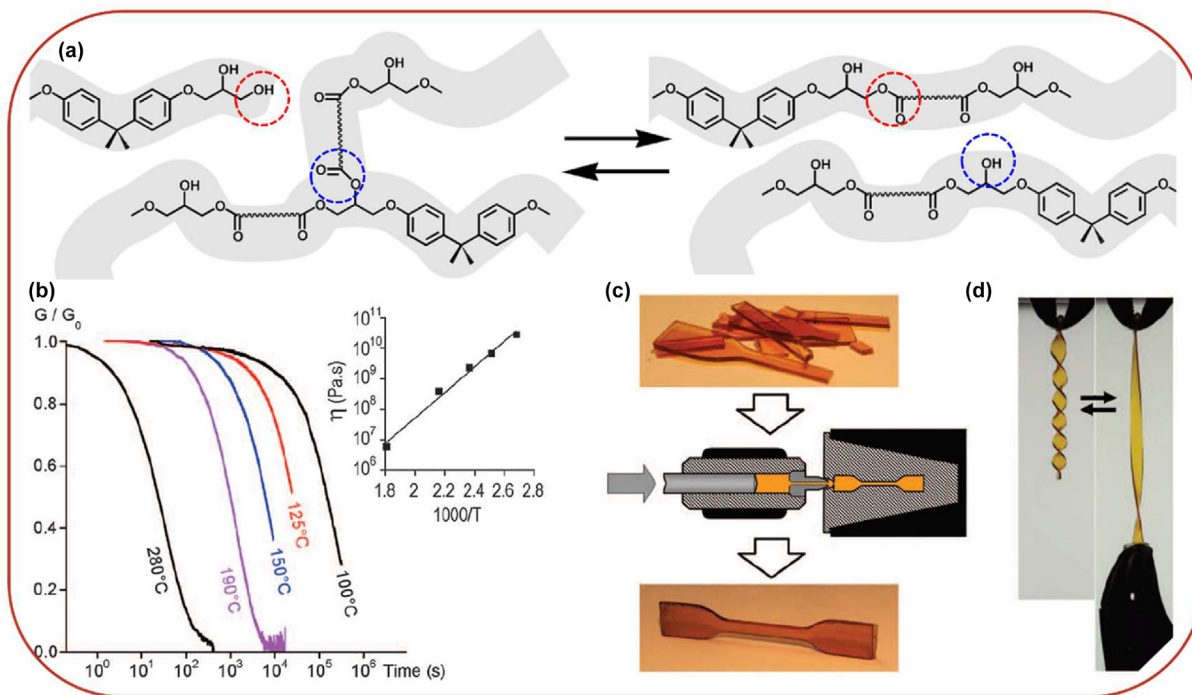


FIGURE 3.1

(a) Illustration of transesterification in hydroxyl-ester networks. (b) Normalized stress relaxation at different temperatures. The inset shows the temperature variation of zero-shear viscosity. (c) Reprocessing the broken pieces in an injection machine to recover its initial aspect and properties. (d) Reshaping the sample into a fusilli-shape. Reproduced with permission [17]. Copyright 2011, American Association for the Advancement of Science.

times of ~ 63 s at 150 °C (Fig. 3.2b) [66]. Internal catalysis was achieved through the close proximity of the neighbouring carboxylic acid group, which could attack the ester moiety to reversibly form an activated phthalic anhydride, which is more susceptible to attack by another alcohol. Although this reaction proceeds through a dissociative mechanism, the stress relaxation of this CAN follows Arrhenius behaviour ($E_a \sim 120$ kJ mol $^{-1}$) and the overall network integrity was retained even after 3 cycles of reprocessing, indicating vitrimer-like behaviour.

Another example of catalyst-free transesterification vitrimers was reported by Ojha et al. in 2020 [34]. Here, the authors utilised diethyl malonate as cross-linkers with poly(hydroxymethyl methacrylate) (Fig. 3.2c), with the β, β' -activated diester promoting the rate of transesterification such that the catalyst-free exchange could occur at 150 °C ($E_a \sim 110$ kJ mol $^{-1}$), while addition of $\text{Sn}(\text{Oct})_2$ could lower the processing temperature to 110 °C ($E_a \sim 82$ kJ mol $^{-1}$). Replacing catalysts with well-designed monomers could increase the safety and recyclability of transesterification vitrimers since catalyst leaching is no longer an issue.

As an alternative to tuning the carboxylic acid group, the “alcohol” can also be modified to lower the E_a of transesterification. He et al. incorporated the oxime moiety into polyesters to produce poly(oxime-ester) (POE) [79]. As the pK_a of oxime is lower than that of aliphatic alcohols, the replacing conventional ester bonds with oxime-ester bonds allowed for a catalyst-free oxime-transesterification exchange reaction (Fig. 3.2d). The results from small molecule model study revealed that the Arrhenius activation energy of catalyst-free oxime transesterification ($E_a \sim 63.5$ -

kJ mol $^{-1}$) is lower than that of conventional epoxy ester system containing catalysts ($E_a \sim 88$ kJ mol $^{-1}$). An excess amount of free oxime was incorporated in the polymer to promote associative exchange mechanism. Increasing the amount of free oximes resulted in vitrimers with faster relaxation times (from 5102 to 2725 s at 100 °C) and lower T_v (from 43 to 12 °C).

Other stimuli, such as light and solvent, have also been explored in transesterification vitrimers. For instance, light-activated vitrimers were developed by incorporating carbon nanotubes (CNTs) [81] or gold nanospheres [82] into the polymer network (Section 4.5.1). Light energy could be absorbed by these nanoparticles and converted to heat, enabling localised healing of the vitrimers through the photothermal effect. Solvent activated vitrimers were developed by Ji's group to program 2D flat epoxy-based vitrimer sheets into sophisticated 3D architectures at room temperature [29]. This vitrimer was synthesized by using TBD as a catalyst during the polymerization of epoxy and acid monomers. In doing so, TBD was also covalently incorporated into the network. During reprocessing, by employing good solvents for TBD (such as tetrahydrofuran and dichloromethane), chain stretching could be induced, activating the incorporated TBD to act as catalysts, reducing the activation energy of transesterification, and enabling reshaping, self-healing, and repurposing. At the same time, no catalyst leaching was observed under ambient operating conditions.

There has also been avid interest in bio-based transesterification vitrimers to minimise dependence on non-renewable chemical feedstock. These include polylactide vitrimers [83], as well as vitrimers based on poly-functional epoxidized soybean oil

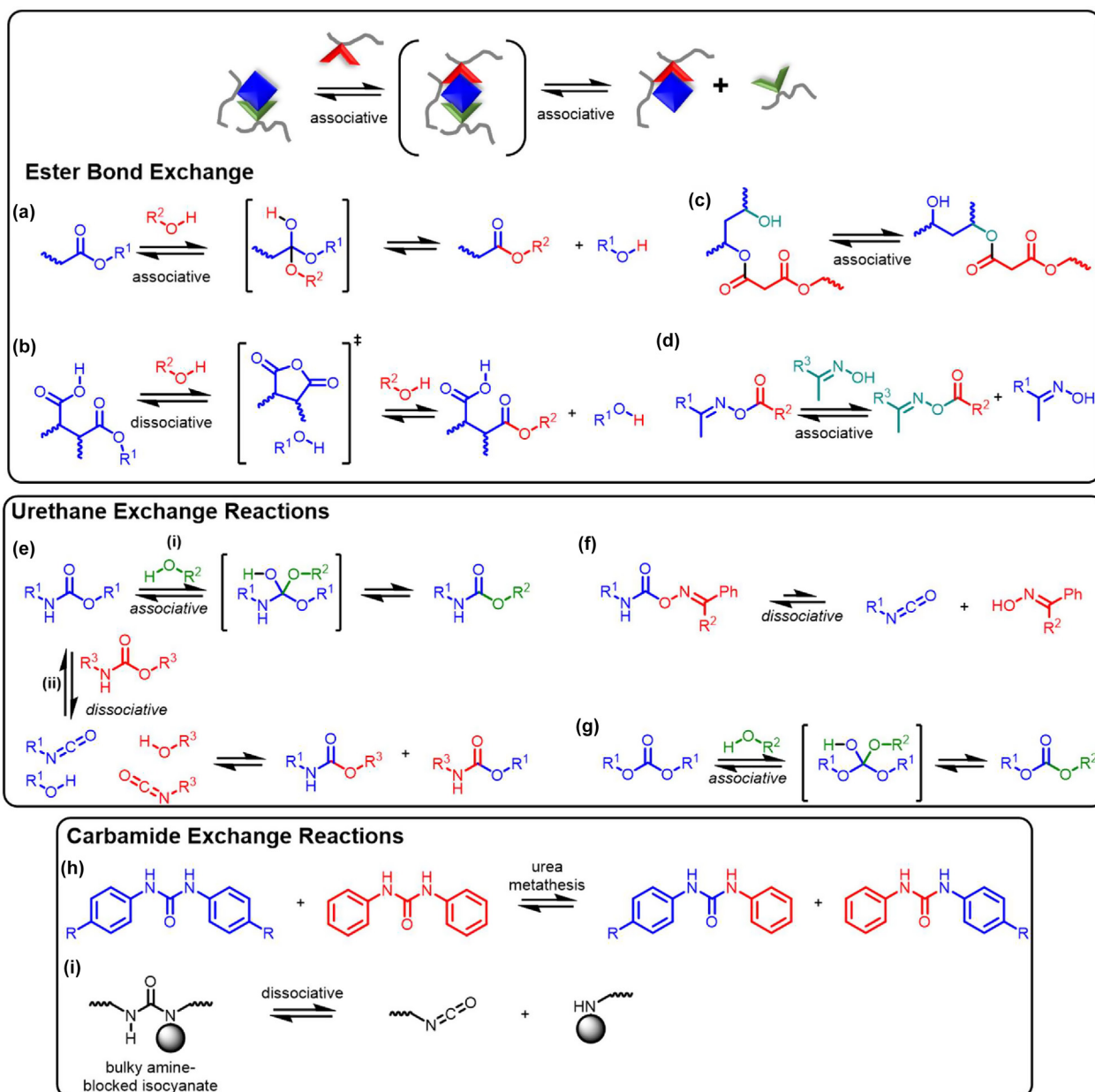


FIGURE 3.2

Ester bond exchange: (a) associative transesterification in epoxy-acid vitrimers; (b) catalyst-free dissociative mechanism in phthalate monoester transesterification by Du Prez et al. [78]; (c) catalyst-free β, β' -activated diester-promoted transesterification [34]; (d) catalyst-free associative oxime-ester transesterification [79]. Urethane exchange reaction via (e) (i) associative transcarbamoylation or (ii) dissociative urethane reversion via isocyanate and alcohol; (f) oxime-promoted dissociative transcarbamoylation [80]; (g) carbonate exchange via associative transcarbonation [63]. Carbamide exchange: (h) N, N'-diaryl urea metathesis; (i) dissociation of urea linkages with bulky amine substituent via isocyanate and amine.

[84–86] or lignin derivatives [87,88]. The use of biomass feedstock for vitrimers has multi-fold advantages – renewability, recyclability, biocompatibility and even biodegradability (under specific conditions) – and further refinement and adoption of these technologies could drastically improve the sustainability of plastics.

Carbamate and carbonate bond exchange

Instead of using the carboxylic acid esters, carbamic acid esters have also been utilised to synthesise transcarbamoylation vitrimers. Hillmyer and co-workers first developed polylactide vitrimers based on isocyanate-alcohol exchange reactions in 2014

[83]. Using a highly active $\text{Sn}(\text{Oct})_2$ catalyst, these polymers possessed T_v ($\sim 60^\circ\text{C}$) similar to T_g values and exhibited comparatively short stress relaxation times of 50 s at 140°C ($E_a \sim 150 \text{ kJ mol}^{-1}$).

While polyurethanes (PUs) represent a class of polymeric materials with extensive industrial applications, the reprocessability of PU-based thermosets was poorly understood and re-processing was inefficient until recently. Recently, a mechanistic study of stress relaxation in urethane-containing polymeric networks was presented by Hillmyer et al. [27]. The study thoroughly examined the stress relaxation behaviour of PEO-based and PLA-based polymers cross-linked with carbamate

bonds and suggested that the likely mechanism of stress relaxation is a dissociative tin-catalysed carbamate exchange reaction which proceed *via* isocyanate intermediates (Fig. 3.2e(ii)). The effects of temperature, catalyst content, and polymer structure on the relaxation behaviour of the polymeric network were also examined and it was shown that both materials exhibit Arrhenius-like stress relaxation.

While the discovery of re-processable PUs is a welcomed progression, the use of tin catalyst remains highly undesirable due to issues such as catalyst leaching and deactivation which limits material longevity, as well as the high toxicity of tin-based catalyst. Considering these issues, a network based on catalyst-free urethane exchange reaction is highly desired. Furthermore, an associative urethane exchange reaction mechanism is also highly desired to endow other beneficial properties such as solvent resistance. One way of achieving such material properties relies on the introduction of co-functional moieties into the polymeric network to effect changes in exchange mechanism. Pertinent to the topic, Hillmyer et al. reported the introduction of free hydroxyl moieties to produce poly(hydroxyl-urethane), a new class of PU-like materials with catalyst-free relaxation behaviour [26]. The polymer produced was glassy at room temperature ($T_g = 53\text{ }^\circ\text{C}$) and exhibited Arrhenius-like stress relaxation behaviour (8 hours for *ca.* 75% relaxation at $160\text{ }^\circ\text{C}$). The topology-freezing transition temperature (T_v) was determined to be $111\text{ }^\circ\text{C}$. The authors attributed the stress relaxation behaviour to mechanically activated associative transcarbamoylation promoted by the free hydroxyl groups (Fig. 3.2e(i)). Another advantage of this system is that the synthesis from cyclic carbonates and amines, as well as the exchange mechanisms both do not require the use or production of toxic isocyanates.

In 2017, Zhang and Rowan synthesised catalyst-free poly(alkylurea-urethane) networks by reacting the trimer of 1,6-hexamethylene diisocyanate with aminoethanols bearing *N*-alkyl substituents of different sizes [89]. While the polymer from the bulky 2,2,6,6-tetramethyl-4-piperidinol showed conventional dissociative behaviour of blocked isocyanates (Fig. 3.2e(ii)), the equilibrium constant of carbamate formation increased for less bulky aminoethanols; with concentrations as low as <1% isocyanates species at $200\text{ }^\circ\text{C}$ for the ethyl and isopropyl substituents. Despite the small amount of isocyanate dissociation, and almost constant cross-linking density even at high temperatures, these polymers could still be reprocessed at temperatures between 110 to $190\text{ }^\circ\text{C}$, exhibiting vitrimer-like Arrhenian flow ($E_a \sim 132\text{ kJ mol}^{-1}$) and $T_v \sim 74\text{ }^\circ\text{C}$ (for ethyl). This study highlighted that polymers based on dissociative dynamic bonds could be tuned to exhibit vitrimers-like behaviour by controlling the equilibrium constant of the reaction.

Analogous to the work by He's group [79], oxime chemistry is another promising strategy that can be exploited to prepare catalyst-free vitrimeric PUs. One such work was recently presented by Liu et al. involving the integration of oxime with urethane to produce poly(oxime-urethane) (POU) as a PU-like material [80]. The POU exhibited Arrhenius-like stress relaxation behaviour which was attributed to the oxime-promoted transcarbamoylation *via* a dissociative mechanism (Fig. 3.2f). Experimentally, the oxime-carbamate bond was shown to be reversible at *ca.* $100\text{ }^\circ\text{C}$, a facile re-processability condition rela-

tive to conventional PU materials ($>200\text{ }^\circ\text{C}$). Theoretically, it was revealed that mild temperature to achieve bond reversibility is mediated by the characteristic oxime-nitrone tautomerization.

In addition to transcarbamoylation, replacing the carboxylic acid with carbonic acid likewise generates carbonate vitrimers. Hillmyer's group developed hydroxyl-rich polycarbonate vitrimers ($T_g \sim 25\text{ }^\circ\text{C}$), which could undergo transcarbonation exchange reactions (Fig. 3.2g), in 2018 [63]. Catalysed by $\text{Ti}(\text{O}i\text{-Pr})_4$, these polymers displayed stress relaxation times of ~ 200 s to 1000 s at $170\text{ }^\circ\text{C}$ ($E_a \sim 80\text{--}120\text{ kJ mol}^{-1}$), with kinetics increasing with both catalyst loadings and pendant alcohol concentration. Zhao and co-workers utilized similar carbonate vitrimers to form composites with cellulose [90] to form a hydrophobic paper with self-healing properties.

Carbamide (Urea) bond exchange

An alternative functional moiety that can be employed as a cross-linker is the urea moiety. Li et al. reported the introduction of free urea moieties to produce poly(urethane-urea) [64]. The introduction of the urea moiety produced a copolymer consisting of hard and soft segments; the former endowed enhanced mechanical properties while the latter imparted the flexibility required for dynamic exchanges. In this instance the vitrimer-like property of the PU-like material arises as a result of an *N, N'*-diaryl urea exchange (Fig. 3.2h) rather than a carbamate bond exchange.

Polyurea represents another class of nitrogen-containing polymer which holds industrial significance. In 2013, Cheng et al. reported an instance of exploiting steric factor of bulky amines to induce dynamic exchanges in polyurea (Fig. 3.2i) [91]. The isocyanate functional group presents a *viable* solution for the design of dynamic covalent interactions. In contrast with ketenes which are unstable, isocyanates are reasonably stable under ambient conditions, and rapidly reacts with amines to form ureas. Through the incorporation of bulky substituents on the nitrogen atom of the urea bond, urea linkages can reversibly dissociate into the corresponding isocyanate and bulky amines, giving rise to dynamic relaxation properties. Polyurea incorporating such steric effects can be readily synthesized by replacing regular amine with bulky counterparts. Through examining a series of five amines, this work showed that the dynamic exchange of urea linkages can be controlled by tuning the steric bulkiness of the substituent attached to the urea nitrogen. Subsequently, the optimal urea moiety, 1-(tert-butyl)-1-ethylurea, was introduced into a poly(urethane-urea) network which exhibited vitrimer-like properties. These results suggest that such design incorporating the role of steric effects may be readily integrated into wide range of materials, bringing modular and tunable dynamic properties to traditional polyurea and urea-containing polymers such as poly(urethane-urea).

Dynamic transacetalation and transimination

Acetal bond exchange

Acetal chemistries have been extensively explored as a synthetic strategy for syntheses of complex supramolecular assemblies [92,93]. Recent works have suggested that the dynamic nature of acetal exchange reactions could also be adopted to develop vitrimer(-like) materials. Acetal exchange can occur through

two distinct mechanisms: transacetalization and acetal metathesis. The former refers to the alcoholysis of acetal (Fig. 3.3a(i)), that is, a free hydroxyl group reacts with an acetal and replaces part of the acetal structure to form a new acetal while the latter refers to the exchange reactions between two acetals (Fig. 3.3a(ii)).

In their recent work, Zhu et al. exploited acetal chemistry for the design of a malleable and recyclable polymer networks (Fig. 3.3d) [65]. Taking into consideration the impact of toxic metal catalysts, the acetal dynamic networks were prepared *via* the catalyst-free “click” addition of poly(styrene-co-styrene-OH) and 1,4-cyclohexanedimethanol divinyl ether which proceeds without the release of any small molecules by-products. The heat-induced stress relaxation behaviour of the polymer network based on the acetal motif exhibited Arrhenius-like temperature dependence. It was found that relaxation rate was dependent on the free hydroxyl content of the network, indicative of

hydroxyl-promoted transacetalization being the main relaxation mechanism. The T_v of the network, depending on the hydroxyl content, ranged from 61 °C to 103 °C. Furthermore, these acetal-based network demonstrated excellent mechanical and chemical recyclability. Hot press recovery could be achieved in 10 min under 15 MPa at 150 °C with well-preserved mechanical properties. The monomer recovery of these acetal-based network was also efficient and simple, achieving a 92% recovery after a 1-h treatment in hot water at 100 °C (Fig. 3.3d). However, owing to the high relaxation temperature, sample aging occurred, resulting in slight deterioration in relaxation property. In follow-up work, the same team showed that the chemical stability and mechanical properties can be adjusted by finetuning the chemical environment adjacent to the acetal linkages (Fig. 3.3b) [94]. Additionally, this work showcased how a conventional thermoset resin, such as phenolic resin, could be adapted to form a vitrimeric network through one-step “click” cross-linking.

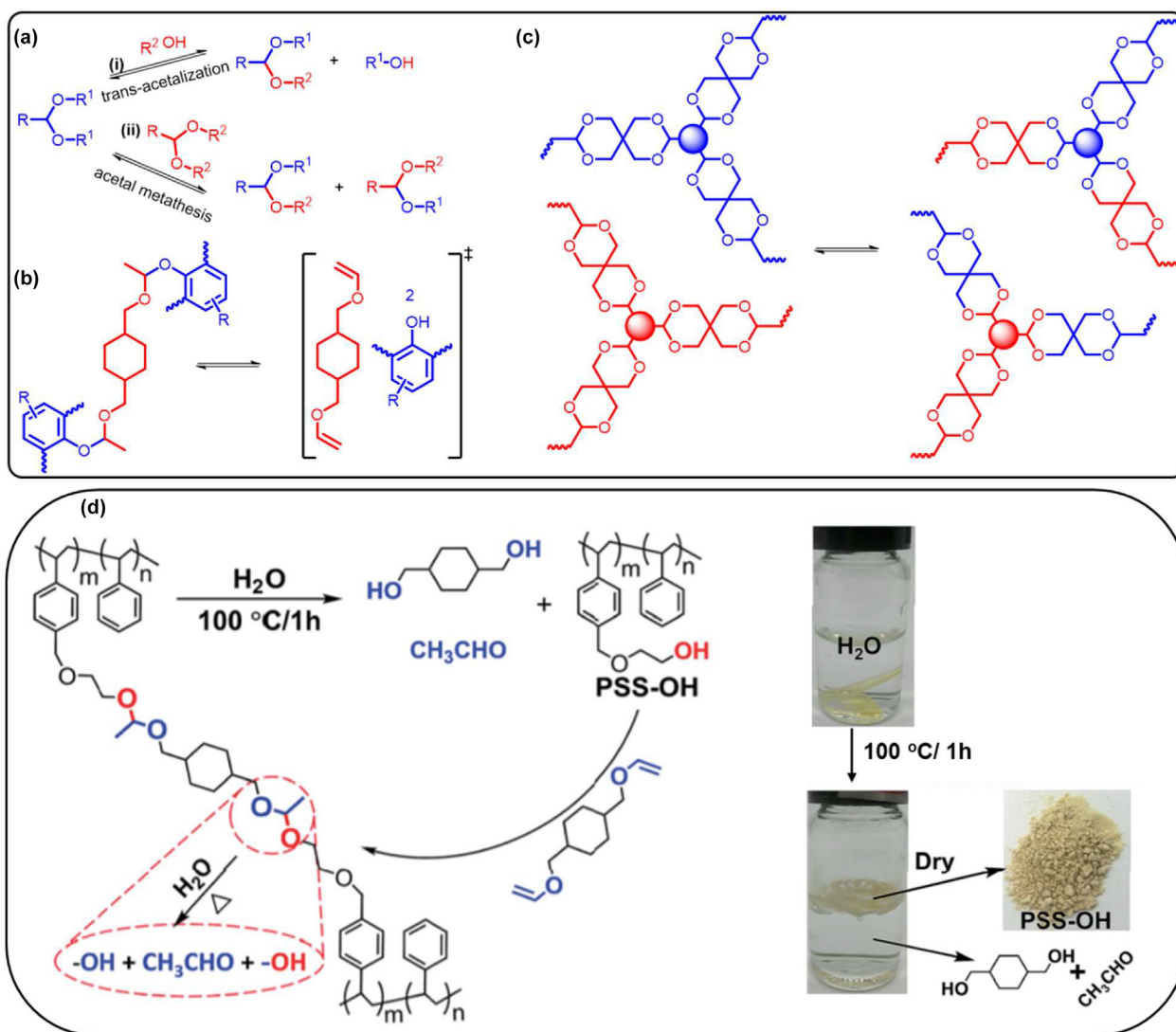


FIGURE 3.3

(a) Acetal exchange *via* (i) transacetalization between acetal and free hydroxy moiety or (ii) acetal metathesis. (b) Catalyst-free dissociative acetal exchange in phenolic vitrimers with cyclohexyldimethanol divinyl ether cross-linkers [94]. (c) Catalyst-free acetal metathesis in spirocyclic acetal network [95]. (d) Degradation recycling of the acetal dynamic network in hot water: mechanism and photographs [65] Reproduced with permission [65]. Copyright 2019, Royal Society of Chemistry.

Yu et al. demonstrated a re-processable elastomer operating on the basis of catalyst free acetal metathesis in a cross-linked spirocyclic acetal polymer (Fig. 3.3c) [95]. The mechanism and kinetics of the exchange process were studied using model compounds and the Arrhenius activation energy of the catalyst-free metathesis was determined to be $\sim 57 \text{ kJ mol}^{-1}$. Under this context, the presence of free hydroxyl groups within the polymeric network was not necessary, eliminating potential side reactions (such as dehydration and oxidation) at high re-processing temperature. Meanwhile, the elimination of acidic catalysts also avoids acid-mediated degradation. Additionally, spirocyclic acetals showed improved thermal stability over acyclic acetals. The high refractive index of these polymers also make them promising candidates for applications in optical devices.

Imine bond exchange

In 2014, Zhang et al. reported an instance of catalyst-free polyimine material with water-driven malleability at ambient temperature [96]. The polymer produced was hard and glassy at room temperature ($T_g = 56 \text{ }^\circ\text{C}$) and exhibited Arrhenius-like stress relaxation behaviour (30 min for *ca.* 90% relaxation at $80 \text{ }^\circ\text{C}$). The material exhibited excellent recyclability being remouldable even from powdered states under facile conditions (45 min under 90 kPa at $80 \text{ }^\circ\text{C}$) with well-preserved mechanical strength. More interestingly, the polyimine materials possess hydrolytic resistance which allowed it to relax in water. Furthermore, it was revealed that the stress relaxation of the polyimine in water is comparable to the behaviour observed at elevated temperature. As this was not observed in other solvents, the authors hypothesised that hydrolysis of a small percentage of imine (insignificant based on solid-state ^{13}C NMR) promoted amine/imine exchange (Fig. 3.4a). This water-induced reprocessability also alleviates material aging caused by conventional high temperature re-processing conditions which typically limits the lifespan of the recycled material.

In a more recent work, Smulders et al. reported a quantitative structure–property relationship (QSPR) between dianiline monomers and the macroscopic material properties of their corresponding polyimines [98]. The physical properties of five selected dianiline monomers with differing electronic properties (quantified by their respective Hammett parameter σ , where a higher σ value relates to a greater electron-withdrawing effect) were studied (Fig. 3.4c). The study revealed a simple, often linear, correlation between σ values and a range of dynamic material properties such as E_a , T_v and creep ($\dot{\gamma}$) (Fig. 3.4c). Through this direct correlation based on the Hammett equation of a molecule-based physical parameter (σ) to macroscopic property of polymer, dynamic material properties could be tuned in a quantitative and predictable manner, representing a step forward for the designability of vitrimers with highly precise material properties for specific applications.

Bio-based polymers hold great promise for the development of green and sustainable materials. The integration of dynamic covalent interactions with bio-based polymers to endow intrinsic controlled degradability to bio-based polymers is highly sought after. To this end, Dhers et al. reported on the instance of bio-based polyimine vitrimer fabricated from 100% renewable monomer sources (Fig. 3.4b) [97]. The polyimine network was

prepared from fructose-based monomer furandialdehyde and a mixture of amine monomers derived from vegetable oil. Remarkably, the fabricated materials exhibited superior mechanical properties, thermal stability and chemical resistance as well as excellent re-processability. The materials showed typical Arrhenius-like stress-relaxation with an experimental activation energy of *ca.* 60 kJ mol^{-1} . Short relaxation times (for full relaxation) ranging from *ca.* 20 min at $40 \text{ }^\circ\text{C}$ to 40 seconds at $80 \text{ }^\circ\text{C}$ were observed. The fast relaxation time was attributed to the associative transamination of the imine linkages in the presence of excess amines. The fabricated materials were also found to be extremely stable under hydrolytic conditions which can be partially attributed to the hydrophobic nature of the amines used.

Dynamic exchange of conjugated systems

Ketoamine bond exchange

Du Prez and co-workers reported one of the first catalyst-free vitrimers in 2015 [67]. The group's vinylogous urethane (Vurethane) vitrimers were based on ketoamines, formed from amine attack on β -keto esters, which are remarkably stable towards hydrolysis. A follow-up study in 2017 demonstrated that the exchange reaction proceeds *via* conjugate addition followed by elimination, with low uncatalyzed E_a of $\sim 60 \text{ kJ mol}^{-1}$ and rapid stress relaxation ($\sim 3 \text{ min}$ at $150 \text{ }^\circ\text{C}$) [99]. The authors also elucidated the impact of various additives on stress relaxation. While protic acids (e.g. *p*-TsOH, H_2SO_4) accelerated the stress relaxation with little change in E_a (Fig. 3.5a), Lewis acids (e.g. dibutyltin laurate) drastically lowered the E_a , indicating a different exchange mechanism (Fig. 3.5b). Addition of bases (e.g. triazabicyclodecene, 1,5-diazabicyclo[4.3.0]non-5-ene) instead increased both the E_a and stress relaxation time (Fig. 3.5c). These findings enabled the authors to tune the viscoelastic properties of not only elastomeric vitrimers ($T_g \sim -25 \text{ }^\circ\text{C}$), but also rigid vitrimeric networks ($T_g \sim 87 \text{ }^\circ\text{C}$) [99]. Following these studies, vinylogous urethane vitrimers have been synthesised from many different commodity polymers, such as polydimethylsiloxane (PDMS) [100], poly(methyl methacrylate) (PMMA) [101] and epoxy [102].

Ketoamine-type vitrimers based on other vinylogous acyl compounds have also been discovered. Du Prez et al. systematically studied the dynamic exchange reactions of vinylogous urethane, amides and urea. The authors found that more electron donating groups at the carbonyl led to increased exchange kinetics, with vinylogous ureas (Vureas) thus possessing the most rapid exchange. Vurea vitrimers prepared had uncatalyzed stress relaxations of as low as 57 s at $170 \text{ }^\circ\text{C}$, and with 0.5 mol% *p*-TsOH, this could even be lowered to 2.4 s. These Vureas were further explored for use in prepreg composites together with carbon fibres [104].

Fluoropolymers are a class of polymer characterized by their high chemical resistance and friction reducing surface properties, which are significant in various high-performance material applications. Du Prez et al. introduced the catalyst-free vinylogous urethane vitrimer chemistry into perfluoropolyether (PFPEs) to endow the thermosetting material with viscoelastic properties (*i.e.* fluorinated vitrimers) [103]. The PFPEs were synthesised *via* a facile solvent-free protocol and demonstrated a novel dual vitrimer relaxation behaviour (Fig. 3.5d). The observed phe-

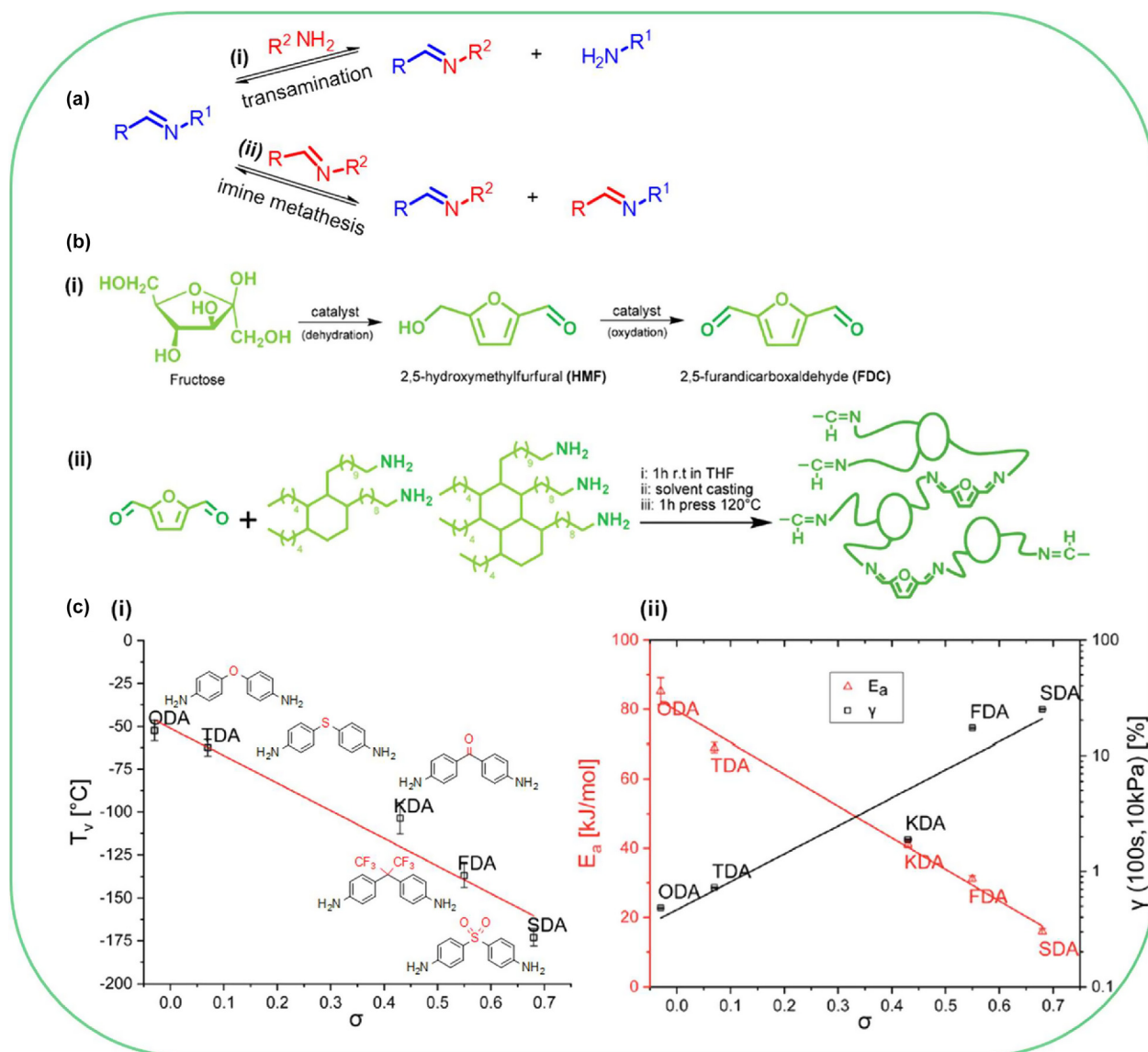


FIGURE 3.4

(a) Imine exchange *via* (i) transamination between imine and free amine moiety or (ii) imine metathesis. (b) Fabrication of bio-based polymeric material: (i) synthesis of fructose-based bio-monomer FDC, followed by (ii) poly-condensation reaction of FDC with bio-based mixture of amines (DTA). Reproduced from Ref. [97] with permission from The Royal Society of Chemistry; (c) Quantitative structure–property relationship (QSPR) study of aniline monomers with (i) topology freezing temperature (T_v) and (ii) Arrhenius activation energy (E_a) and creep (γ) as a function of Hammett constant, σ . Adapted from Ref. [98] Published by The Royal Society of Chemistry.

nomenon was attributed to the co-existence of two mechanistically distinct transamination processes with significantly different activation energies which occur at different temperature ranges. The gradual and moderate decrease of the viscosity in the lower temperature range was ascribed to an amine exchange which proceeded *via* a pathway involving an activated iminium intermediate (Fig. 3.5d(i)). At a higher temperature range however, a higher energy barrier Michael-type conjugate addition becomes the dominant transamination pathway due to its greater temperature dependence (Fig. 3.5d(ii)), resulting in a sharper and more pronounced temperature response. The results from the study also showed that transition point of the two temperature ranges is seemingly dependent on the free amine composition, further substantiating the notion that the low barrier

process is outcompeted by the high barrier process at higher temperatures. In summary, the novel dual viscosity profile arises from the same transamination occurring *via* two distinct exchange mechanisms, involving different reactive species. The discovery of such novel material properties illustrates the need to further our understanding the mechanism behind vitrimeric material behavior. Undoubtedly, the understanding of the peculiarities behind well-established chemistries when integrated into existing material will facilitate design of more new materials with precise rheological profiles for niche application.

More recently, poly(diketoenamine) (PDK) vitrimers have been reported. In 2019, Helms and co-workers reported that condensation of β -triketones with amines *via* ball-milling forms PDK networks with high T_g (>120 °C) and catalyst-free low E_a

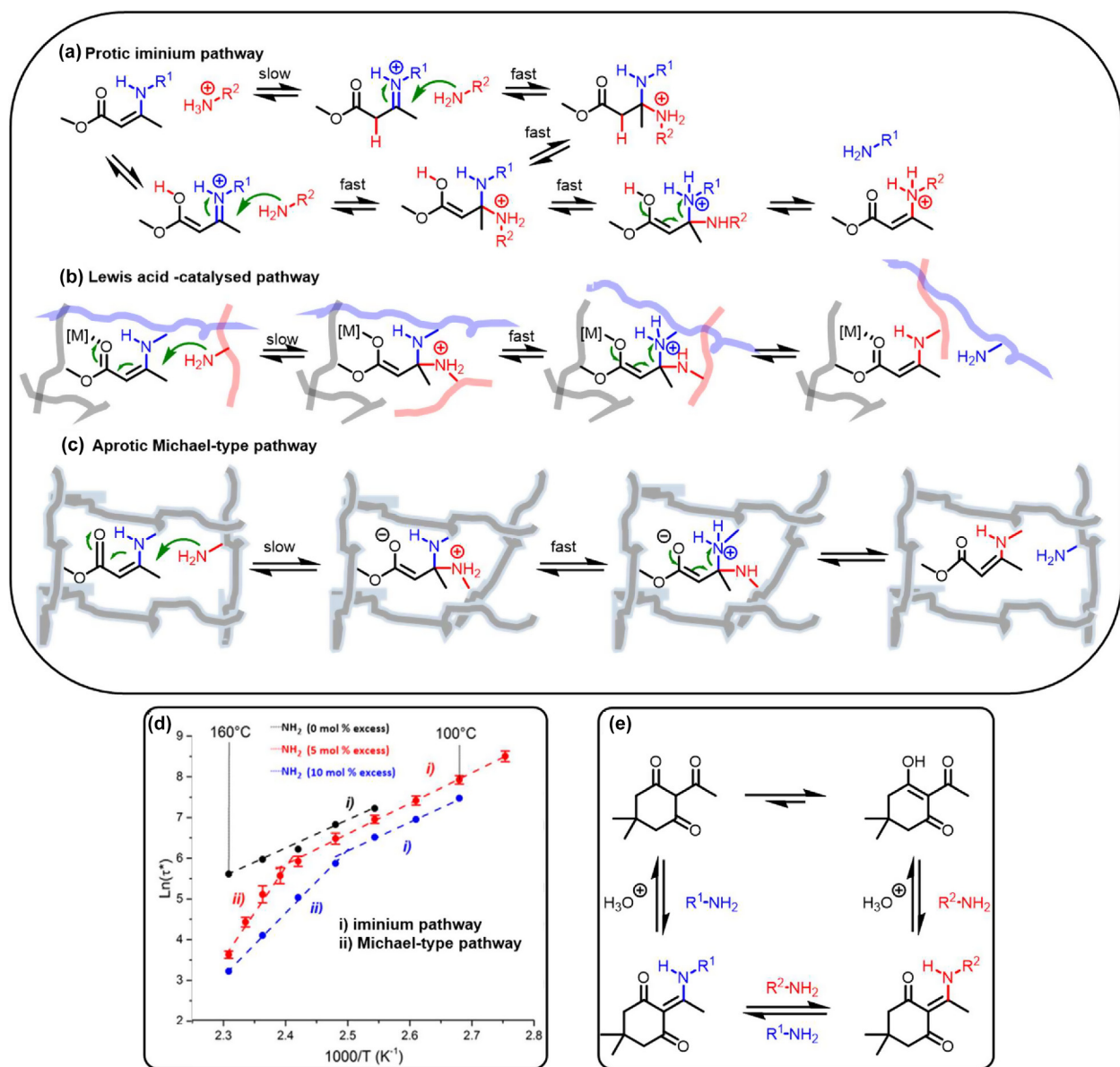


FIGURE 3.5

Transamination of ketoenamines *via* (a) pathway at low temperature or under acidic/neutral conditions involving an iminium intermediate. (b) Lewis acid-catalysed pathway. (c) Michael-type pathway at high temperature or under basic conditions. (d) Arrhenius plots indicating the temperature-dependent mechanistic change in PFPEs with vinyllogous urethane cross-links. Reproduced with permission from Ref. [103]. Copyright 2018, American Chemical Society; (e) Reaction mechanism showing the reversible formation of diketoenamines. Triketones and amines favour the spontaneous formation of diketoenamine bonds, which will hydrolyze under strongly acidic conditions to reform a triketone and an ammonium salt.

($\sim 50 \text{ kJ mol}^{-1}$) exchange reactions [68]. Another advantage of this system is the ability to recover both the triketone and amine monomers in $>90\%$ purity under acid depolymerisation (Fig. 3.5e); this ease of recovery is rare even the broader field of covalent adaptable networks (CANs). In 2020, the group studied how polymer design could impact the thermal and rheological properties of the vitrimers: incorporation of flexible (linear long-chain) amines lowered the vitrimer T_g , while rigid amines increased T_g , following the Flory-Fox equation [105]. Increasing conformational entropy also led to decreasing the E_a and relaxation times of the vitrimers. These findings provide useful guidelines for tuning vitrimers properties through polymer design.

Thiol ether conjugate addition–eliminations

Apart from amines, Meldrum's acid derivatives can also form reversible covalent bonds with other nucleophiles. In 2018, Ishibashi and Kalow developed silicone vitrimers based on thioetherification of Meldrum's acid alkylidene (Fig. 3.6) [69]. Catalyst-free "click" conjugate addition–elimination of thiofunctionalised PDMS (13–17%) to Meldrum's acid derivative MA (2 mol%) at 120°C resulted in cross-linked silicone networks which could be reprocessed at 150°C under 9 tons in a hot press at least 10 times. The reversible, associative exchange mechanism enabled the vitrimers to exhibit Arrhenius stress relaxation ($E_a \sim 64 \text{ kJ mol}^{-1}$) behaviour with $T_v \sim -6^\circ\text{C}$. Following up on

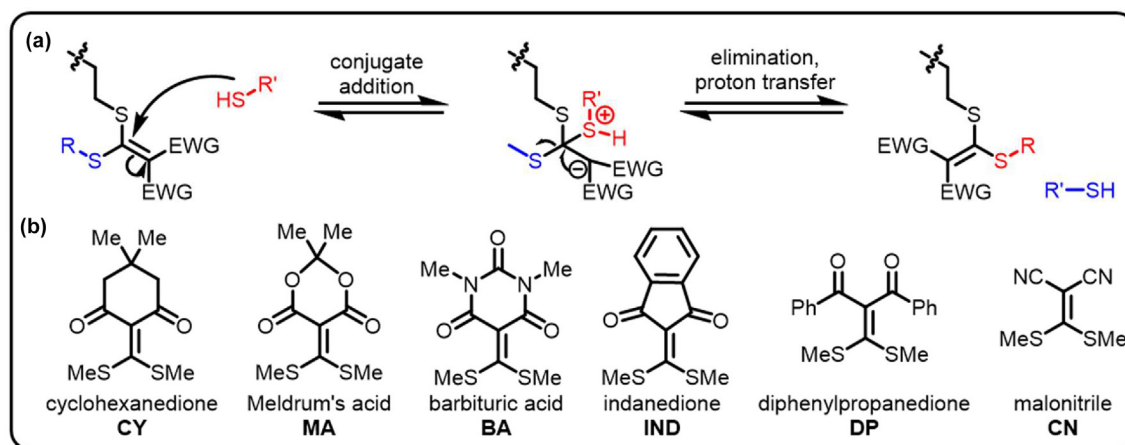


FIGURE 3.6

(a) Reaction mechanism of the conjugate addition–elimination exchange reactions of a thiol ether-based cross linker. (b) Chemical structures of the various conjugate acceptor cross-linkers that were studied in Ref. [106], with the derivative CY having the fastest stress-relaxation.

this work, the group studied a series of conjugate acceptor cross-linkers (Fig. 3.6b) and the properties of their resulting vitrimers with the same thio-functionalised PDMS [106]. Stress-relaxation studies revealed that while the E_a of networks with different cross-linkers were similar, the relaxation time for the cyclohexanedione derivative CY was the fastest, which could be attributed to the unhindered structure and heightened reactivity of the cross-linker to nucleophilic attack.

Dynamic transalkylation in polyionic systems

Transalkylation of N-centred salts

Ionic vitrimers were first reported in 2015 by the group of Drockenmüller. A network comprising poly(1,2,3-triazole) cross-linked by difunctional alkylating agents, exhibited malleability and reprocessability at 170 °C (Fig. 3.7a) [107]. Poly(1,2,3-triazolium ionic liquid)s (PTILs) with the bromide counterion exhibited Arrhenius stress-relaxation ($E_a \sim 140 \text{ kJ mol}^{-1}$) and short relaxation times (30 min at 130 °C), while the iodide counterion led to slower stress-relaxation. As vitrimers were originally established as materials in which the polymeric networks can undergo topology rearrangement due to an associative dynamic exchange reaction between functional moieties in the network, the initial mechanism proposed was associative–nucleophilic attack of pendant triazoles on the alkyl triazolium species. However, a more in-depth mechanistic study from the same group showed that a dissociative pathway – nucleophilic attack of halide counterion on the alkyl triazolium species, releasing free triazole and alkyl halide – was actually dominant (Fig. 3.7b) [28]. Despite the dissociative exchange mechanism, PTILs still possessed vitrimeric properties. To explain this phenomenon, the authors showed that the rate-limiting step of the overall exchange was the dissociation of the alkyl triazolium, and reformation of cross-links was rapid. Hence, the cross-link density remained constant across a wide temperature range (100–170 °C), in contrast with networks based on Diel–Alder adducts. This finding, in conjunction with the work by Rowan et al., [89], that cross-link density could be maintained even with a dissociative exchange mechanism, widened the field of vitrimers-like materials.

Guo et al. recently reported an instance of C–N transalkylation of pyridinium salt [70]. As an alternative to vulcanization, nanofillers are often used as mechanical reinforcement for neat rubber to produce rubber composites. However, its application usually results in additional obstructions for chain mobility and network rearrangement in the resultant composite. This work reported the incorporation of exchangeable covalent cross-links in the interfaces between the rubber and nanoparticles as a resolution to this dilemma. The butadiene-styrene-vinylpyridine composites were prepared using (3-bromopropyl)-trimethoxy-silane modified silica (Si-Br) as crosslinkers, forming pyridiniums in the rubber-nanoparticle interfaces. As expected, the mechanical properties of the composite were improved compared to neat rubber and Young's modulus is a function of Si-Br loading. The composites demonstrated vitrimeric viscoelasticity with Arrhenius-like stress relaxation behaviour. Small model molecules study revealed the C–N trans-alkylation of pyridinium salt with alkyl halide at elevated temperature (Fig. 3.7c) and the fast relaxation behaviour of the composites was attributed to the C–N trans-alkylation of pyridinium at the rubber-nanoparticle interface. The composites were also shown to be thermally reprocessable without significant loss of mechanical properties.

Another transalkylation system was reported by Konkolewicz et al., who demonstrated that anilinium salts could also form vitrimeric materials [71]. The authors copolymerised 2-hydroxyethylacrylate with 4-(*N,N*-dimethylamino)styrene and anilinium cross-linkers to obtain networks with high malleability at 60 °C and Arrhenius stress-relaxation ($E_a \sim 60 \text{ kJ mol}^{-1}$) [108]. The authors studied the correlation between kinetics of dynamic exchange of anilinium salts in small molecules and the vitrimer-like flow behavior of polymeric materials with anilinium linkages [108]. Similar to the PTIL systems [28], the exchange proceeds *via* an indirect $\text{S}_{\text{N}}2$ mediated by the bromide counter-anion (Fig. 3.7d). Despite the dissociative exchange pathway, constant crosslink density was observed over a wide range of temperatures. The results from the small model molecule study revealed that both the association and dissociation of anilinium linkages have similar activation energies, suggesting

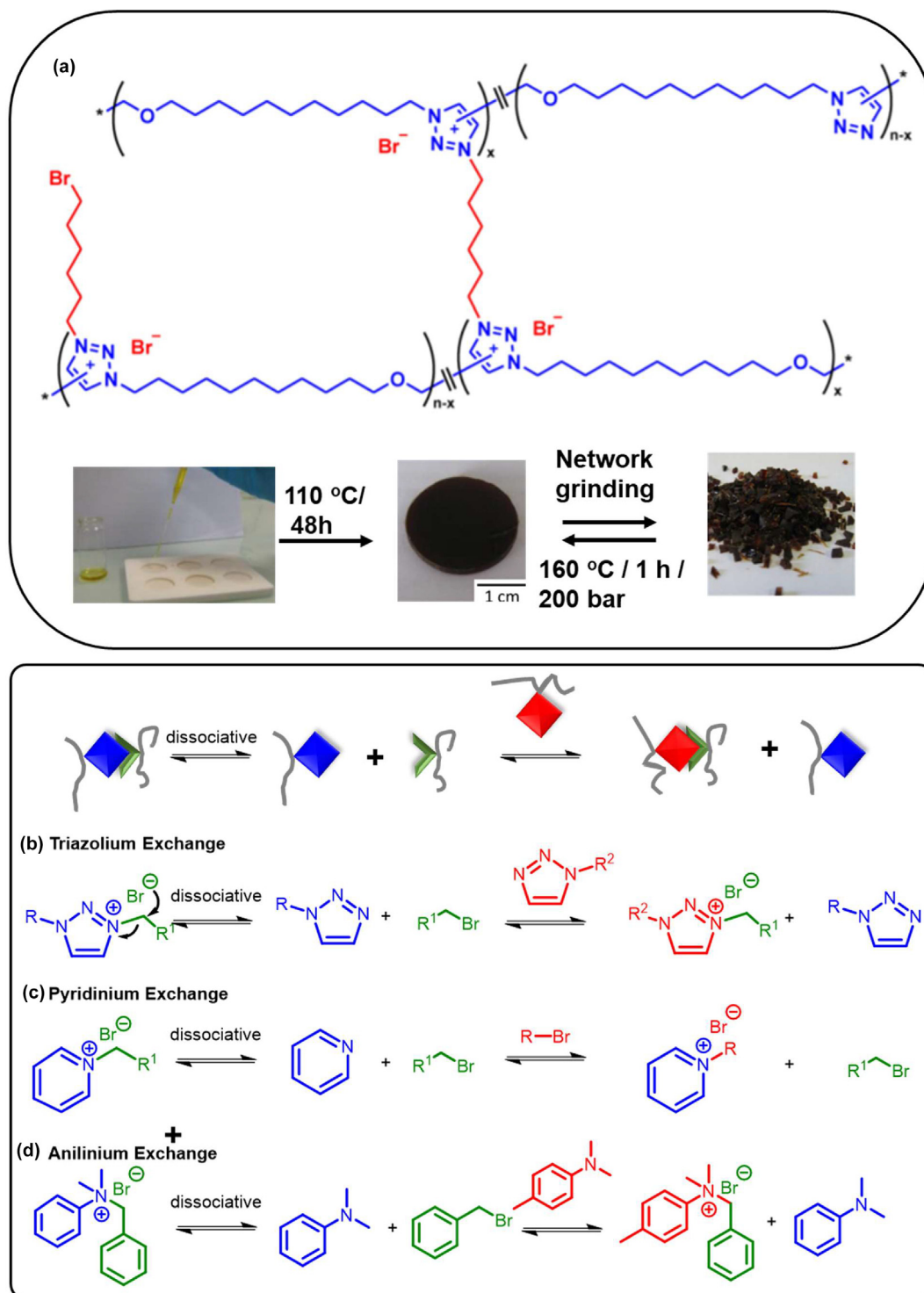


FIGURE 3.7

Dissociative mechanism in the transalkylation of: (a) and (b) triazolium salts [28,107]; (c) pyridinium salts [70]; and (d) anilinium salts [71,108]. Reproduced with permission [107]. Copyright 2015, American Chemical Society.

that the retention of constant cross-link density could be due to a rapid de-crosslinking and re-crosslinking phenomena. In contrast to traditional dissociative CANs such as the Diel–Alder adducts, in which the thermodynamics at elevated temperature significantly favors the dissociation of adducts, in the anilinium system the drive toward an increase in dissociation rate is bal-

anced by an equally large drive for the reassociation of reactive species back into anilinium adducts. As such, anilinium linkage proves to be a unique dissociative system with its measurable and nontrivial fraction of the dissociated bond (dissociative nature) while at the same time temperature-independence of the fraction of cross-linkers (associative nature).

Transalkylation of sulfonium salts

In addition to cationic N-centred salts, sulfonium salts can also undergo dynamic covalent exchange. The reversibility of sulfide-sulfonium salt reaction was previously reported by Goethals et al. [109]. Based on this precedence, Du Prez et al. recently reported the fabrication of catalyst-free poly(thioether) networks based on the dynamic sulfide-sulfonium salt exchange reaction [72]. Through a model small molecule study, it was established that the exchange mechanism proceeded *via* a classical S_N2 -type reaction of sulfonium salts with thioether nucleophiles with Arrhenius activation energy *ca.* 108 kJ mol⁻¹. The associative, concerted cross-linking reaction produced polymers which exhibited vitrimer-like properties ($T_v = 65$ °C), thus endowing simple recyclability at elevated temperature (few min at 160 °C).

Today, rubber is generally recognized as a strategically important material. However, to produce rubber with sufficient elasticity, toughness, as well as solvent resistance, the most common approach to date is still vulcanization – the treatment of rubber with sulfur to form C–S bonds which inevitably hinder the subsequent recycling, reprocessing or even re-use of rubber products due to the formation of strong C–S linkages. Encouraged by the results from Du Prez et al., Zhang and co-workers reported on a facile yet efficient way (60 min at 160 °C) to recycle existing sulfur-cured rubbers through the addition of trimethylsulfonium iodide (TMSI) during re-molding procedure to initiate the of sulfide-sulfonium salt exchange [110].

Dynamic heteroatom bond exchange

Boronic ester (B–O) exchange

Guan and co-workers first demonstrated the use of boronic ester metathesis in bulk solid-state polymers in 2015 [111]. The authors showed that polycyclooctene polymer containing 20% 1,2-diol groups could be cross-linked by metathesis with a *bis*-dioxaborolane (Fig. 3.8a). The rate of dynamic transesterification could be tuned with the design of cross-linker, with the *bis*-dioxaborolane cross-linker bearing a neighbouring N atom possessing 5 orders of magnitude faster exchange compared to the corresponding O-bearing cross-linker in small molecule studies. Stress-relaxation studies of the vitrimers showed similar results – vitrimers with N-containing cross-linker released stress much faster (<5 min for 2% strain) compared to O-containing cross-linker (>20 min) for temperatures between 35 to 55 °C; and only the N-containing cross-linker could facilitate self-healing of the polymer at 50 °C. Surprisingly, while small molecule boronic esters are susceptible to hydrolysis, these vitrimers could be immersed in water overnight without any changes in mass or mechanical properties.

Leibler et al. introduced these dioxaborolane cross-linkers into commodity thermoplastics to prepare catalyst-free vitrimers (Fig. 3.8b) [73]. PMMA and polystyrene (PS) vitrimers were prepared by incorporation of dioxaborolane-functionalized monomers during polymerisation, and cross-linked *via* metathesis with a *bis*-dioxaborolane. The PMMA vitrimers had stress relaxation time of ~35 to 1300 s at 160 °C, viscosity activation energy of ~76.7 kJ mol⁻¹, and could be molded at 200 °C under 12 bars in only 15 s. High-density polyethylene (HDPE) vitrimers were prepared by reactive grafting of maleimide-dioxaborolane to

the as-formed polymer before cross-linking. In all the above examples, the vitrimers possess similar T_g to the original thermoplastics and could be reprocessed several times by extrusion or compression- or injection-moulding, but they showed better solvent and creep resistance even at higher temperatures. Nicolay's group followed up with demonstrations that reactive grafting of dioxaborolane functional groups could be achieved by nitroxide radical coupling to HDPE [112] and radical thiol-ene addition to polybutadiene [113].

Boroxines are formed from dehydration of boronic acids, and thus can also undergo similar dynamic B–O exchange reactions. Guan et al. synthesised boroxine networks (Fig. 3.8c) with ≥89% of boroxine (~11% unreacted boronic acid) but found that these were brittle; addition of 4-undecylpyridine (1:1 ratio, coordinated to boroxine) as plasticiser resulted in strong and malleable vitrimers, which exhibited relaxation times of ~100 s at 75 °C and Arrhenius flow ($E_a \sim 79.5$ kJ mol⁻¹), with $T_v \sim -0.5$ °C [74]. In addition to reprocessing, the monomers could be recycled by boiling in water. This work paved the way for further explorations into N-coordinated boroxine vitrimers networks, such as dual-dynamic covalent networks with imine-coordinated boroxines (discussed in Section 3.6.1) [114,115].

Silyl ether (Si–O) exchange

In addition to B–O bonds, Si–O bonds can also be harnessed in vitrimer chemistry. Guan and co-workers reported the first example of a silyl ether exchange-based vitrimers in 2017 (Fig. 3.9a(i)) [37]. Similar to their study on boronic esters [111], the authors showed that bisalkoxysilane cross-linkers bearing a γ -N atom possessed 3 orders of magnitude faster exchange than the corresponding γ -C cross-linker in small molecule studies. When PS containing 9 mol% hydroxy groups was reacted with these cross-linkers (0.75 mol% wrt hydroxyl on PS), the *bis*- γ -N cross-linked vitrimers exhibited a shorter stress relaxation time at 180 °C (260 s) in comparison to the γ -C cross-linked vitrimers (779 s). Similarly, *bis*- γ -N cross-linked vitrimers possessed lower $E_a \sim 81$ kJ mol⁻¹ and $T_v \sim 47$ °C than the *bis*- γ -C cross-linked vitrimers ($E_a \sim 174$ kJ mol⁻¹, $T_v \sim 117$ °C).

In the above study, excess hydroxyl groups in the PS enabled associative exchange with the cross-linkers but could also participate in undesired side reactions at elevated temperature such as dehydration. These limitations were addressed through direct silyl ether metathesis in 2019 reported by the same group [116]. PE containing 6 mol% trimethylsilyloxy groups was cross-linked with *bis*(methoxydimethyl)silyloctane *via* silyl ether metathesis at 80 °C with camphorsulfonic acid as catalyst (Fig. 3.9a(ii)). The resulting vitrimer exhibited stress relaxation time of 130 s at 170 °C, with calculated $T_v \sim 45$ °C. Despite the relatively low T_v , the vitrimer showed better creep resistance at 80 °C compared to the linear polymer; it also transitioned into a rubber state above $T_m \sim 93$ °C, while the linear polymer flowed freely. The vitrimer had high thermal stability (minimal loss below 400 °C) due to the lack of free hydroxyl groups, and could be reprocessed at 150 °C at least 3 times with mechanical properties and gel fractions remaining almost constant.

Lu and co-workers harnessed the silyl ether motif to develop a vitrimers with the highest known T_g to date [117]. The authors designed a benzoxazine resin (P-mdes) with high density of

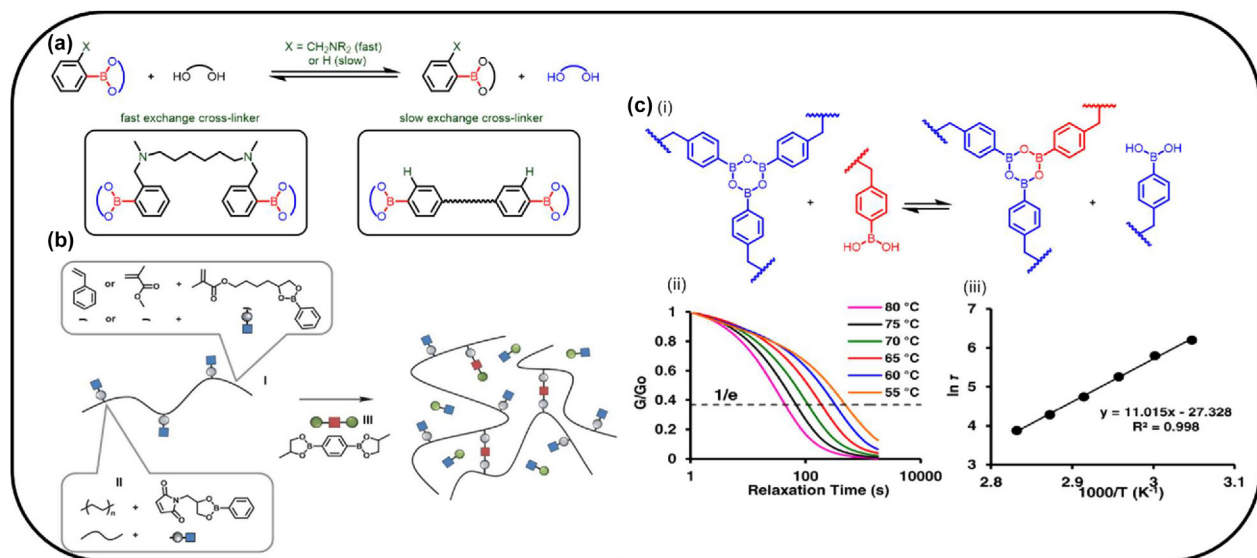


FIGURE 3.8

(a) Manipulating the kinetics of dynamic dioxaborolane exchange by fine-tuning the neighbouring group [111]. (b) Synthetic scheme of vitrimers. (i) Synthesis of copolymers that contain pendant dioxaborolanes by using functional monomers. (ii) Reactive processing (grafting of dioxaborolanes) of commercial thermoplastics. (iii) Metathesis *via* the cross-linking of polymers. This figure is reproduced from Ref. [73] with permission from American Association for the Advancement of Science. (c) (i) Design of boroxine-based thermoset polymers *via* boroxine exchange mechanism to achieve its polymer network. Malleability study of the network (ii) Stress relaxation tests at various temperatures and (iii) Arrhenius plot with linear fit [74]. Reproduced with permission from Ref. [74]. Copyright 2018, American Chemical Society.

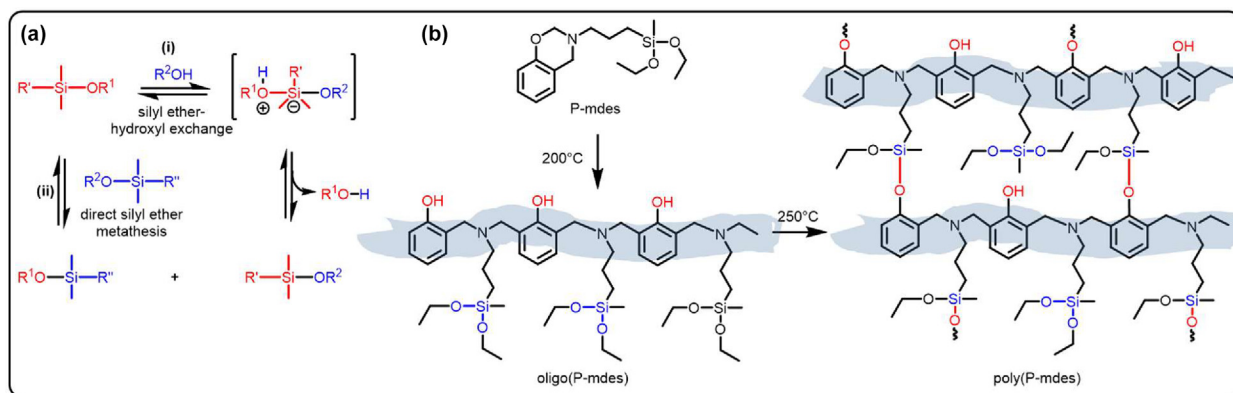


FIGURE 3.9

(a) Silyl ether exchange *via* (i) silyl ether-hydroxyl exchange with a free alcohol [37] or (ii) direct silyl ether metathesis [116]; (b) Synthesis of benzoxazine poly(P-mdes) with $T_g \sim 301$ °C [117].

dynamic Si-O-Ph crosslinks (Fig. 3.9b), resulting in a polymer with high $T_g \sim 301$ °C and high thermal stability up to ~ 396 °C. This polymer could be reprocessed under 10 MPa at 220 °C for 2 h, maintaining >75% of its original tensile strength after 3 cycles. While the polymer could tolerate immersion in different solvents at 50 °C for 24 h, it could be recycled to its monomer by treatment in acid under those conditions.

Disulfide (S-S) bond exchange

The dynamic covalent character of disulfide bonds has been exploited in the synthesis of vitrimers. Generally, most studies have indicated that the self-healing properties of vitrimeric materials with aromatic disulfide bonds are promoted by the radical-mediated reactions [118] instead of metathesis (Fig. 3.10a). For

instance, spectroscopic studies conducted by Nevejans et al. have revealed the mechanism of spontaneous aromatic disulfide exchange to involve the homolytic cleavage of the disulfide bond followed by the radical transfer of sulfur-containing radicals [119]. When a nucleophile such as triethylamine or tri-*n*-butylphosphine (TBP) is added as catalyst, the reaction proceeds also *via* thiolate anions, generated by reduction of the disulfides. Thus, both radical-mediated and thiol-mediated exchange reaction occurs simultaneously. In addition, a higher nucleophilicity may also favour the formation of these sulfur-based anions to promote disulfide exchange.

Based on aromatic sulfide as the dynamic moiety, Odriozola and co-workers synthesized epoxy vitrimer materials from inexpensive and commercially available precursors diglycidyl ether

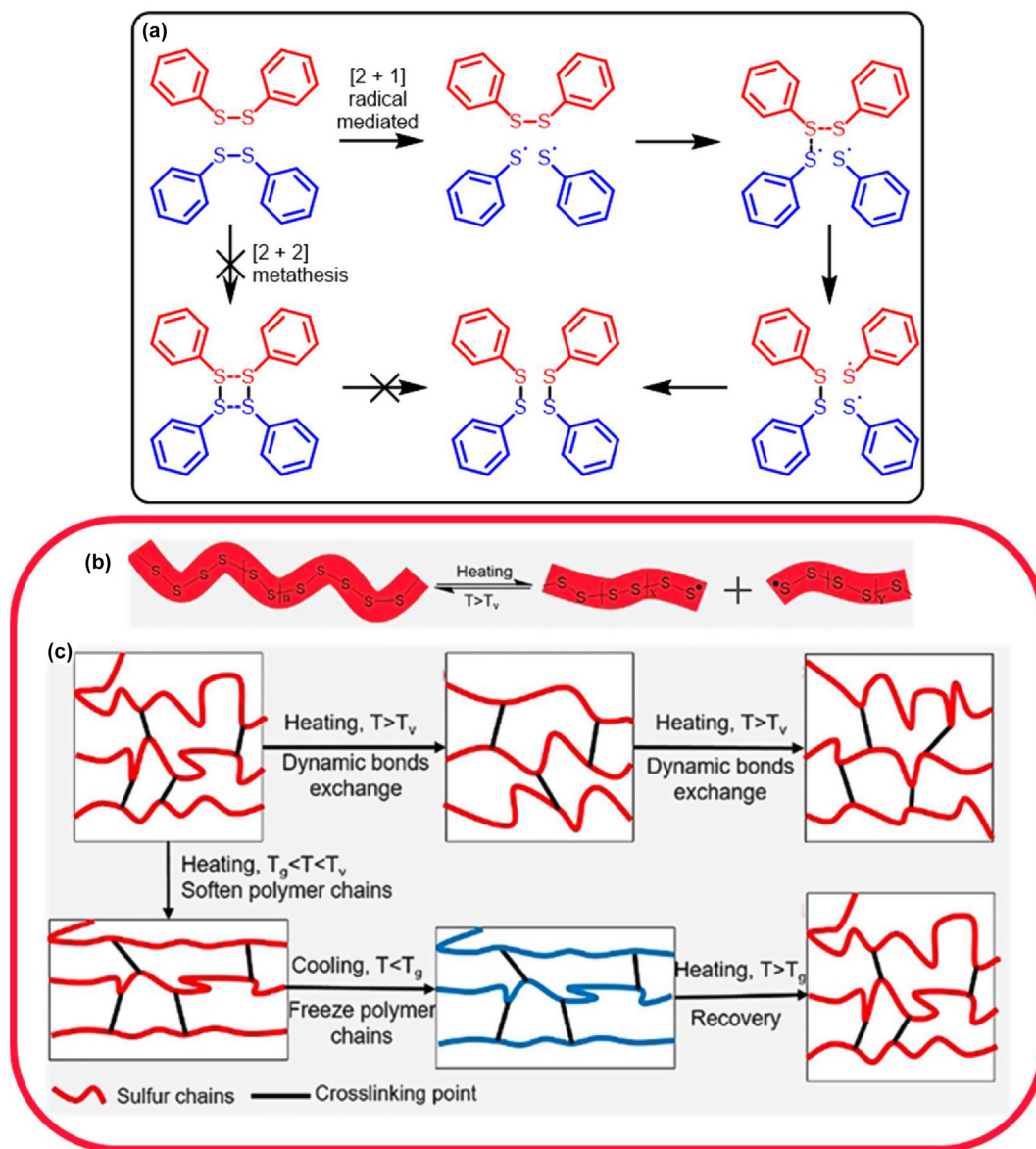


FIGURE 3.10

(a) Schematic representation of a [2+1] radical mediated reaction mechanism for the cross-linking of aromatic disulfides. The [2+2] metathesis mechanism is highly unlikely based on the lack of evidence to indicate a possible metathesis transition state. (b) Schematic illustration of non-aromatic disulfide bond exchange reaction and (c) the effect of polymer structure changes on the dynamic property of the polymer network. This figure is reproduced from Ref. [121] with permission from Wiley.

of bisphenol A (DGEBA) and diethyltoluenediamine (DETDA) with 4-aminophenyl disulfide (4-AFD) as the cross-linker [75]. The authors reported that such a novel vitrimer exhibited rapid exchange reactions with fast relaxation times from 180 min at 130 °C to 20 seconds at 200 °C, and with a sufficiently low Arrhenius activation energy (55 kJ mol⁻¹). More importantly, the hypothetical T_v value of the vitrimer (-13 °C) is lesser than its T_g (127 °C) highlighting the nature of a rapid disulfide exchange reaction associated with the epoxy vitrimer. Good reprocessing, repairing, and recycling properties are also reported which are not possible with conventional epoxy composites after the curing process. Such properties would greatly favour the use of the epoxy vitrimer in industrial applications, including fiber-reinforced polymer composites (FRPCs). Another disulfide-

based epoxy vitrimer was also used by Odriozola and co-workers to investigate its mechanochromic properties *via* mechanical stress with changes in time and temperature [120]. Mechanochromism of the vitrimer was evident either by hitting it with a hammer or grinding with a mortar at room temperature. In both instances, an immediate green colouration was observed and disappeared gradually after the vitrimer was left alone for 24 h. The mechanically assisted excision of the aromatic disulfide crosslinks resulted in the formation of sulfenyl radicals with a characteristic green coloration upon hammering or grinding. When the epoxy vitrimer was hit with a hammer and placed in an oven at 150 °C, the disappearance of the green colouration was more rapid and lasted in less than 30 seconds. The similar effect of colour disappearance was attributed to the radical-

mediated exchange mechanism of the sulfenyl radicals in the polymeric network and would accelerate when heated above its T_g -value.

Non-aromatic disulfides can also be used as cross-linkers in vitrimeric materials. Yan et al. synthesized an inverse vulcanized sulfur-polymer network that is capable of thermal reprocessing and plasticity (Fig. 3.10b and c) [121]. The reshaping is possible by heating the fully cross-linked vitrimer film to its T_g value (45.6 °C), and its desired shape can be locked with the freezing of its polymer chains. In a different study, Tsuruoka et al. reported the infinite possibility of fine tuning the mechanical properties of the polymer synthesized *via* the fusion of two heterogeneous cross-linked polymers (CLPs) in varying mixing ratios and using bis(2,2,6,6-tetramethylpiperindin-1-yl)disulfide (BiTEMPS) as a crosslinker for dynamic covalent bonding [122]. More importantly, self-healing and reprocessing properties are also evident with the synthesized polymer that exhibit dynamic sulfide exchange at various mixing ratios of the CLPs crosslinked by BiTEMPS and conventional covalent bonds between 2:1 to 5:1.

Besides the disulfide (S–S) bond exchange, the light-driven and wavelength-controlled reversible exchange between disulfides and diselenides (Se–Se) to form Se–S bonds is an example of a dynamic metathesis and is important for controlling the composition of the mixture of light-sensitive vitrimers at various wavelengths. Fan et al. employed the aforementioned dynamic metathesis with di-(1-hydroxylundecyl)-diselenide and diphenyl disulfide as the precursors [123]. The manipulation of the wavelength of the irradiated light is critical for metathesis of the diselenide and disulfide compounds under UV irradiation to form Se–S bonds, while visible-light irradiation can drive the reversal of the exchange reaction with the breakage of Se–S bonds.

Vitrimers with multitype dynamic exchange bonds

In the previous Sections, we have discussed the different types of dynamic covalent exchange bonds used in vitrimers. Vitrimers could also contain more than one type of dynamic exchange bond, whether covalent (Section 3.6.1) or non-covalent (Section 3.6.2), conferring several advantages to the network. These include more rapid stress relaxation [114,115,124], increased creep [125] or stress resistance [126,127], and response to additional stimuli or even orthogonal control of dynamism (Section 4.5).

Vitrimers with dual dynamic covalent exchange bonds

The imine and boroxine chemistry of vitrimers were described in the previous subSections (3.2.2 and 3.5.1 respectively). Vitrimers possessing both of these dynamic exchange bonds are known as dual-dynamic networks. For instance, Delpierre et al. synthesized catalyst-free non-isocyanate polyurethane (NIPU) vitrimers with boroxine/iminoboronate-based cross-linked double networks [114]. The N-coordinated boroxine could reversibly exchange under ambient conditions, governed by humidity. At 45% relative humidity for 48 h, Young's modulus was at 502 MPa with 3.36% strain at break and 9.8 MPa stress at break, highlighting its good self-healing property. At high temperatures both the B–O boroxine bonds and C=N iminoborate bonds could simultaneously exchange. The dual-dynamic network thus ensured

excellent reprocessability (80 °C) and mechanical resistance properties (Young's modulus of 551 MPa with 3% strain at break and 11 MPa stress at break, when neat). Utilising the same boroxine/iminoboronate cross-linker, Yang et al. prepared a polybutadiene-based vitrimeric material [115]. Due to the hydrophobic polybutadiene backbone, this vitrimer was resistant to humidity, and only exhibited Arrhenius-dependent exchange with $E_a \sim 58 \text{ kJ mol}^{-1}$. Upon heating, both the B–O boroxine bonds and C=N iminoborate bonds simultaneously exchange, resulting in sharp decrease in relaxation time (1.46 s at 100 °C). Consequentially, the polymer material prepared with 12% cross-linker possessed excellent properties such as strong malleability (12.35 MPa tensile strength), high reprocessing upon recycling over multiple times, and thermal-induced shape-memory behaviour with restoration of the initial entropy elastic shape upon heating.

In another instance, Chen *et al.* synthesized a dual dynamic epoxy vitrimer based on two simultaneous exchange reactions – disulfide metathesis and carboxylate transesterification (Fig. 3.11) [124]. Using 4,4'-dithiodibutyric acid (DTDA) as the disulfide-containing carboxylic acid and DGEBA as the epoxy moiety, the vitrimer was formed with TB as transesterification catalyst. Consequentially, the dual dynamic epoxy vitrimer possessed a rapid stress relaxation time at 180 °C that was 28 and 122 times faster than that of the single-disulfide (without TBD) and single-ester (by replacing DTDA with sebacic acid) vitrimers respectively. In addition, the highly efficient rearrangement of the polymer chain network within the dual dynamic epoxy vitrimer can impart the property of plasticity into cross-linked polymers and facilitate exchange reactions on the timescale that are more rapid than the single dynamic vitrimer. The dynamic properties of the novel epoxy vitrimer are enhanced by the dual exchangeable cross-linking properties of both disulfide bonds and carboxylate ester bonds, thereby promoting a more rapid rearrangement of polymer chains with a lower temperature of malleability (65 °C) than the single vitrimers, and also much lower than that of many permanently cross-linked polymers or vitrimers.

Vitrimers with additional non-covalent interactions

Instead of dual dynamic networks, vitrimers may also comprise dynamic covalent exchange bonds with non covalent interactions such as metal coordination or hydrogen bonding.

Introduction of some permanent cross-links into vitrimers has been explored as a *viable* solution to improve creep resistance [128,129]. However, introduction of too many permanent covalent cross-links would render the polymer unrecyclable. For example, Torkelson and co-workers showed that while transesterification vitrimers with up to 40 mol% permanent cross-links could achieve full reprocessability with >65% creep resistance, increasing the amount of permanent cross-links to 60 mol% resulted in poor reprocessability [128]. As such, an alternative solution is to increase the stability of the dynamic covalent bonds through metal cation coordination. Recently, Wang and co-workers explored such a strategy in polyimine-metal complex vitrimers [125]. A metal content of up to 5 mol % of the polyimine-metal complex vitrimer is resulted in higher T_g values (132–170 °C for M = Cu(II), Fe(III), or Mg(II)) than the

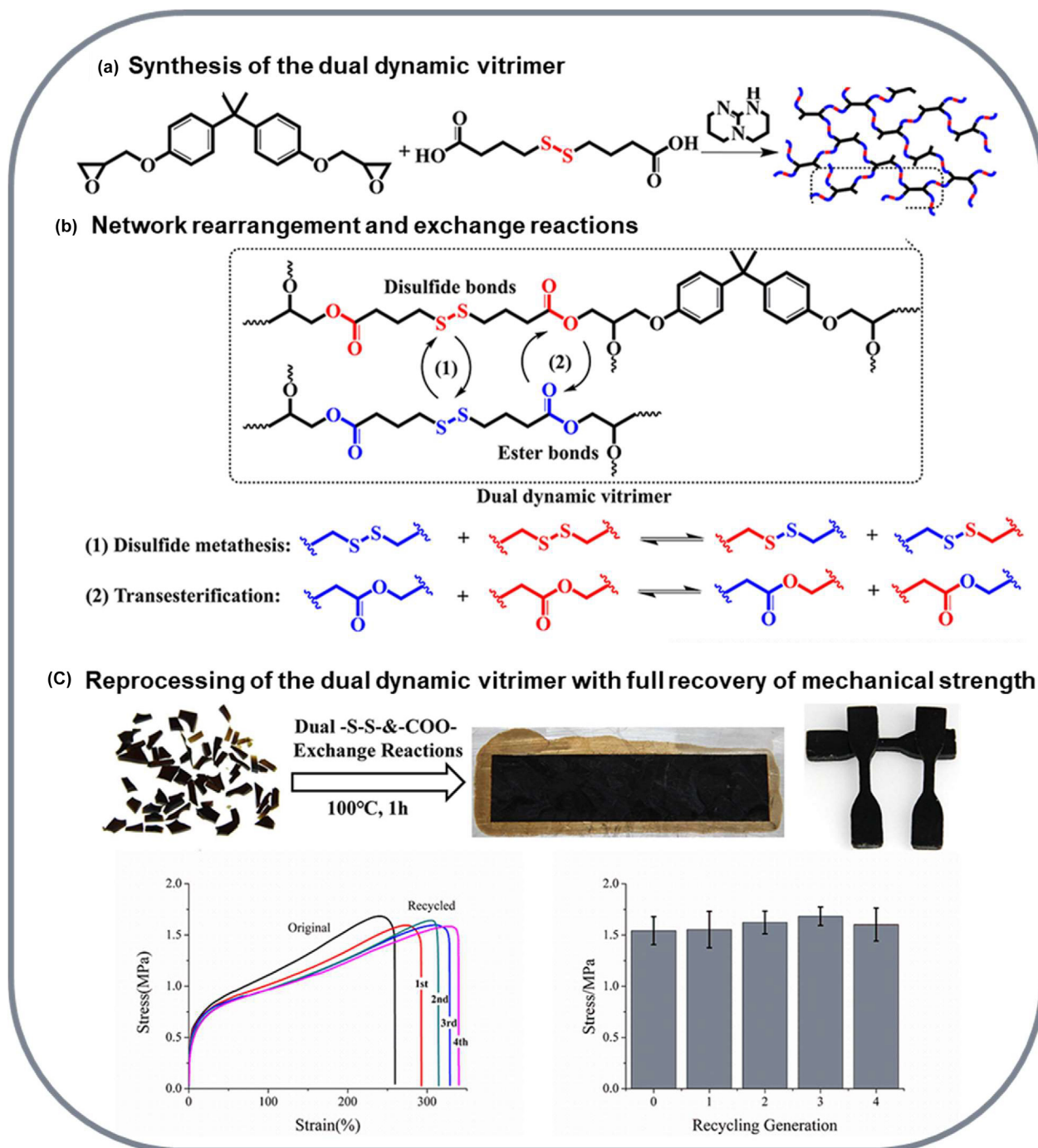


FIGURE 3.11

(a) Synthesis of the dual dynamic vitrimer with a cross-linked structure by reacting DGEBA and DTDA in the presence of the transesterification catalyst TBD at 180 °C for 4 h. (b) Simultaneous occurrence of disulfide metathesis and carboxylate transesterification to cause the rearrangement of the polymeric chains in the dual dynamic vitrimeric network. (c) Successful reprocessing of the dual dynamic vitrimer by hot pressing. The stress–strain and stress–recycling graphs show the full recovery of the mechanical strength after four cycles. This figure is reproduced from Ref. [124] with permission from American Chemical Society.

polyimine in the absence of a coordinating metal center due to a greater crosslink density of the complex vitrimer and the rigidity of its segmental chain. Creep reduction was also dependent on the metal loading as well as the stability of the coordinated metal complex.

Metal coordination can also act as sacrificial bonds. Chen et al. prepared dynamic dual cross-linked elastomeric vitrimers by incorporating boronic ester bonds and sacrificial Zn(II)–O

coordination bonds into a commercially available epoxidized natural rubber (ENR) (Fig. 3.12) [126]. A dithiol-bearing boronic ester was used as a cross-linker with ENR. The elasticity is attributed to the presence of the dynamic covalent boronic ester bonds, while the sacrificial bonds are able to reversibly dissociate and associate to allow energy dissipation. As a result, the elastomeric vitrimers formed from ENR cross-linked with the dithiol-bearing boronic ester ranging from 1 to 10 wt% are able

to achieve 80% or more recovery ratios of the mechanical properties (elongation at break and Young's modulus).

Sacrificial hydrogen bonds may also be incorporated into these networks to further improve the mechanical properties of the vitrimers. Liu and co-workers have successfully prepared a vitrimer that incorporated sacrificial hydrogen bonds and exchangeable β -hydroxyl ester linkages into the vitrimeric network [127]. These bonds and linkages were realized with the use of sebacic acid as a cross-linker with ENR, and to initiate simultaneous grafting with *N*-acetylglycine (NAG) *via* the chemical reaction between epoxy and carboxyl groups. With various wt % ratios of NAG relative to ENR up to 8 wt%, the recovery ratios of the original mechanical properties (breaking strain and Young's modulus) are extremely high with percentage values $\geq 90\%$. Moreover, stress-strain curve analyses have also indicated good retention of the mechanical properties after single, double and triple successive recycling of the vitrimer with 4 wt% NAG relative to ENR. These excellent results of the experimental mechanical properties are due to the sacrificial and reversible nature of the hydrogen bonds to dissipate significant mechanical energy during stretching, while elasticity is governed by the presence of the exchangeable ester covalent cross-linkages.

Depending on their respective activation energies, the dynamic covalent bond could be the sacrificial bond instead of

the hydrogen bond. A study conducted by Zhang et al. investigated the hierarchical dynamics of a transient polymer network using poly(*n*-butyl acrylate) (PBA) cross-linked by orthogonal dynamic bonds with the use of rheology and solid-state NMR spectroscopy [130]. The T_g value of the pyrimidinone derivative with dynamic covalent boronic ester bonds from diboronic ester (DE) (PBA-UPy-DE) as the cross-linker (-17.3 °C) is found to be lower than the pyrimidinone derivative with the use of *p*-divinylbenzene (DVB) as the permanent covalent cross-linker (PBA-UPy-DVB, -19.3 °C). Moreover, rheological studies revealed that the dynamic covalent B–O bonds exchange at much lower temperatures than hydrogen bond interactions between the UPy dimers, such that PBA-UPy-DE network has a lower activation energy (35.6 kJ mol $^{-1}$) than both the PBA-UPy-DVB and PBA-UPy networks (both 43.6 kJ mol $^{-1}$).

Synergetic effects from the dual crosslinking systems will significantly contribute to the desired properties of vitrimers, such as enhanced mechanical strength, and improved creep and solvent resistance. To design an effective dual cross-linked dynamic system, two reversible bonds bearing large different activation energies (active temperatures) will be attractive. It would be advantageous to have greatly differing active temperatures in a single material to intensify the dimensional stability at the service temperature. Given the external stimuli-responsiveness pro-

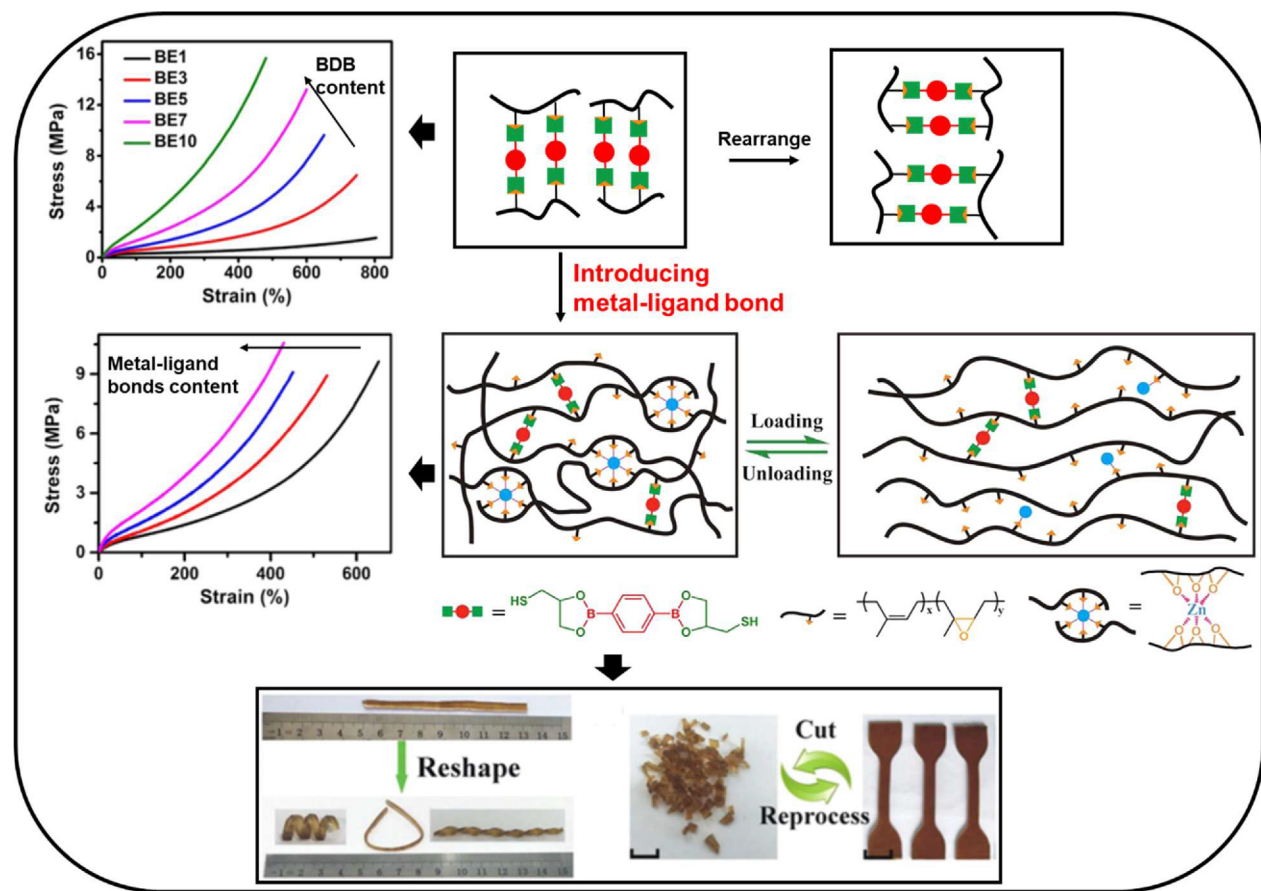


FIGURE 3.12

Schematic diagram showing the reversible breaking and reforming of Zn^{2+} -O coordination bonds during the loading and unloading tests. The epoxidized natural rubber (ENR) has ENR x - y networks with dual cross-links of dynamic boronic ester bonds and noncovalent Zn^{2+} -O coordination bonds. This figure is reproduced from Ref. [126] with permission from American Chemical Society.

file of vitrimeric materials, it will be appealing to introduce two exchangeable bonds that respond to distinct stimuli respectively, allowing the resultant vitrimers to tune properties in an on-demand fashion. Beyond that, the good compatibility of the two crosslinking systems is necessary as well.

Design strategies of vitrimers

In this Section, we have discussed a variety of dynamic covalent bonds and their applications in vitrimers(-like) materials. Here, we would like to highlight some of the recurring themes to tune the properties of the vitrimers.

Choice of dynamic covalent bond. There are two main strategies to develop a vitrimer: (1) employing new polymers that involved exchangeable bonds to generate dynamic crosslinking networks with rearrangeable backbones; and (2) introducing crosslinkers into commercially available prepolymers, such as incorporating a fraction of dynamic covalent cross-links into thermoplastics. In both strategies, the choice of dynamic covalent bond is key to the control of vitrimers properties (see Table 3.1). For instance, if a room temperature malleability, or a low T_v , is desired, dynamic covalent bonds with low E_a , such as boronic esters, imines and ketoenamines, should be chosen. In contrast, if the vitrimer should only be malleable at higher temperatures, then dynamic covalent bonds with high E_a , such as esters, carbamates, silyl ethers and triazolium salts, should be incorporated.

Another key decision is in the compatibility of the polymer backbone and the cross-linker, especially for thermoplastic-based vitrimers. For example, for thermoplastics with pendant hydroxyl groups can easily be functionalized for ester-type, acetal, boronic ester and silyl ether cross-links; while those with pendant amine groups can be functionalized for imine and ketoenamine cross-links. If the polymer backbone has no reactive groups, then the cross-linkers can be installed by reactive grafting [73,112,113]. Similarly, it is important to select a dynamic covalent bond suitable for the polymer application, such as triazolium, pyridinium or anilinium salts for polyionic vitrimers (Section 3.4).

Yet another possibility is to have more than one type of dynamic covalent bond. The vitrimers produced with this strategy could possess higher malleability and more rapid stress relaxation than single exchange bond vitrimer. Temperature-tunable malleability and shape memory behavior can be achieved by using dynamic covalent bonds with different activation energies, thus when the vitrimer is heated, only the crosslinkers with lower E_a can exchange initially, while both crosslinkers can exchange once the temperature is sufficiently high. However, care must be taken in the selection of the dynamic covalent cross-linkers to ensure that there is no cross-reactivity between the crosslinkers. For example, introducing imine crosslinks into epoxy-acid vitrimers with pendant hydroxyl groups would result in the hydrolysis of the imine crosslinks. In addition to orthogonal crosslinks, cooperative crosslinks can be used such as in the boroxine/iminoboronate examples, where the N-coordination of the boroxine lowers its E_a to enable room-temperature exchange.

Having chosen the polymer backbone and the cross-linker, fine-tuning of the vitrimers properties can be achieved through the following strategies:

Maintaining a constant crosslink density. Conventionally, vitrimers are based on dynamic associative exchange reactions. One strategy to promote the associative mechanism in the vitrimer is to add an excess of free nucleophile in the polymer network; transesterification and transcarbamation vitrimers with pendant hydroxyl groups are key examples of this [17,26]. However, these reactive pendant groups can be easily oxidized, resulting deterioration of the polymer properties and also reduced recyclability of the vitrimer. Hence, other approaches to maintain crosslink density are desirable.

Although there are many examples of vitrimer(-like) materials with dissociative mechanism, it should be noted that their equilibria lie towards bond formation and the cross-link density remains unchanged with temperature. This consideration can be incorporated through judicious selection of cross-linkers to minimise the dissociative mechanism, such as by using less hindered substituents in blocked isocyanates [89], or by choice of counter-anion in polyionic systems [28,108].

Another approach to maintain constant crosslink density without the requirement for super-stoichiometric nucleophiles is by using dynamic covalent crosslinks which undergo exchange *via* direct bond metathesis. Examples of these chemistry include ureas [64], imines [96], dioxaborolanes [73], and silyl ethers [116].

Lowering the reprocessing barrier. To lower the stress-relaxation activation energy, one method is to introduce and tune the reactivity through the use of different catalysts or additives [76,77,99]. While catalysts help to speed up the kinetics of dynamic bond exchange, they can also increase the side reactions of the polymer, or leach out of the polymer. One strategy for developing catalyst-free vitrimers is to tune the cross-linkers so as to lower the E_a . Using the transesterification exchange as an example, one could either introduce an electron-withdrawing group to the carboxylic acid functionality [34] or lower the pK_a of the alcohol functionality [79] to increase its reactivity (Section 3.1.1).

Alternatively, several examples of internal catalysis through neighboring group participation have also been demonstrated [30]. These include acid activation of phthalate monoesters towards transesterification [78], hydroxyl activation of urethanes towards transcarbonylation [26], and amino activation of dioxaborolanes [111] and silyl ethers [37] towards hydroxyl attack, albeit with possible changes in mechanism. In fact, Du Prez and co-workers postulate that Leibler's original epoxy-acid systems could also be described as internally activated β -hydroxyl esters [30], although catalyst is still required for this system. While the obviation of catalyst is advantageous, the need for excess reactive groups poses stability issues as discussed above.

Increasing the stability and reprocessability. While vitrimers supersede traditional thermosets in their ability to be reprocessed, they may lose some of their mechanical properties after a few cycles. With respect to dimensional stability, an often applied strategy is to introduce a percentage of permanent cross-links [128,129], stronger dynamic cross-links [124,125] or weaker stress-relieving cross-links [126,127] to the system (Section 3.6). For the former, it should be noted that there is a fine balance between the percentage of dynamic and permanent cross-links to maintain good recyclability while reducing creep; Torkelson

and co-workers have described theory to quantitatively predict the optimal percentage of dynamic to permanent cross-links using a modified Flory–Stockmayer theory which should prove useful to vitrimer design [128].

As for hydrolytic stability, incorporation of hydrophobic backbone or groups will help to protect moisture-sensitive moieties in the vitrimer such as imines [96,97], or iminoboronates [115] from hydrolysis. Minimizing the number of reactive groups in the vitrimer can also increase the lifespan of the vitrimer; to this end, it is favorable to employ exchange reactions based on metathesis instead of attack from pendant moieties [95,116].

There are multiple examples of these design considerations being implemented across many of the dynamic covalent bond motifs, and it is our hope that these insight can be overarching design strategies for the design of novel vitrimers with both high malleability and stability.

The emerging applications of vitrimers

Vitrimers have aroused great enthusiastic interest in myriad fields, such as functionally tunable devices, car industries, soft robots, and aerospace [12,62,131–133]. Generally, vitrimers can be prepared by two methods. Most vitrimers were developed by using new polymers that involved exchangeable bonds between the backbones to generate dynamic crosslinked networks. Another more universal vitrimeric preparation method has also been developed, in which, crosslinking agents were introduced into commercially available and inexpensive prepolymers (*i.e.* thermosets and thermoplastics) to form dynamic crosslinking networks with a significantly improved performance. Taking advantage of the reversible exchange of covalent motifs upon heating, vitrimers with changeable topologies displays a variety of functionalities, including recycling, self-healing, welding, stress relaxation, and multiple shape changing, paving the way for numerous opportunities in engineering for real applications. Moreover, introducing multi-functional moieties into polymer networks also generates new advanced vitrimeric materials that respond to multi-triggers (such as light, pH and redox agent).

Vitrimers for material circulating applications

Thermoset materials, such as polyurethanes, formaldehyde resins, and epoxy resins, though extensively used in industry and our daily life, have resulted in growing environmental concerns due to their high stability. Inappropriately managed thermoset waste sometimes end up in the oceans, where their durability prevents them from being biodegraded, and their presence often adversely affects aquatic life [134]. In best-case scenarios, thermoset waste management usually involve either incineration, which releases carbon dioxide and other pollutants into the atmosphere, or the landfill, where they persist in for a long time due to their lack of biodegradability. More significantly, in the long term, plastics are made from petroleum feedstock, which though abundant at present, is still a finite resource. Hence, converting these unrecyclable thermoset materials and/or wastes into recyclable materials for reuse is a valuable step for the development of sustainable growth. This Section discusses how vitrimers and vitrimerisation can be a *viable* solution to this problem.

Recycling of vitrimers

Vitrimers are potentially able to function as a type of recyclable thermosets. There are two main mechanisms of vitrimer recycling, namely hot press, and solvent dissolution (Fig. 4.1) [135–140]. In most cases, vitrimers can be reprocessed by hot-pressing their fragments or debris into new robust integrated film for reusing due to their dynamic covalent bonds [12,37,116,135]. Du Prez's group also reported an imine based vitrimer which could be reprocessed by extrusion [141]. The reformed vitrimer specimen contains a continuous network architecture analogous to the fresh sample, and exhibits comparable mechanical behaviours. The second vitrimer reprocessing system is solvent depolymerization of the polymer network into monomers or oligomers. These fragments can then be re-polymerised to generate new vitrimer samples after solvent evaporation. For instance, Evans and co-workers developed a poly(ethylene oxide)-based network containing dynamic boronic ester bonds for ion transport and electrolyte applications [142]. The mechanical properties and conductivity of the vitrimer were found to be dependent on the concentration of (trifluoromethanesulfonyl)imide (LiTFSI). This polymer could then be dissolved in a solvent, and recycled back to its original monomers, which could be repolymerised to generate a new vitrimer with comparable conductivity. Another example was reported by Feng et al., using 4-aminophenyl disulfide as a multifunctional amine crosslinker in the amine-epoxy polymerization system [143]. In this system, both heating and pressing could trigger the exchange of disulfide bond, resulting in the rearrangement of the network. Both hot pressing and solution processing could reprocess the vitrimer to obtain mechanical properties comparable to the original sample. Other examples of solution processing include the boroxine based vitrimers reported by Guan [74], and the PDK vitrimers reported by Helms [68].

Converting conventional thermosets into vitrimers for recycling applications

Conventional thermosets sometimes contain dynamic covalent bonds which exhibit high stability even at high temperatures due to their high activation energy. A novel strategy to enable their recycling is to apply the concept of vitrimers to them by introduction of a catalyst in a process called “vitrimerisation” by Manas-Zloczower and co-workers. In the first example, the group infused Sn(Oct)₂ catalyst into conventional polyurethane or epoxy-anhydride samples by swelling the polymers in a solution of the catalyst in dichloromethane at room temperature, or in dimethylformamide at 140 °C [144]. The vitrimerized samples could then be reprocessed up to two times by compression molding and extrusion, albeit with noticeable reduction in modulus and strength. In a later example, epoxy-anhydride thermoset was ball-milled with Zn(OAc)₂ to form metal-polymeric ligand complexes through solid-state mechanochemical reactions [145]. The resulting vitrimerized epoxy could be recycled at least three times with similar mechanical performance.

Ji et al. demonstrated that conventional liquid crystalline epoxy thermosets (LCETs) could be reprocessed even without addition of catalyst simply by allowing the polymer more time to relax under strain at high temperature [146]. This is known as the time–temperature equivalence principle. An unaligned

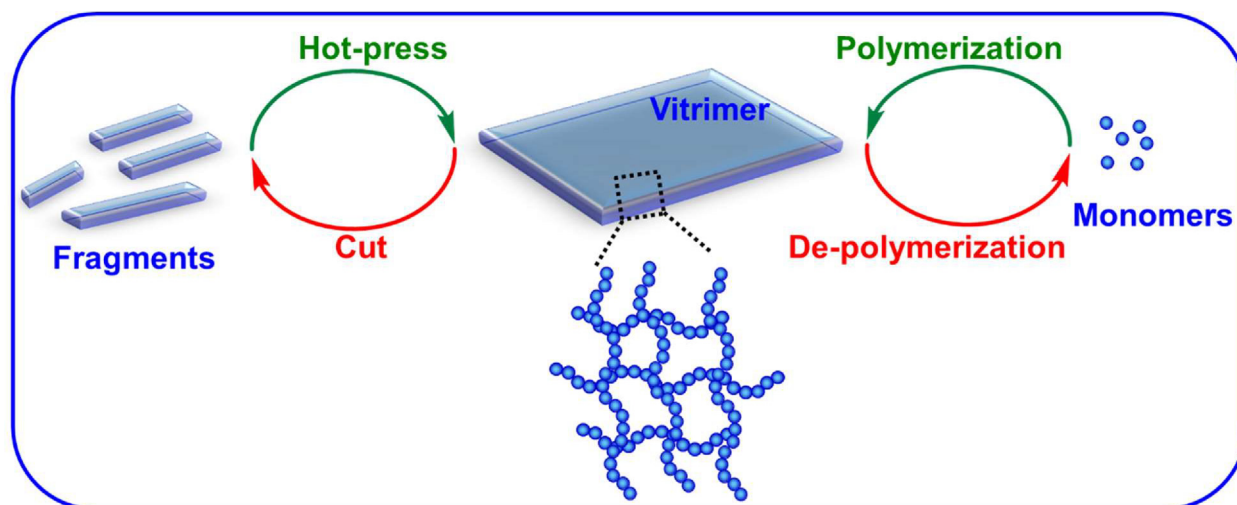


FIGURE 4.1

Schematic illustration of vitrimers recycling mechanisms.

epoxy-acid LCET was prepared and stretched by 30% at 180 °C for 2 h. In this process, transesterification occurred in the isotropic phase, leading to uniaxial alignment of the mesogens in the liquid-crystal phase upon cooling. This work stemmed from the group's previous finding that even conventional epoxy thermosets have T_v which are independent of catalyst loading [38]. The transesterification reaction ($E_a \sim 100 \text{ kJ mol}^{-1}$) simply occurs at a slower rate and thus requires higher temperature and longer time for reprocessing [147,148]. These findings are promising starting points for the recycling of current thermoset polymers, which may take many years to replace depending on industry's rate of adoption of new materials.

Vitrimers for self-healing and reusable adhesives applications

Polymer materials are vulnerable to damages from long-term wear and tear as well as external forces, leading to performance drop and potentially ending in catastrophic failures. As such, polymers with crack-healing capability are highly desirable for extending material lifetime by preventing fatal structural disintegration, mitigating material-waste problems, and reducing the overall cost. Different types of healing and welding can be achieved depending on the interface, such as identical polymer network surface self-healing (A-A fusion), incompatible polymer networks interfaces adhesion (A-B fusion), and different type of materials welding (Fig. 4.2).

Self-healing refers to the recovery of not just the external macroscopic shape of the material, but also its internal mechanical properties (such as modulus, mechanical strength, and toughness) [149–152]. The self-healing of identical vitimer debris (A-A fusion), can be ascribed to the presence of covalent adaptable bonds, which enables dynamic chain-exchange reactions and topology rearrangements under external stimuli. Garcia and coauthors indicated that the identical polymer network self-healing process underwent the following three steps (Fig. 4.2a) [150]. Initially, an adhesive process would take place with the genesis of a relatively weak 2D interfacial restoration. Chain-interdiffusion would then convert this interphase interaction into a volume interaction. Finally, the interphases disap-

pears, resulting in full healing of the material [150]. Theoretically, materials bearing the dynamic covalent bonds are able to self-repair indefinitely if the healing is controlled by reversible exchangeable motifs. To date, most examples of self-healing polymers are relatively soft materials, restricting their practical applications significantly. As such, self-healing vitrimers with high chain mobility, as well as an integrated cross-linked network, resulting in excellent self-healing property along with rigid mechanical properties, are of growing research interest.

Lei and co-authors studied the self-healing capability of poly-urea vitrimers (HTPUs) by using hindered urea bonds as the dynamic cross-link [153]. Upon heating, the speed of hindered urea bonds breaking and reforming is dramatically accelerated. When the temperature was further raised to 120 °C, the exchange rate was sufficiently high to activate the polymer chains' mobility and completely repair the scratches on the sample. Moreover, the repaired film possessed strong mechanical properties, being stretchable up to 200% strain without tearing, as well as lifting a 0.5 kg weight without breaking at the healed part. Another example of self-healing vitrimers using a dynamic polymer-polymer (P-P) interaction approach was reported by Chen and co-workers [154]. The boronic ester based vitimer displayed superior mechanical performances (*i.e.* tensile strength value of 65 MPa, and Young's modulus value of 2.1 GPa) compared to their small molecular crosslinked counterparts and corresponding thermoplastics. Upon heating, the material displayed fast self-repair behavior along with malleability and recyclability due to the well-dispersed dynamic covalent motifs between polymer chains.

To minimize undesired side reactions, the ideal healing materials should be repairable under mild conditions, which requires the dynamic exchangeable reaction to be relatively facile. However, the crosslinks of a robust material would preferentially employ more stable dynamic covalent bonds. This dilemma was resolved by integrating special exchangeable bonds to polymers, extending self-healing materials to thermal-sensitive devices applications, or materials with complex geometries. For

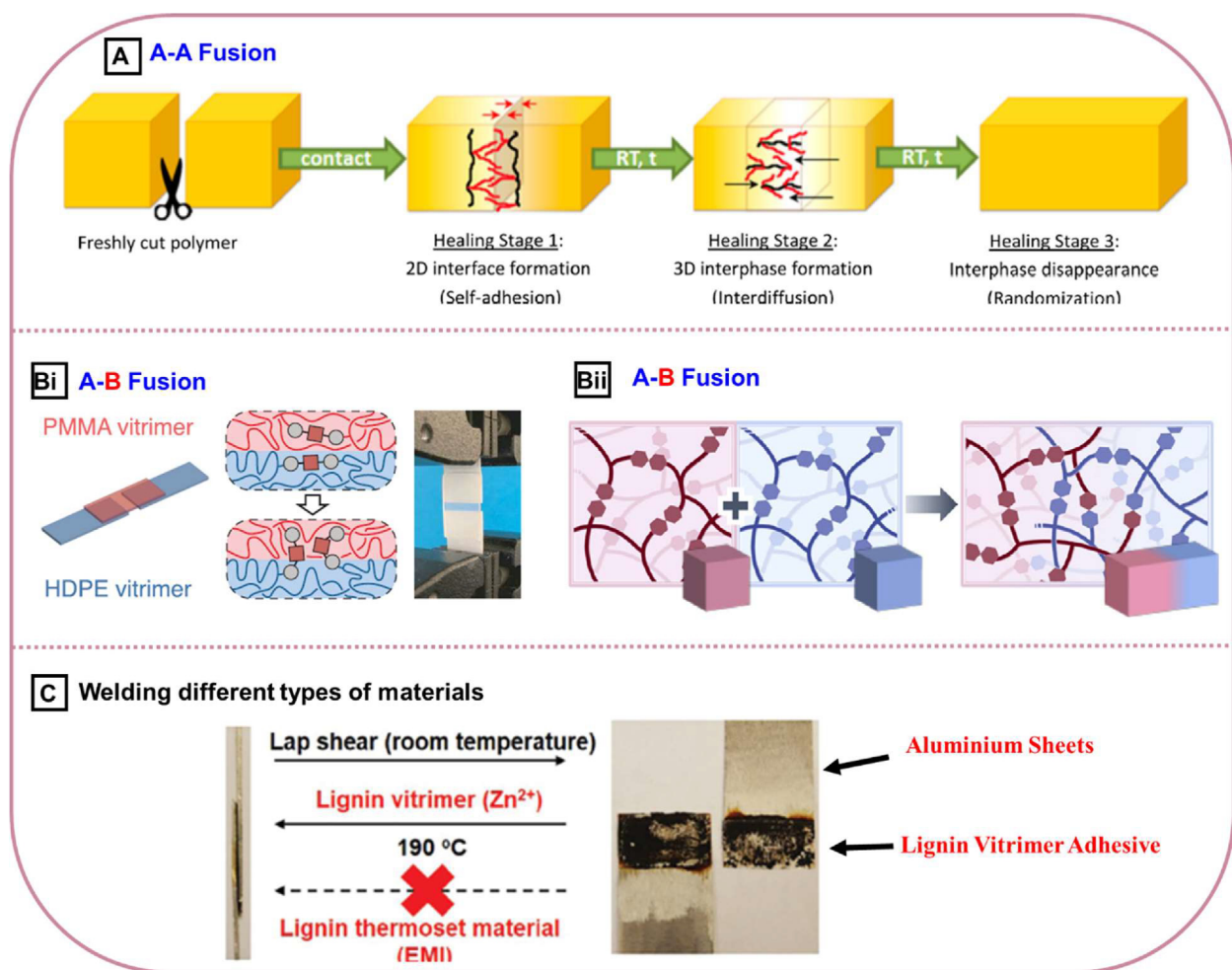


FIGURE 4.2

Schematic illustration of (a) A–A fusion [150], (b) A–B fusion [73,122], and (c) welding different types of materials [88] using vitrimers. Reproduced with permission [150]. Copyright 2016, American Chemical Society. Reproduced with permission [73]. Copyright 2017, American Association for the Advancement of Science. Reproduced with permission [122]. Copyright 2020, Wiley. Reproduced with permission [88]. Copyright 2018, Royal Society of Chemistry.

instance, Jäkle and co-workers utilized Lewis pairs (LPs) (*i.e.* electron-poor Lewis acids (LAs) and electron-rich Lewis bases (LBs)) as novel dynamic crosslinkers [155]. Transient polymer networks were formed between LA-containing PS and LB-terminated telechelic polydimethylsiloxane (PDMS). The mechanical properties of the transient polymer network could be tuned over a wide range by choosing an appropriate LP. Notably, due to the reversible LPs reactions, two edge touching pieces of the polymer networks could spontaneously rejoin at room temperature within around 2 weeks.

Effectively welding different polymeric materials is of great interest in various fields, including microfluidic devices, packaging, robotics, and electronics. However, due to the incompatibility of heterogeneous cross-linked networks, it is challenging to assemble them without tie layers. Interestingly, in some cases, the fusion of vitrimer networks with distinct structures (A–B fusion) can be achieved by modification of the network surfaces using particular dynamic moieties to promote the interface interactions (Fig. 4.2b). For example, Leibler and co-workers utilized the metathesis of dioxaborolanes to prepare vitrimers from different polymer substrates, including PMMA, PS, and even the

permanently cross-linked polyethylene (PE) (Fig. 4.2b(i)) [73]. Due to the presence of pendant polar dioxaborolanes, the heterogeneous polymer networks (such as PE and PMMA) showed some compatibility and adhesion at the first stage. Strong covalent bridges were later formed across the interface and the adhesion was further enhanced *via* the robust dioxaborolanes exchange reactions at 190 °C under 11 kPa pressure. The adhesion strength of the resulting PE-PMMA vitrimer reached around 11500 N/m after welding for 10 min, and exceeding the strength of pure PMMA vitrimer when the welding time was prolonged to 20 mins. Recently, Otsuka and co-workers developed a novel method to bond two distinct polymer networks using the thermal bond-exchange reaction of BiTEMPS (Fig. 4.2b(ii)) [122]. Due to the topological and exchangeable BiTEMPS moieties at the material interface, two different networks could be fused at the molecular level in the bulk material. The mechanical behaviors of the assembled bulk materials could also be adjusted by varying the component ratios.

The use of dynamic exchange reactions to induce strong surface interaction upon topology rearrangement are not only suitable to polymers, but also for other types of materials (such as

metal, wood, ceramic, and engineering plastics), as vitrimeric adhesives have the capability to weld onto the surface of other materials. Compared to traditional adhesives (*i.e.* epoxy resins, phenol–formaldehyde resins, organosilicons, and urea–formaldehyde resins), vitrimer adhesives possesses outstanding properties, including high transparency, strong adhesion, excellent mechanical properties, recoverability, as well as chemical resistance [156,157]. Zhang and co-workers demonstrated a fully bio-based epoxy vitrimer system (Se-EP/Oz-L) with high lignin content as a recoverable adhesive (Fig. 4.2c) [88]. This thermal-responsive vitrimeric adhesive displayed outstanding self-repairing and shape-changing properties. They demonstrated that this new vitrimeric adhesive showed similar lap-shear strength in the cohesive failure experiment with commercial epoxy-based glues for the binding of aluminum sheets. In contrast to common disposable adhesives, the vitrimeric adhesive gave the aluminum parts the ability to reversibly detach and re-bonded on demand, due to the robust transesterification exchange reactions at elevated temperatures. Another vitrimeric adhesive from dynamic polythiourethane (PTU) was prepared by introducing exchangeable thiocarbamate bonds [158]. The obtained transparent PTU adhesive possesses good water-resistance, reprocessability, and outstanding bonding property for different types of materials including glass, metal, and wood.

Vitrimers for shape memory and smart actuators applications

Shape memory polymers (SMP) is a unique class of cross-linked elastomer that features programmable shape morphing behavior under external stimuli, having great potential in applications including biomedical devices, smart actuators, robotics, electronic devices, and automation equipment. Generally, a polymer film with a dramatic variation of modulus with temperatures demonstrates great potential of becoming a thermal-responsive SMP. Traditional SMPs have dual-shape changing behavior. At a temperature above T_g , the polymer chain segment is activated to allow the deformation under external force, causing the reduction of system entropy. The deformed shape will temporarily be fixed after cooling. Because of the entropic nature of the chain conformation change, the deformed polymer can recover its original shape upon reheating above T_g . This entropy change directed dual-shape morphing behavior is polymer elasticity (Fig. 4.3a). Another important polymer behavior is plasticity, which is traditionally opposed to elasticity. Polymers with dynamic exchangeable bonds exhibit plasticity, being capable of reconstructing the polymer's shape permanently in response to external forces. The polymer is first programmed at a temperature above T_v , whereby the dynamic covalent bond is sufficiently activated to rearrange the network topology under external load. Upon cooling, a new permanent shape is acquired. This topology rearrangement is caused by covalent bond exchange without corresponding change of entropy. This new permanent shape is non-recoverable, and will be kept intact upon temperature change in the absence of an external stress.

The elastic nature of SMPs enables their temporary shape fixation and later recovery on demand. However, traditional SMPs with only a single shape-changing cycle are unable to fulfill the increasing requirement for geometric complex multifunctional devices. In contrast, vitrimers combining both elasticity and

plasticity, could be programmed with multiple shape memory effects. This enables the continually shifting of the material into various sophisticated and geometrically complex 3D structures, which could be useful in aerospace and soft robotics applications.

A paradigm for introducing plasticity into an elastic polymer network was demonstrated by Xie's group, who used poly (caprolactone)-diacrylate and a tetrathiol crosslinker to prepare a network with ester crosslinkers that displays elasticity and plasticity under distinct triggering temperatures (Fig. 4.3) [159]. In this system, the cumulative nature of the plasticity allowed the fabrication of parts with complicated 3D structures that are considered to be impossible in other systems. The same group also modified a classical shape-changeable polyurethane thermoset to exhibit reworkability by introducing an exchangeable transcarbamoylation reaction [160]. The modified polyurethane thermoset contains both thermal phase transition and dynamic covalent motifs, and could undergo multi-type shape reshuffling. Robust thermadaptable shape memory polymers with high T_g are also highly desirable in high performance smart devices with self-folding and self-deployable properties. Such materials have been demonstrated by Gu and colleagues, who described a new type of thermadaptable shape memory polymer (EPSi) based on dynamic silyl ether linkages [43]. The resultant EPSis showed adjustable high T_g (from 118.1 to 156.4 °C) without compromising its mechanical strength. Notably, these EPSis exhibit excellent thermadaptable self-folding properties, with shape fixity ratio (R_f) ranging from 97.1 to 98.9%, shape recovery ratio (R_r) ranging from 95.6 to 99.8%, as well as a good shape retention ratio ranging from 80.5 to 86.3%. The macroscopic shape of EPSis could be converted from planar films into various 3D structures. Pan and coworkers fabricated sequence-rearranged reconfigurable co-crystalline networks, which showed great potential in biomedical devices [161]. Due to the dynamic transesterification nature, the obtained network exhibited tunable melting point, relatively high crystallinity, and possesses excellent shape reconfigurability property at body temperature, which facilitates the manufacturing of sophisticated shapes.

Soft actuators with pre-set shapes undergoing defined locomotion in response to external stimuli (*i.e.* heat, light, solvent, and electricity) are of great interests in fields such as soft robotics, energy generators, motors, and fluid propellers. To date, polymer materials, such as SMPs, liquid crystalline elastomers (LCEs) and gels, have been extensively used for the fabrication of smart 3D materials. Among which, LCEs with reversible shape-changing property have attracted great attention. Generally, under external programming, LCE polymer chains and mesogens undergo gradual orientated aligning, and the mesogen alignment can be fixed by crosslinking. By selectively tuning the LC alignment and its crosslinking distribution, LCN actuators are able to undergo an order–disorder phase-transition, giving rise to the possibility of controllable reversible actuation (Fig. 4.4a) [162]. Recently, the exchangeable LCE (xLCE) has aroused extraordinary interest, especially for the fabrication of elaborate 3D actuators with robust mechanical, recyclable, and reprogrammable functions as well as more efficient actuation.

The main technological barrier in thermal-responsive soft actuator is the contradiction between thermal-induced repro-

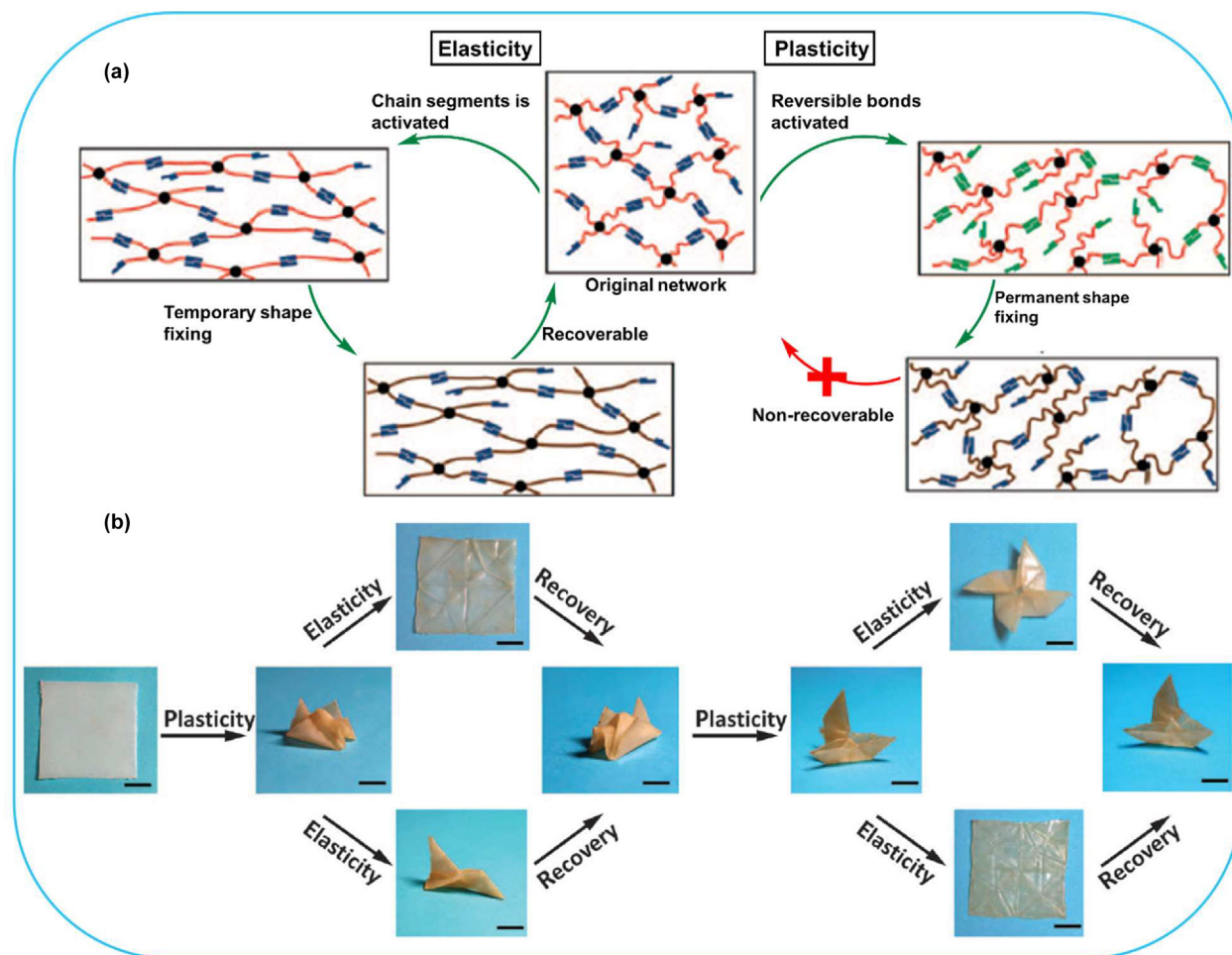


FIGURE 4.3

(a) Design of network with thermally distinct elasticity and plasticity. (b) Shape manipulation *via* thermally distinct elasticity and plasticity. Reproduced with permission [159]. Copyright 2016, American Association for the Advancement of Science.

grammability, and stability. The programming of an actuator is caused by network topology rearrangement due to the exchanging of linking moieties, which is triggered by heating. However, at high temperatures, some undesired network topology change will also happen if the chain-connections are too weak, resulting in low operational stability, and finally failing the pre-set architecture and actuation performance. Accordingly, the prudent selection of exchangeable reactions to avoid the overlaps between the actuator operation temperature and material programming temperature is a key factor in designing advanced actuation systems. In the past decade, dynamic exchangeable reactions such as transesterification, transcarbamoylation, and boronic ester exchange reactions, are widely used for the fabrication of advanced actuator systems [162].

For example, Yu et al. engineered a new adaptable main-chain LCE system by utilizing thermally induced transesterification [163]. The network benefits from both the advantages of traditional LCE (*i.e.* isotropic phase transition), as well as a dynamic crosslinked network, which renders malleability, stress relaxation, surface welding, as well as recyclability. The exchangeable boronic-ester reaction was introduced by a Michael-addition thiol-acrylate reaction to develop a new class of LCE by Terentejv

and coworkers [164]. They explored a new concept of “partial vitrimer network” material, where both the permanent and exchangeable networks were incorporated into a single material. The ratio of the corresponding components were rationally controlled to tune the fraction of the permanent and exchangeable parts in the network, achieving a material “sweet spot”, with an optimum balance between elasticity and plasticity. Such a material system was capable of maintaining the integrity of the network while simultaneously minimizing the creep. Very recently, Ji group developed an efficient swelling-heating method to reversibly turn on/off the thermal reprogrammability of a common siloxane LCE, fundamentally addressing the conflict between the operation stability and thermal reprogrammability (Fig. 4.4b) [165]. In this system, an anionic catalyst was used to control the switching ability of the network reprogrammability by altering the catalytic ability. When the network was immersed in a catalyst/solvent solution, the catalyst was able to enter into the network due to its good solubility, triggering the siloxane chain rearrangement, which could be quenched by heating (catalyst deactivation). As such the polymer was stable even at high temperatures. The network dynamics could be continually switched on/off by repeating the swell/heating cycle.

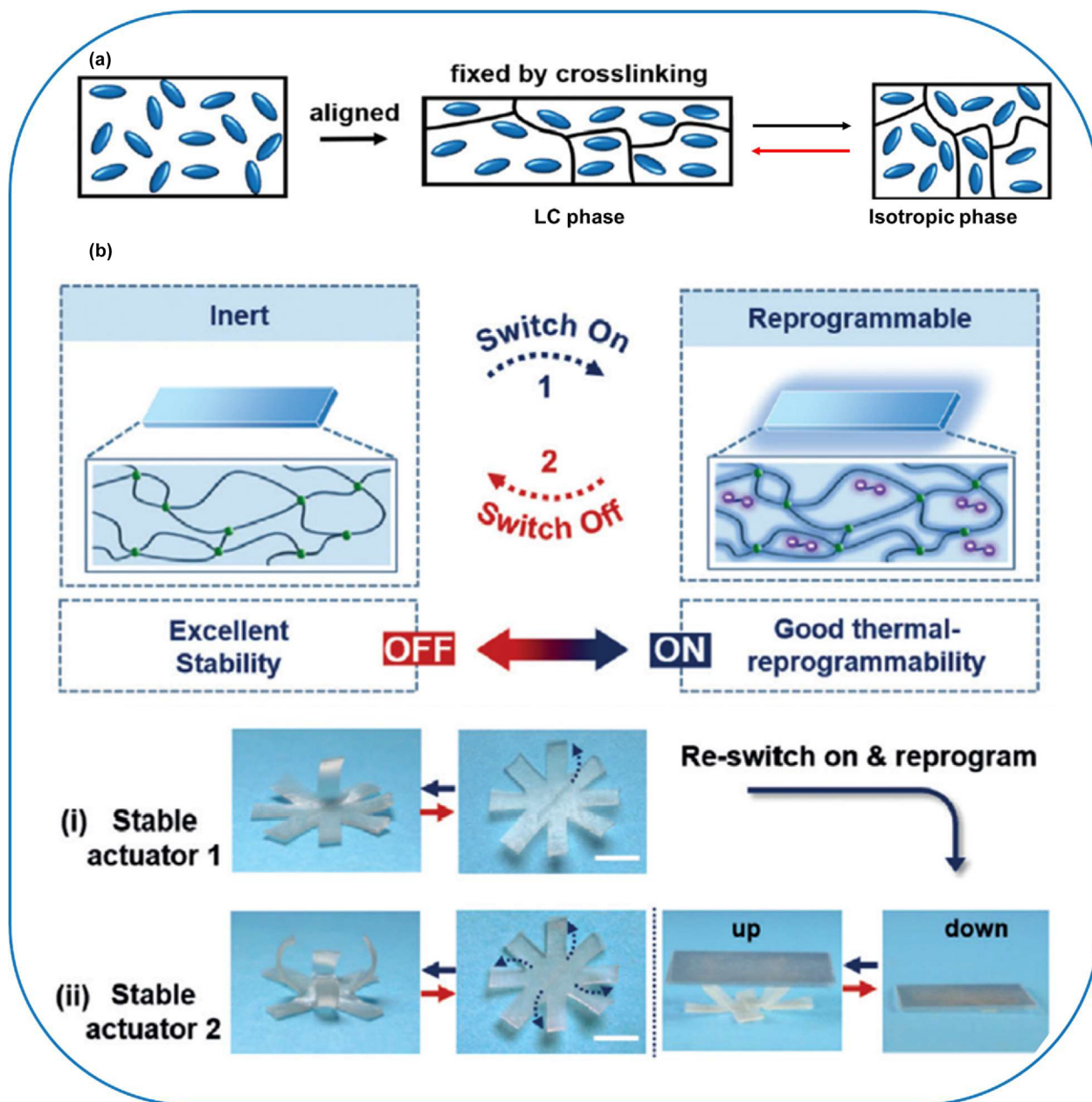


FIGURE 4.4

(a) Image illustration of the actuation mechanism of LCEs. The alignment is fixed through crosslinking. After that, LCEs show a reversible shape deformation on account of LC-isotropic transition [162]. (b) (Top) Illustration of switching on/off the thermal reprogrammability, and (bottom) the demonstration of re-switching on the thermal reprogrammability and reprogramming the one-arm bending motion (i) into four-arm bending motion (ii) for raising up objects [165]. Copyright 2020, Royal Society of Chemistry. Reproduced with permission [165]. Copyright 2020, Wiley.

Moreover, taking advantage of this strategy, many machine-like and biomimetic actuators were prepared and underwent reversible pre-defined locomotion.

Vitrimers for 3D printing applications

3D printing represents an excellent fabrication technique to manufacture geometric complex 3D devices with high accuracy. However, conventional 3D objects obtained by the layer-by-layer construction strategy showed low mechanical strength, resulting in restrictions for practical engineering. The combination of 3D printing technology and vitrimers leads to recyclable 3D devices

with sophisticated structures and precise control of the fabrication process, without compromising the robustness of objects, facilitating the large-scale application in various fields, including actuators, SMPs, and electronic/optical materials.

A recyclable epoxy vitrimer was developed as 3D printing ink by Qi and coworkers (Fig. 4.5) [166]. This ink could be printed into geometric complex parts, which subsequently recycled by dissolving in hot ethylene glycol as a solvent to generate a polymer solution (a new vitrimer ink) for the next round of 3D printing. The designed vitrimer ink could be printed four times and while retaining outstanding printability. Schlögl and coworkers

discovered a new liquid transesterification catalyst (*i.e.* oligomeric methacrylate phosphate) which showed excellent solubility in a variety of acrylates, good stability in the thiol-click reaction, and could be covalently bonded to the network [167]. This catalyst exhibited excellent catalytic activity in thiol-acrylate vitrimers with improved mechanical properties. The prepared materials were amendable to digital light processing to manufacture precise 3D soft active devices with triple-shape memory and self-repair ability. Zhang et al. prepared a robust and reprocessable acrylate vitrimer for the photo-3D printing applications *via* combing exchangeable β -hydroxyl esters and sacrificial hydrogen bonds based on the reaction between diacry-

late prepolymer, tetrahydro-furfuryl acrylate, and acrylamide [168]. When the composition of acrylamide was increased to 20 wt%, the resulting vitrimer exhibited dramatically increased tensile strength (40.1 MPa) and Young's modulus (871 MPa) compared to unmodified acrylate vitrimers, while still retaining its reprocessability. This material was used to precisely fabricate recyclable 3D objects with multiple structures by using stereo lithography 3D printing.

Multifunctional and multi-responsive vitrimer systems

Multifunctional and multi-responsive vitrimer systems have been developed by incorporation of functional molecules

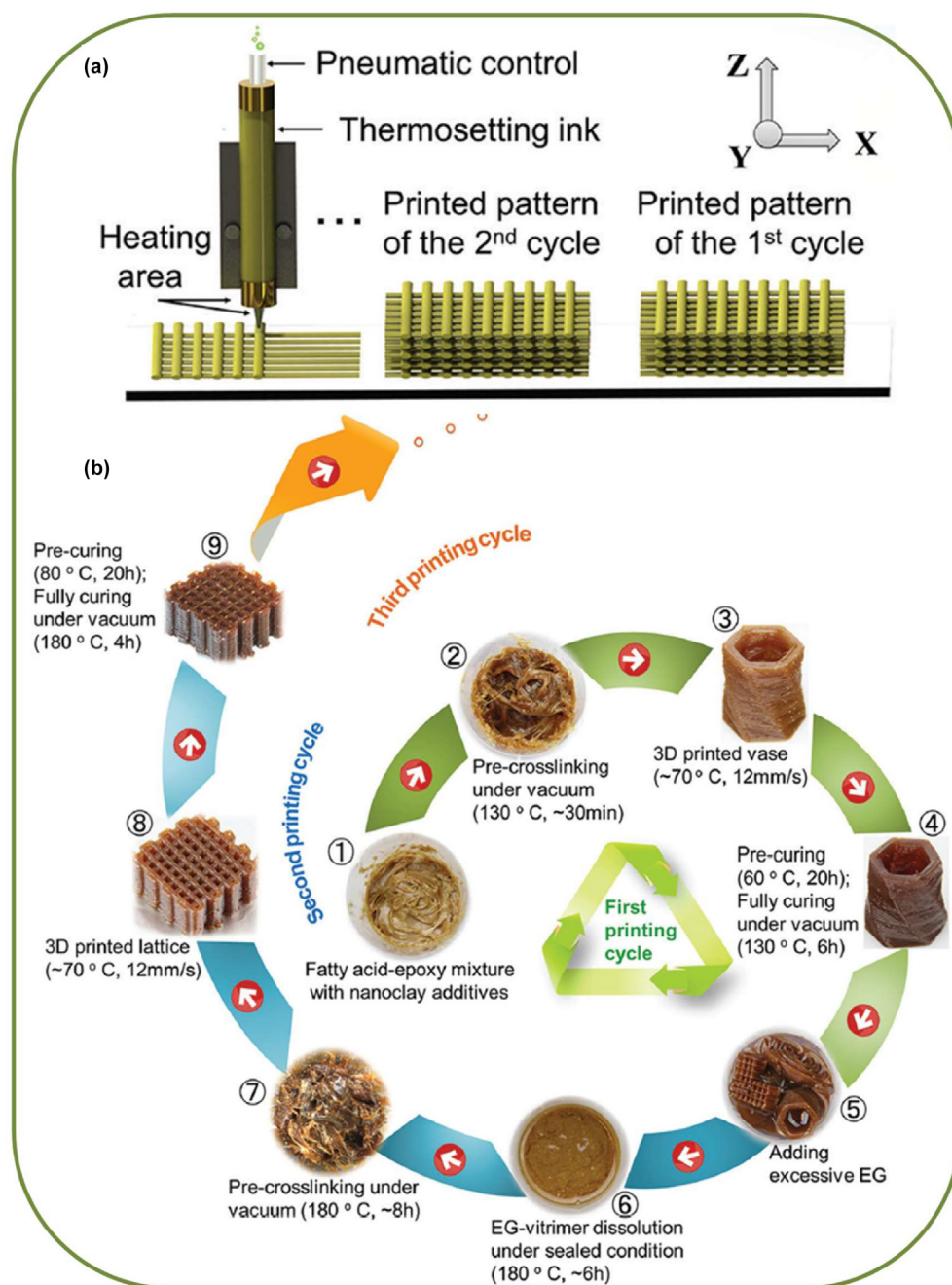


FIGURE 4.5

Schematic illustration of (a) 3D printing of vitrimeric ink; (b) the crosslinking/dissolution/recrosslinking cycle of recyclable 3D printing of nanoclay-reinforced vitrimer epoxy. Reproduced with permission [166]. Copyright 2017, Royal Society of Chemistry.

directly into the vitrimeric networks. These modified vitrimers often exhibit improved properties and interesting stimuli responsive behaviour. Apart from temperature, the modified vitrimeric systems also show the possibility of responding to a variety of external stimuli, including light, pH, solvent, redox conditions, and electrical current.

Light-triggered vitrimers

Light-triggered vitrimers with their unique advantages, are of continually growing research interest [50]. Compared to thermal-triggered vitrimers, photo-sensitive vitrimers often exhibit improved properties, such as enhanced healing speed. Furthermore, parameters of light are also highly variable; either the wavelength, intensity, or polarization can be tuned in a controlled fashion, and precise remote and regional control over these vitrimers are more conveniently achieved. These advantages offer new vitrimeric system various opportunities in engineering real applications, particularly, in the smart actuator field. An actuator with the ability to optically reconfigure can display a new actuation behavior, such as light-fueled locomotion behaviors, which is desirable in developing materials for soft robotics applications. In cooperation of photo-induced reversible reactions, such as azobenzene *trans*–*cis* transition [169], anthracene [4+4] cycloaddition [170], and disulfide/ diselenide metathesis, in the polymer main chain or side chain are appealing strategies to prepare photo-responsive vitrimers.

Ikeda and coworkers engineered a reprogrammable photomobile LCE with both thermal-induced dynamic covalent bonds and photo-switchable moieties in the network [171]. In this system, a dual functional azobenzene-based chemical was selected as both mesogens and photochromic groups to link the polysiloxane backbone to generate the network. Upon heating, mesogens could be aligned and fixed in the LC phase during the external programming. Because of the limited extinction coefficient, the light-induced *trans*–*cis* transition of the azobenzene group mainly occurred near the surface of the sample. Under UV or visible light irradiation, the surface azobenzene mesogens enable to change, leading to the rearrangement of the crosslinking strands and eventually causing macroscopic flow (*i.e.* reversible bending motions).

Furthermore, they discovered that the function, motion, and other performances could be effectively adjusted by altering the initial macroscopic shape. A novel LCN with Diels-Alder dynamic bonds in the main-chain (LCDANs) was developed for actuator programming and reprocessing was reported by the Zhao group recently (Fig. 5.1a) [172]. *Via* the formation and cleavage of D-A bonds, the LCDAN was capable of reversible transformation between the ordered and disordered phase, offering the possibility to be remolded into complicated 3D structured actuators, such as helices, origami, and other various 3D architectures. Furthermore, light-driven 3D actuators (wheel-shape and caterpillar-shape) were prepared simply by laminating a photo-switchable azobenzene-based LCDAN strip with a commercially available polyimide film (Kapton), displaying efficient photo-fueled locomotion. Zhao group also fabricated a reprocessable photo-controlled LCN containing azobenzene moieties in the polymer main chain [173]. By combined the energy from

both azobenzene photoisomerization and network strain energy, an unprecedented photoinduced mechanical force (up to 7 MPa) could be achieved, enabling the rolling or moving of large-size 3D actuators, including wheels and spring-like motors, along with a controllable direction and speed. Recently, the same group developed a novel liquid crystal polymer network (LCN) contained anthracene, which underwent the reversible photocrosslinking under different wavelength UV irradiation (Fig. 5.1b) [174]. The obtained LCN could selectively alter the distribution of crosslinking domains, resulting in the actuation behavior in a controlled manner. Taking advantage of this mechanism, the LCN actuator was able to realize optical reconfiguration of origami, and also as a light-fueled microwalker with different locomotion behaviors.

Apart from 3D actuators, vitrimers with photo-sensitive chromophores have also been applied in fabricating materials with tunable surface topologies, and spatial control of reprogramming. Wolf and co-authors demonstrated that aliphatic diamines underwent thermal exchange reactions while aromatic diamines only responded to photo-irradiation [170]. Exploiting this, a photoactivated vinylogous urethane vitrimer was prepared by carrying out the polymerization of 1,12-dodecane diamine, 1,12-dodecanebisacetoacetate, and 1,5-diaminoanthracene with different molar ratio. The vitrimeric behaviors of the material was ascribed to the dynamic exchange of vinylogous urethane bonds upon heating in the network. Additionally, due to the formation of anthracene dimers under UV irradiation, the vitrimer exhibited tunable rheological properties and glass transition temperature. This photo-responsive vitrimer also possessed rapid scratch healing behavior with a tunable onset temperature. Bowman *et al.* used the dynamic thiol-ene reaction to photocure the vitrimer material using the bi-functional norbornene monomer comprising both ester bonds and pendant OH moieties [175]. Analogous to thermally cured vitrimers, the reported photo cured vitrimer system exhibited a strong Arrhenius dependence of the stress relaxation time with inverse temperature from 145 to 175 °C, suggesting a relaxation controlled by the transesterification reaction rate. Exploiting the reversible nature of the transesterification reaction, this vitrimeric system showed excellent performance in the nanoimprint lithography (NIL), due to its ability to continually change surface features. Additionally, complicated hierarchical structures could be obtained by combining NIL and photopatterning. Xu and co-workers used visible light to trigger the plasticity of polyurethanes (PUs) thermoset which contained diselenide bonds. Both shape memory and light-induced plasticity were tunable by altering the diselenide bond content [176]. Triggered by visible light, these PUs thermoset possessed the advantage of spatial control while avoiding the undesired damage caused by heat or UV light. Subsequently, positive tone patterns with rewritability was attained by using an epoxy-anhydride vitrimer (*o*-NBE) formed by the reaction between hexahydrophthalic anhydride with 1,5,7-triazabicyclo[4.4.0]dec-5-ene [177]. The resulting *o*-NBE comprises both photolabile chromophores *o*-nitrobenzyl esters, as well as thermal-activated hydroxyl ester groups. Under the UV irradiation, *o*-nitrobenzyl ester links in the network were broken, increasing vitrimer solubility, and precise micropatterns (size ~ 20 μm) were

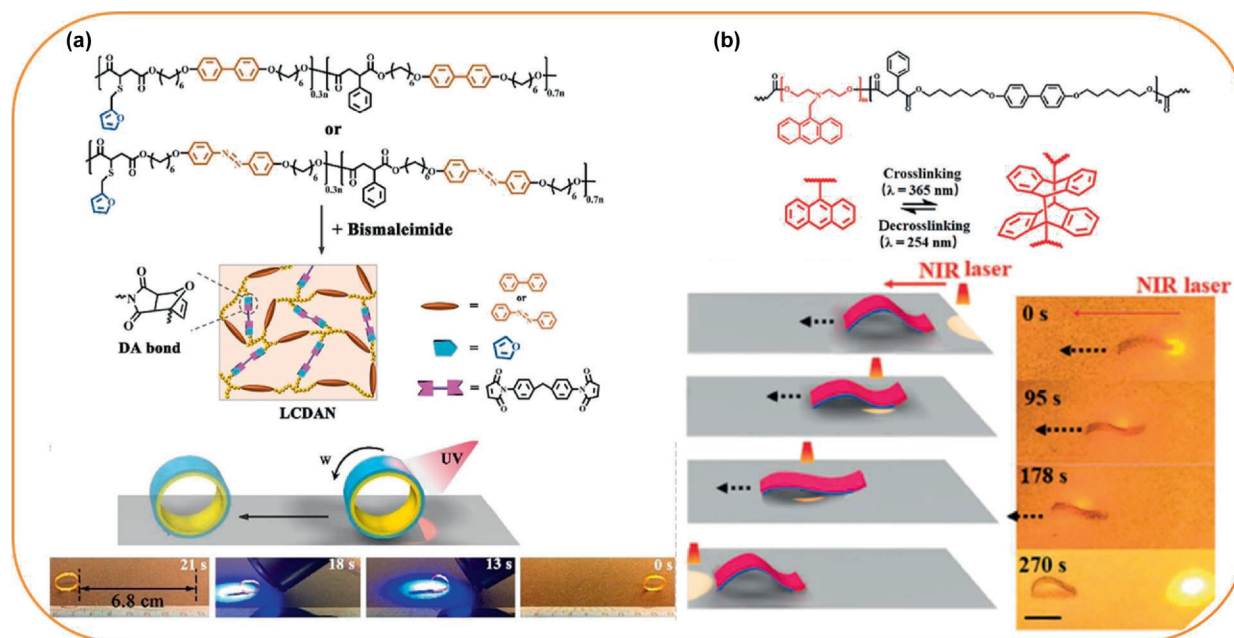


FIGURE 5.1

(a) Chemical structures of two main-chain liquid crystalline polymers and an AZO-LCDAN/Kapton bilayer wheel executing rolling motion under UV-light irradiation [172]. (b) Chemical structure of the anthracene-containing liquid crystal polymer, and the walking of an arch-shaped actuator along the laser scanning direction (from right to left) by reversible flattening/arching shape change as laser spot moves on [174]. Reproduced with permission [172]. Copyright 2020, Wiley. Reproduced with permission [174]. Copyright 2019, Wiley.

achievable by photolithographic techniques. The polymer patterns were subsequently fully erased at the temperature above T_v due to the reversible reaction of the hydroxyl ester.

Multiple stimuli responsive vitrimers

Oligoanilines with a well-defined molecular structure, shows excellent electro-activity, metal ions absorption capability, strong photo-thermal effect, and good solubility in common solvents, and are promising materials for multiple stimuli responsive vitrimers. Ji and co-authors developed low-cost multi-stimuli responsive and multi-functional vitrimeric composites by copolymerizing aniline trimer (ACAT, an oligoaniline) with epoxy monomers [178]. Besides heat, the modified vitrimer systems also responded to light, pH, voltage, metal ions, and redox chemicals. The obtained material retained the features of starting materials (such as the malleability/recyclability of vitrimers and metal ions absorption of oligoanilines), while simultaneously exhibiting new properties, such as photo-induced self-healing/weldability, and pH-activated shape memory. Very recently, Zhang *et al.* converted a conventional vitrimer system into multiple responsive ACAT-vitrimer by incorporating oligoaniline through the polycondensation reaction of terephthaldehyde, m-xylylene diamine, and tris (2-aminoethyl) amine [179]. The ACAT-vitrimer was responsive to three stimuli, including heat, light, and amines. Moreover, the prepared material exhibited excellent thermal stability, weld ability, as well as recyclability.

Vitrimeric composites

Vitrimer systems with enhanced performance and multi-responsiveness is necessary for the development of next generation materials. In this context, two kinds of advanced vitrimer

systems will be introduced. We first focus on vitrimer composites formed by adopting nano-fillers into the polymer matrix (Section 5.1). In Section 5.2, we will introduce the malleable material-reinforced vitrimer composites obtained by immersing vitrimers into commercially available materials.

Advanced vitrimer composites from nanoparticle additives

Nanoparticles with advanced inherent properties, are promising additives to improve the properties of vitrimers. Some of the most common nanoparticles include graphene and carbon nanotubes (CNTs), which endows the composites with enhanced mechanical properties, as well as electrical conductivity. In addition, due to the photo-thermal effect, the resultant vitrimer composites can be constructed and reconstructed into sophisticated 3D structures by localised heating. For instance, a graphene-epoxy-vitrimer composite with dynamic covalent transesterification bonds was developed to show thermally reconfigurable shape memory behaviors [180]. The resultant composite exhibited stable shape memory property with constant shape fixity and recovery values ($R_f > 99\%$, $R_r > 98\%$). As illustrated by the DMA analysis, the vitrimer composite had a shape retention ratio of 100%, facilitating the fabrication of the arbitrary 2D or 3D newly permanent shape. In addition, with the incorporation of graphene nanosheets, the vitrimer composite displayed NIR triggered shape recovery behavior. Liu *et al.* incorporated imine-containing networks into graphene grafted polymers [88]. Besides reinforcement for the material, grafting of graphene to the cross-linked network also allowed light activated behaviour.

One of the key barriers in preparing vitrimer composites is the homogenous dispersion of nano fillers in the matrix. Due to their large aspect ratio, van der Waals, and strong π - π interactions,

nano-fillers tend to aggregate in the vitrimer matrix, forming a non-uniform structure, which sometimes results in unstable behaviors. Some strategies to surmount this problem include ultra-sonication [181], introduction of dispersants [81], and surface modification [82].

A carbon nanotube-polyurethane (CNT-PUV) vitrimer composite was developed [181]. Ultra-sonicating the mixture of CO, melted PEG, CNTs and ethyl acetate enabled the CNTs to be well-dispersed in the mixture solution. The prepared CNT-PUV vitrimer composite possessed dual-triggered shape memory and reconfiguration behavior because of transcarbamoylation reactions of carbamate bonds.

Ji group developed carbon nanotube (CNT) dispersed liquid crystalline vitrimers (LCVs). With the help of a dispersant (PIM), CNTs were homogeneously dispersed in the material matrix [81]. Due to the strong photothermal effect of CNTs, the resultant vitrimeric composite experienced dynamic light-activated transesterification, enabling various sophisticated 3D architectures to be built and rebuilt under light irradiation (Fig. 5.2). In addition, the LCV film exhibited tunable thermal, mechanical, and actuation properties, under shining light without screws, glues, or molds.

Guo *et al.* synthesized styrene-butadiene rubber (SBR)/graphene composites by engineering imine bonds into both rubber bulk network and SBR-graphene interface [182]. The incorporation of well-dispersed graphene resulted in multi stimuli vitrimeric composites with significantly enhanced mechanical properties. The dynamic exchange of imine bonds in both the bulk network and SBR-graphene interphase, enabled the topology rearrangement of the network, facilitating the ready material recycling as well as the repeated construction of geometrically complex shapes either under heating or IR irradiation. A new kind of electromagnetic shielding materials (SEMs) was developed by doping vitrimer matrix with MWNT/Fe₃O₄ composite [183]. To improve the additives' dispersion, polypyrrole (ppy) wrapped MWNTs and Fe₃O₄ were prepared with satisfactory dispersion in the vitrimer matrix. As demonstrated by the reflection loss experiment, the prepared SEM exhibited a superior electromagnetic shielding capacity compared to its original counterparts. In the lap-shear test, samples exhibited a comparable self-bonding effect either under mechanical force or magnetic force, demonstrating a similar transesterification speed and deformation efficiency.

Apart from graphene and CNTs, other inorganic fillers (such as gold nanoparticles, and silica) are also be used to prepare vitrimer composites with strong mechanical properties, reprocessability, and recyclability. Gold nanoparticles showed an excellent photothermal effect and selective-spectrum absorption property which can be adjusted by the structure. Efficient incorporation of gold nanospheres with vitrimer materials can be used to prepare light-sensitive vitrimeric composites that only respond to the selective wavelength, increasing the stability of the material under visible light. However, due to the high-temperature vitrimer curing process, naked gold nanoparticles are vulnerable to aggregation, resulting in the weakening of the plasmon resonance of the nanospheres. To increase the stability of gold nanoparticles during the procedure of vitrimers, Ji and coworkers used polydopamine to modify gold nanospheres,

which could be well dispersed into epoxy vitrimers [82]. Due to the strong photothermal effect of the polydopamine-modified gold nanoparticles, the obtained composites offering efficient healing and shape-reshifting by light, as well as light-directed surface patterning and re-patterning. Recently, the optical self-repairing properties of a polarizing film was achieved by using the synergistic effect between Au nanorods (AuNRs) and a vitrimer. Chen and co-workers engineered a three-step phase transfer process to obtain a polarizing film with a stable and monodispersed AuNRs in a polyvinylpyrrolidone polymer matrix [184]. The prepared polarizing film exhibited vitrimer properties due to the dynamic reversible exchange reaction of carbamate bonds. Interestingly, the damaged film could be in situ healed by the photothermal effect of AuNRs triggered by laser irradiation.

Silica was also used to improve the vitrimer mechanical properties. Guo and colleagues disclosed a robust crosslinked elastomer system *via* C-N transalkylation of pyridinium and implemented this chemistry to modify the silica surface, preparing a smart elastomeric composite by hot-pressing. Because of the powerful covalent interfacial bridges and the uniform dispersed silica nanoparticles, the yielded composites possessed superior mechanical strength. Due to the dynamic nature of C-N transalkylation reactions of pyridiniums in the network, the designed composites could be continually reprocessed at elevated temperatures.

Apart from inorganic nanoparticles, organic nanoparticles are also used to improve the properties of vitrimeric composites. In contrast to inorganic nanoparticles, organic nanoparticles were easy to disperse homogeneously into the polymer matrix without any further dispersion step. For example, Ji and coworkers utilized organic polydopamine (PDA) nanoparticles to prepare vitrimeric composites to successfully build 3D structures (Fig. 5.3) [185]. Notably, this vitrimer composite was prepared in the absence of dispersant, surface modification, or sonication.

Ni and co-workers engineered a new vitrimeric paper, with polycarbonate as a matrix, and natural cellulose paper acted as the reinforcing framework [90]. Through *in situ* polymerization of monomers in the cellulose paper, the porous structures of the original paper could be fully filled, resulting in a robust vitrimeric paper. As demonstrated by the cross-section scanning electron microscope (SEM), blank paper comprises a random intertexture of natural cellulose fibers with very high porosity. The resultant vitrimeric paper not only possesses exceptional mechanical robust and great thermal/chemical stability, but also displayed various smart behaviors, including shape-memory, self-healing, and reshaping. Walther and colleagues combined cellulose nanofibrils (CNFs) and vitrimer nanoparticles to achieve mechanically coherent nano-paper materials [186]. The dynamic transesterification endowed the polydimethylsiloxane-based vitrimer attached to the CNF surface. The resultant nano-paper exhibited flexible, stretchable, and outstanding water resistance properties. Furthermore, this vitrimer was used to glue two nanocomposites as a re-processable adhesive. Recently, a multi-functional carbonized lignin-free wood (CLFW)@Ni-NiS/vitrimer composite was designed with reshaping, self-healing, and shape-memory properties [187]. A hybrid was engineered by assembling the vitrimer with a supercapacitor, possessing high energy

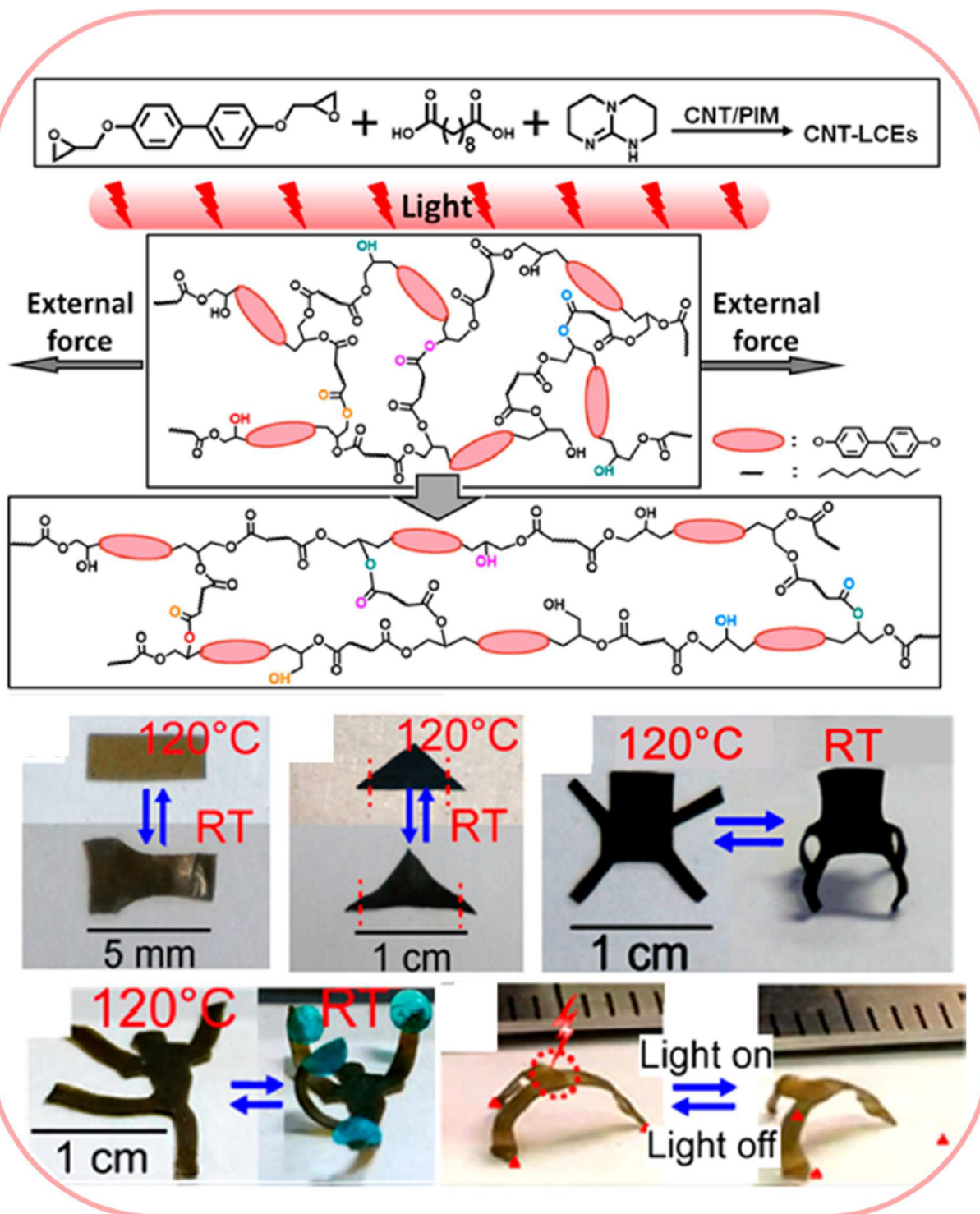


FIGURE 5.2

(Top) Synthesis of CNT-xLCEs and the alignment by light. (Bottom) Reversible actuation and shaping changing of a CNT-xLCE film. Reproduced with permission [81]. Copyright 2016, American Chemical Society.

densities and power densities, and simultaneously exhibiting the improvement of recycling ability, demonstrating the huge potential of wood-based smart materials for applications in supercapacitors, catalysts, and sensors. Most vitrimers are formed by hydrophobic polymer systems, recently, a vitrimeric system based on hydrophilic polymers had been illustrated. Walther

and co-workers demonstrated a waterborne methacrylate-based vitrimer system using heat-activated catalytic transesterification [188]. The corresponding vitrimer featured elastomeric properties and maintained the tensile properties after two recycling cycles. More interestingly, this designed vitrimer system could be used to prepare water-based bioinspired nanocomposites by combin-

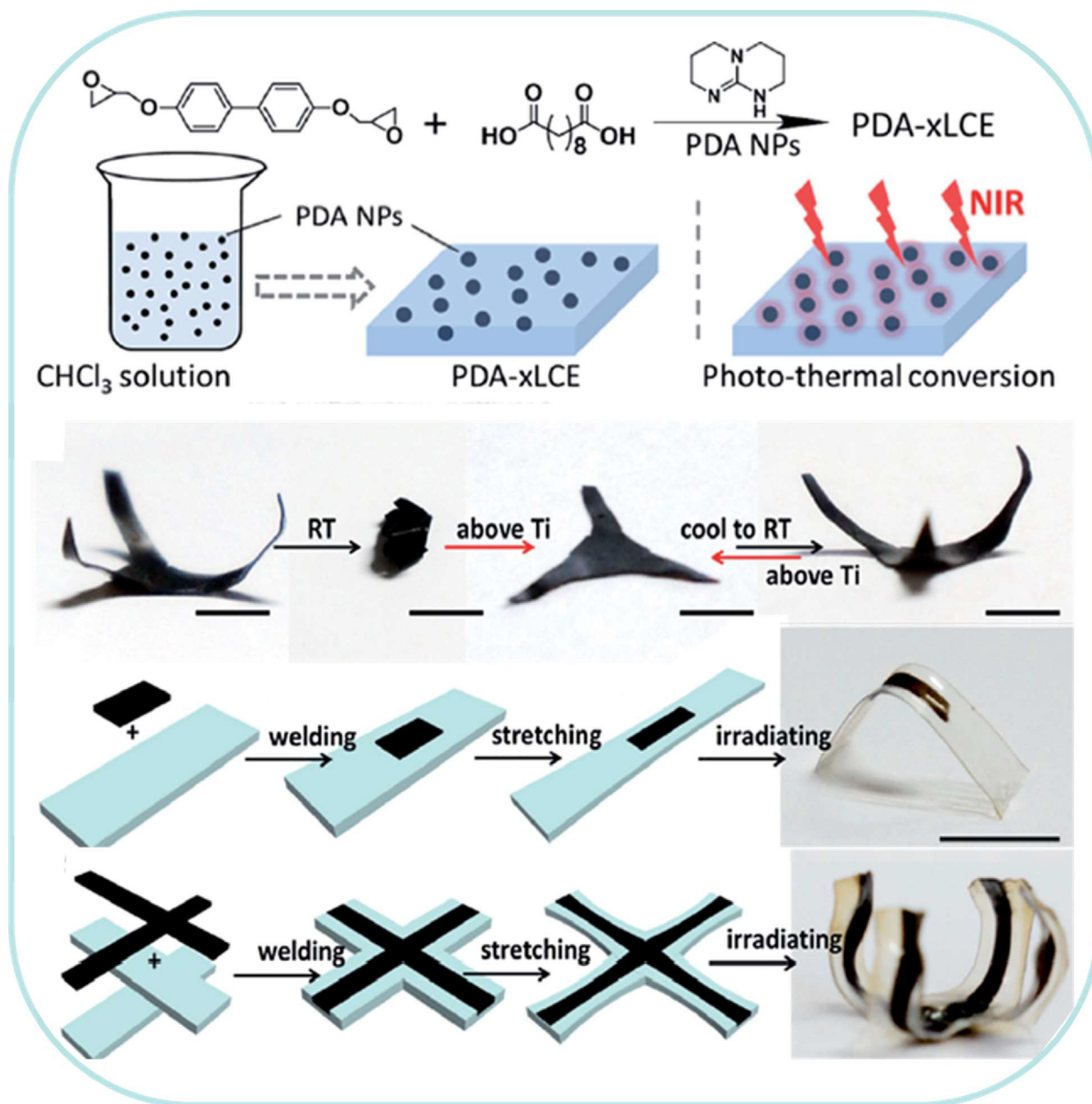


FIGURE 5.3

(Top) Schematic illustration of the process used to prepare the PDA-xLCE sample. (Bottom) Restoration and reversible actuation of deformed dynamic 3D structures of a PDA-xLCE sample and welded blank LCE films/PDA-xLCE sample films. Reproduced with permission [185]. Copyright 2017, Royal Society of Chemistry.

ing the prepolymer with cellulose nanofibrils (CNFs) and nanoclays in a sandwich structure. The obtained transparent film with a very homogeneous structure, and displayed excellent water resistance, which used to be challenging for water-borne bioinspired nanocomposites.

Malleable material reinforced composites applications

Today, fiber reinforced polymer composites (FRPCs) are of great interest as their applications as lightweight alternatives to metals in the aerospace industry and the automotive industry. However, current FRPCs are expensive and impossible to recycle, leading to undesired waste, and pollution with an enhanced overall cost.

Therefore, seeking new materials with robust mechanical properties, good shape-adaptability, and recyclability, to replace the current FRPC is highly sought-after for the development of the sustainable economy. FRPCs based on vitrimers are an extraordinary solution to this demand due to their significantly enhanced mechanical strength, while showing re-processability, reparability and recyclability. FRPCs are easily manufactured from readily available materials (such as carbon fiber) and could thus be easily implemented in myriad fields: transportation, construction industries, energy, and so on. We believe that the development of FRPCs will provide the great possibility to produce lightweight and efficient parts for airplanes, cars, and wind energy sectors.

The following Section gives some reports of FRPC based vitrimers.

Du Prez and co-workers explored a series of vinylogous acyl compounds (urethanes, amides, and urea) for high performance vinylogous acyl based networks with fast intrinsic exchange kinetics [104]. With a simple acid catalyst (0.5 mol % pT_sOH), the obtained networks exhibited very short relaxation times and excellent mechanical properties with a storage modulus value of 2.2 GPa. These vitrimers were exploited as a matrix for the preparation of material composites, as shown in Fig. 5.4a. The resulting composites allowed thermoforming into a triangular shape at 150 °C within 10 mins and fiber recycling by solvolysis. Recently, the same group presented a transparent, rigid, and highly reprocessable catalyst-free epoxy vitrimer system by applying an oligomeric amine-based curing agent to introduce the dynamic vinylogous urethane (VU) bonds [102]. The obtained VU-based vitrimer showed good recyclability and remarkably short stress relaxation times at temperature above

T_g . In addition, this vitrimer was used to prepare glass-fiber-reinforced epoxy composites with the capability of recycling and reshaping.

Odriozola et al. described a disulfide crosslinked epoxy vitrimer, which was first employed for the manipulation of robust fiber-reinforced polymer composites with reshaping and recycling features (Fig. 5.4b and c) [75]. A rapid fabrication technique was developed to prepare FRPCs by heat-pressing vitrimer powder and woven carbon fibers [189]. Moreover, the prepared FRPC samples underwent rapid shape refabrication within a few minutes.

Qi and coauthors reported fully recyclable carbon-fiber reinforced polymer (CFRP) composites based on epoxy vitrimer [190]. The polymer chain of the epoxy matrix in CFRP composites could be cleaved into small segments due to its good solubility in hot ethylene glycol (Fig. 5.5). Moreover, the dissolved epoxy monomer could be re-polymerized and used for the preparation of new CFRP composites with the same level of mechani-

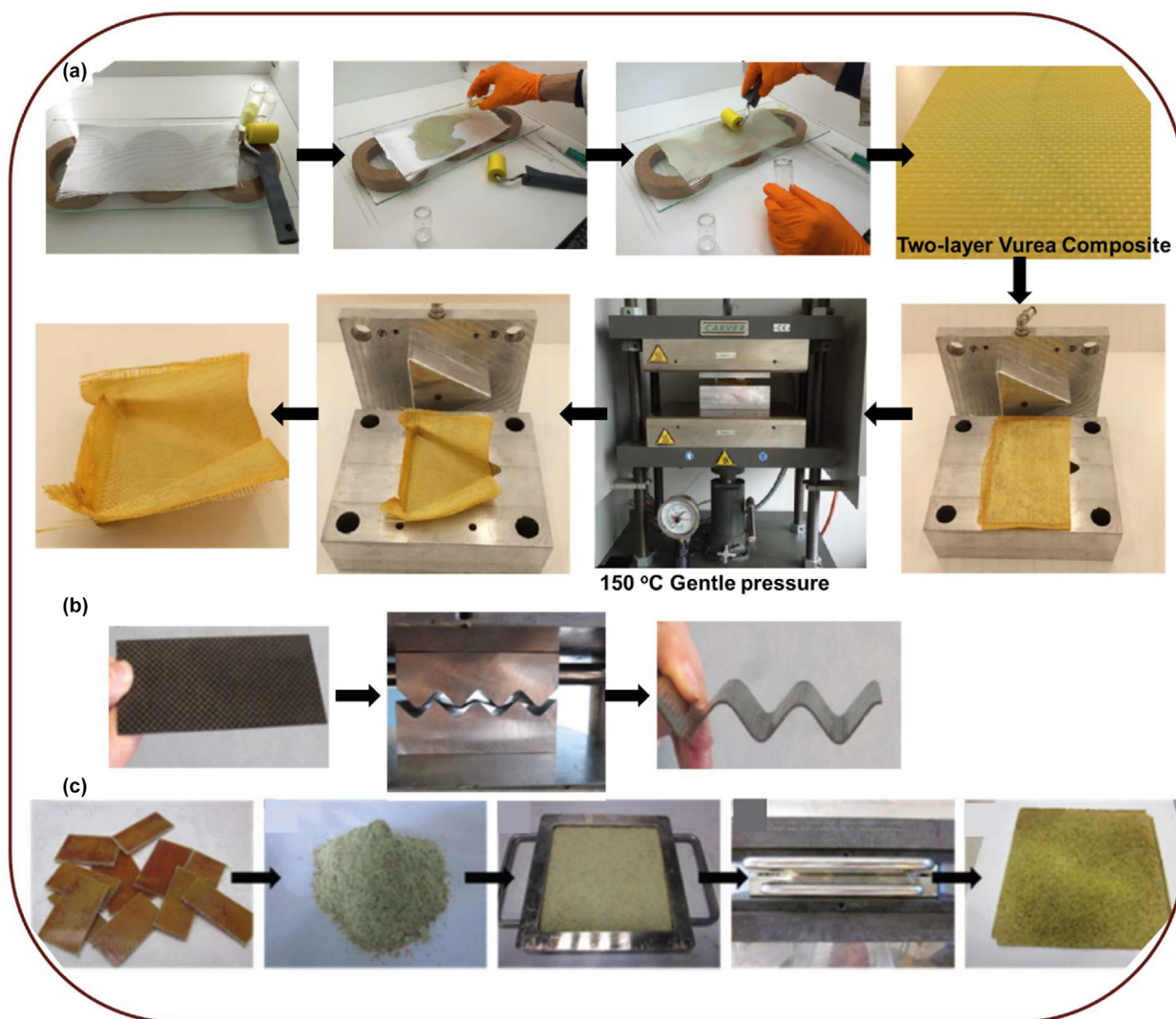


FIGURE 5.4

(a) Pictures illustration of the preparation of a flat Vurea composite and its thermoforming into a triangular shape [104]. (b) Reshaping of a cured composite laminate, and (c) recycling of epoxy composites [75]. Reproduced with permission [104]. Copyright 2018, American Chemical Society. Reproduced with permission [75]. Copyright 2016, Royal Society of Chemistry.

cal strength as original samples. In this system, near 100% materials recycling was successfully obtained.

Zhang and co-workers used polyimine networks as the robust binder to prepare repairable woven carbon fiber composites [66]. These composites were fully reclaimable, with all of the fiber and binder materials reusable. Interestingly, the malleable nature of polyimine networks endowed the capability of welding and remolding of the resulting composites, facilitating the manipulation of a smooth hemispheric structure model, which were strong enough to bear the weight as heavy as 150 kg.

Liu et al. synthesized a fully recyclable CFRP composite using an imine-containing epoxy vitrimer as a hardener [191]. By hot-pressing carbon fiber prepreps and vitrimer matrix, the obtained

CFRC showed the flexural strength and modulus of 1028 MPa and 56 GPa, respectively. Taking advantage of the excellent recycle ability of the vitrimer precursor, the resulting CFRP composite underwent the recycling in a closed-loop process by chemically degrading the material in an amine solvent. Moreover, the degradation products could be used to synthesize fresh vitrimers for further reusing.

Barriers of material reinforced composites in sustainable development are undoubtedly solved by introducing reversible exchangeable bonds to obtain dynamic networks. However, this may reduce the mechanical robustness of materials to some extent. Upon exposure to stimuli, network topology changes caused by the exchanging of the reversible bonds reduce the

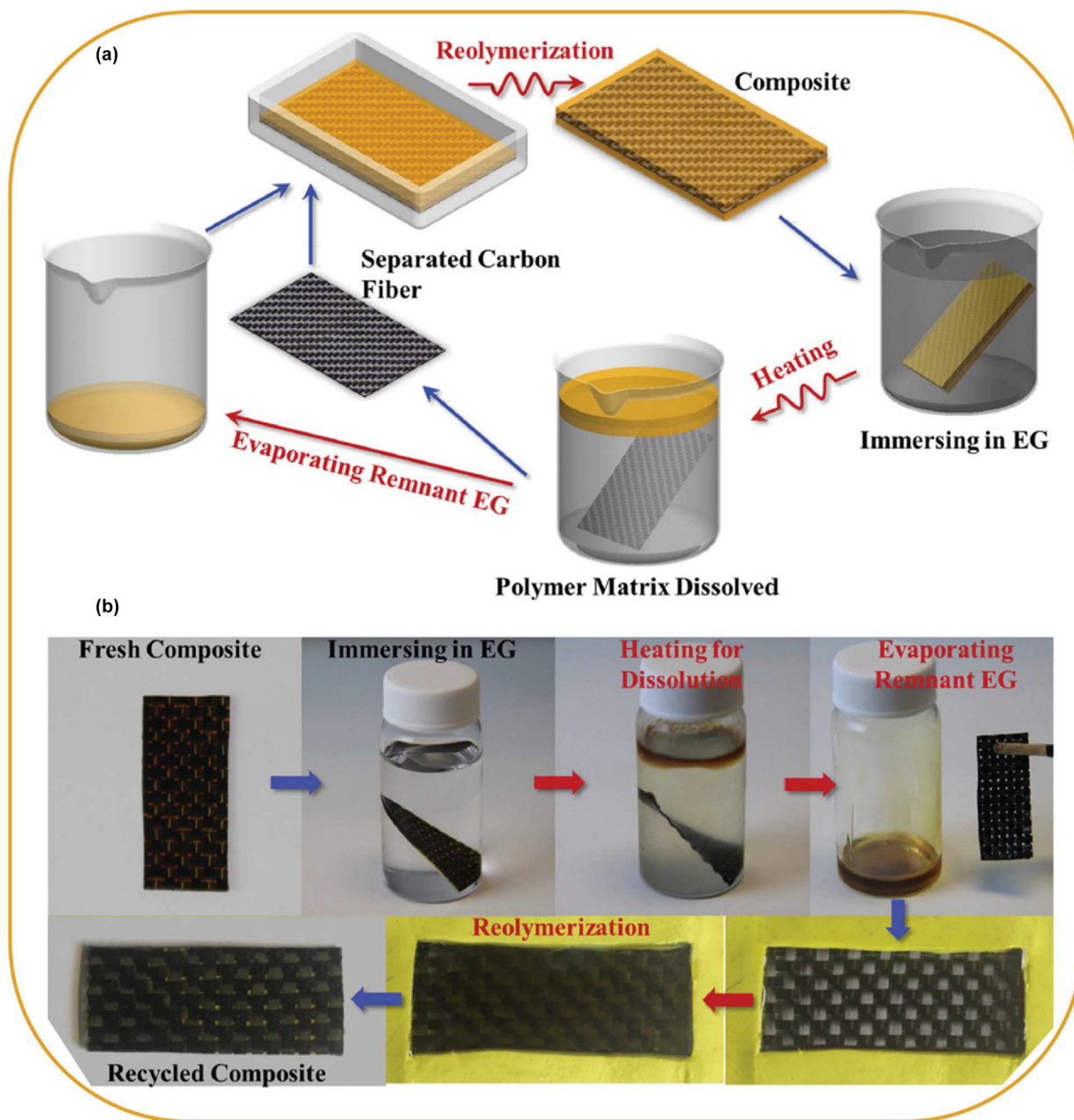


FIGURE 5.5

The recycling procedure for CFRP composites. (a) A schematic view. (b) The experimental pictures. Reproduced with permission [190]. Copyright 2016, Wiley.

integrity of the network and result in a decrease of the material mechanical strength. The contradiction between the material strength and dynamic properties will limit these composites' growth in the global market, especially in applications that require high thermal stability such as devices for aerospace. Thereby, seeking new material reinforced composites with high performance is still necessary for the future. For instance, new strong reversible bonds with associative mechanism and high activation energy can be explored to improve the stability of the material. In addition, dual dynamic crosslinking systems with distinct stimuli can be introduced in a single material, allowing the material to orthogonally control its dimensional integrity upon selectively triggering the external stimulus. Furthermore, catalytic systems can be improved to tune the reversible reaction and network topology reconfiguration in a controlled manner.

Conclusions and perspectives

In this review, we have summarized and given an overview of state of the art vitrimeric materials, which represent a significant leap in the field of materials. As a recyclable type of thermoset, these vitrimeric materials meet the environmental and performance requirement of today's world, representing another step towards a circular economy. In fact, some of these materials have already gone on to be commercialized [192]. However, numerous challenges still remain in bringing vitrimers into widespread commercialisation. Current thermosets are often low-cost materials prepared from readily available feed-stocks. This economic barrier would be an important hurdle for vitrimeric materials to overcome in order to truly replace thermosets. Furthermore, infrastructure and logistical chains would also need to be established to enable end of life recycling. Some groups focus on the conversion of existing materials into vitrimers or vitrimer-like substances [65]. Still others take the concept of vitrimers, applying them to current thermosets to enable reprocessing [144–146]. These works would be key enablers in translating the work in the laboratory to the world, as it would likely be an easier to achieve intermediate step compared to completely replacing thermoset plastics. In addition, the feedstock for these new vitrimeric materials would also have to be considered. Developments in readily available bio-feedstock based vitrimeric materials would also be important in further increasing the sustainability of vitrimeric materials. Furthermore, the processes for material preparation and recycling would also need to be green.

In the past 10 years, an extensive array of both polymeric backbones and choice of crosslinking chemistry have been extensively explored. These reports represent an impressive toolbox from which to choose materials from. However, despite the great fundamental improvement that has been achieved, there is still significant room for innovation and exploration to enhance the engineering feasibility of vitrimeric materials. Some strategies which are employed include 1) development of new advanced vitrimeric systems *via* exploring new dynamic exchange reactions; 2) controlling the activation energy of the existing covalent bonds by appropriate choice of catalysts, solvent, and additives (Section 3.7); 3) balancing the percentage of the perma-

nent and dynamic crosslinks in the network to further increase the stability and reprocessability; 4) combining the physical interactions and covalent crosslinking into the same network to increase the robustness of the material; 5) development of orthogonal control for multiple-stimuli responsive vitrimers, and 6) choice of additives to form vitrimeric composites. These are important parameters in determining the properties of the material eventually formed. Tuning of these parameters would be of paramount importance when exploring vitrimers in specific applications. For instance, every dynamic reaction has its own activation energy (influenced by the catalyst). By considering the desired operating and reprocessing temperature range, an appropriate choice of dynamic reaction will make the ideal material with suitable properties to meet the needs of desired applications. For instance, where ease of re-processability is desirable, the choice of low activation energy dynamic bonds (such as boronic esters) would be appropriate.

However, at present, some limitations are still apparent. Typically reprocessing conditions for currently reported vitrimers typically require a few minutes under high temperature and pressure, with few exceptions [141]. Ideally, for applications such as in injection molding, the reprocessing speed would have to be possible in a few seconds. This would require bonds which rapidly exchange when the appropriate stimuli is applied. Another requirement would be vitrimers which are usable at high temperatures, so as to truly be able to replace thermosets, which are relatively rare [117]. This would require the crosslinking bonds to be more stable and selective such that it does not react with other parts of the polymers even at high temperatures. Beyond replacing existing materials for more environmentally friendly ones, vitrimers also hold great potential as next generation materials with self-healing, shape memory, recoverable adhesives, and malleable properties. All these lead us to be highly optimistic towards the future of vitrimeric materials.

Declaration of Competing Interest

The authors declare that they have no known competing financial interests or personal relationships that could have appeared to influence the work reported in this paper.

Acknowledgements

J.Z and Z. P contributed equally to this work. This work was financially supported by the Agency for Science, Technology and Research (A*STAR) under its AME Young Individual Research Grants (YIRG) Grant (Grant No. A2084c0168 and A2084c0166).

References

- [1] A.L. Andradý, M.A. Neal, *Philos. Trans. R. Soc. B Biol. Sci.* 364 (2009) 1977–1984, <https://doi.org/10.1098/rstb.2008.0304>.
- [2] K.M. Cantor, P. Watts, *Plastics Processing*, in: *Appl. Plast. Eng. Handb.*, 2011, pp. 195–203, <https://doi.org/10.1016/B978-1-4377-3514-7.10012-1>.
- [3] T. Vidil et al., *Prog. Polym. Sci.* 62 (2016) 126–179, <https://doi.org/10.1016/j.progpolymsci.2016.06.003>.
- [4] J. Hopewell, R. Dvorak, E. Kosior, *Philos. Trans. R. Soc. B Biol. Sci.* 364 (2009) 2115–2126, <https://doi.org/10.1098/rstb.2008.0311>.
- [5] B.A. Helms, T.P. Russell, *Chem. 1* (2016) 816–818, <https://doi.org/10.1016/j.chempr.2016.11.016>.
- [6] W. Post et al., *Polym. Rev.* 60 (2020) 359–388, <https://doi.org/10.1080/15583724.2019.1673406>.
- [7] C.J. Kloxin et al., *Macromolecules.* 43 (2010) 2643–2653, <https://doi.org/10.1021/ma902596s>.

- [8] C. Bowman, F. Du Prez, J. Kalow, *Polym. Chem.* 11 (2020) 5295–5296, <https://doi.org/10.1039/d0py90102d>.
- [9] C.J. Kloxin, C.N. Bowman, *Chem. Soc. Rev.* 42 (2013) 7161–7173, <https://doi.org/10.1039/c3cs60046g>.
- [10] S. Majumdar et al., *ACS Macro Lett.* 9 (2020), <https://doi.org/10.1021/acsmacrolett.0c00636>.
- [11] M. Bin Rusayyis, J.M. Torkelson, *Macromolecules* 53 (2020), <https://doi.org/10.1021/acs.macromol.0c01539>.
- [12] M. Podgórski et al., *Adv. Mater.* 32 (2020) 1–26, <https://doi.org/10.1002/adma.201906876>.
- [13] G.M. Scheutz et al., *J. Am. Chem. Soc.* 141 (2019) 16181–16196, <https://doi.org/10.1021/jacs.9b07922>.
- [14] P. Chakma, D. Konkolewicz, *Angew. Chem. Int. Ed.* 58 (2019) 9682–9695, <https://doi.org/10.1002/anie.201813525>.
- [15] N.J. Van Zee, R. Nicolaÿ, *Prog. Polym. Sci.* 104 (2020), <https://doi.org/10.1016/j.progpolymsci.2020.101233>.
- [16] W. Alabiso, S. Schlögl, *Polymers* 12 (2020) 1660, <https://doi.org/10.3390/polym12081660>.
- [17] D. Montarnal et al., *Science* 334 (2011) 965–968, <https://doi.org/10.1126/science.1212648>.
- [18] L.E. Porath, C.M. Evans, *Macromolecules* 54 (2021), <https://doi.org/10.1021/acs.macromol.0c02800>.
- [19] F. Meng, M.O. Saed, E.M. Terentjev, *Macromolecules* 52 (2019), <https://doi.org/10.1021/acs.macromol.9b01123>.
- [20] L. Li et al., *Macromolecules* 54 (2021), <https://doi.org/10.1021/acs.macromol.0c01691>.
- [21] J.J. Lessard, G.M. Scheutz, S.H. Sung, K.A. Lantz, T.H. Epps, B.S. Sumerlin, *J. Am. Chem. Soc.* 142 (2020), <https://doi.org/10.1021/jacs.9b10360>.
- [22] F. Ling et al., *J. Mater. Chem. A* 7 (2019), <https://doi.org/10.1039/c9ta09292g>.
- [23] A. Jourdain et al., *ACS Appl. Mater. Interfaces* 53 (2020) 1884–1900, <https://doi.org/10.1021/acs.macromol.9b02204>.
- [24] B.R. Elling, W.R. Dichtel, *ACS Cent. Sci.* 6 (2020) 1488–1496, <https://doi.org/10.1021/acscentsci.0c00567>.
- [25] M. Guerre et al., *Chem. Sci.* 11 (2020), <https://doi.org/10.1039/d0sc01069c>.
- [26] D.J. Fortman et al., *J. Am. Chem. Soc.* 137 (2015) 14019–14022, <https://doi.org/10.1021/jacs.5b08084>.
- [27] J.P. Brutman et al., *J. Phys. Chem. B* 123 (2019) 1432–1441, <https://doi.org/10.1021/acs.jpcc.8b11489>.
- [28] M.M. Obadia et al., *Adv. Funct. Mater.* 27 (2017) 1–10, <https://doi.org/10.1002/adfm.201703258>.
- [29] Y. Yang et al., *Nat. Commun.* 9 (2018) 1–7, <https://doi.org/10.1038/s41467-018-04257-x>.
- [30] F. Van Lijsebetten et al., *Chem. Soc. Rev.* 49 (2020) 8425–8438, <https://doi.org/10.1039/d0cs00452a>.
- [31] F. Cuminet et al., *Macromolecules* (2021), <https://doi.org/10.1021/acs.macromol.0c02706>.
- [32] H. Zhang et al., *ACS Macro Lett.* (2020), <https://doi.org/10.1021/acsmacrolett.9b01023>.
- [33] M. Delahaye et al., *Polym. Chem.* 11 (2020), <https://doi.org/10.1039/d0py00681e>.
- [34] S. Debnath, S. Kaushal, U. Ojha, *ACS Appl. Polym. Mater.* 2 (2020) 1006–1013, <https://doi.org/10.1021/acsapm.0c00016>.
- [35] Y. Zhu et al., *Chinese J. Polym. Sci. (English Ed.)* (2020), <https://doi.org/10.1007/s10118-020-2479-6>.
- [36] M.L. Williams, R.F. Landel, J.D. Ferry, *J. Am. Chem. Soc.* 77 (1955) 3701–3707, <https://doi.org/10.1021/ja01619a008>.
- [37] Y. Nishimura et al., *J. Am. Chem. Soc.* 139 (2017) 14881–14884, <https://doi.org/10.1021/jacs.7b08826>.
- [38] Y. Yang et al., *Nat. Commun.* 10 (2019) 3165, <https://doi.org/10.1038/s41467-019-11144-6>.
- [39] H. Eyring, *J. Chem. Phys.* 3 (1935) 63–71, <https://doi.org/10.1063/1.1749604>.
- [40] G. Lente, I. Fábíán, A.J. Poë, *New J. Chem.* 29 (2005) 759–760, <https://doi.org/10.1039/B501687H>.
- [41] W. Hu et al., *Adv. Funct. Mater.* 25 (2015) 4827–4836, <https://doi.org/10.1002/adfm.201501530>.
- [42] N. Zheng et al., *Polym. Chem.* 6 (2015) 3046–3053, <https://doi.org/10.1039/C5PY00172B>.
- [43] Z. Ding et al., *J. Mater. Chem. A* 7 (2019) 9736–9747, <https://doi.org/10.1039/c9ta01147a>.
- [44] A.N. Semenov, M. Rubinstein, *Macromolecules* 31 (1998) 1373–1385, <https://doi.org/10.1021/ma970616h>.
- [45] R.J. Sheridan, C.N. Bowman, *Macromolecules* 45 (2012) 7634–7641, <https://doi.org/10.1021/ma301329u>.
- [46] N. Sowan et al., *Adv. Mater.* 33 (2021) 2007221, <https://doi.org/10.1002/adma.202007221>.
- [47] T.F. Scott et al., *Science* 308 (2005) 1615–1617, <https://doi.org/10.1126/science.1110505>.
- [48] J.F. Xu et al., *Org. Lett.* 15 (2013) 6148–6151, <https://doi.org/10.1021/ol403015s>.
- [49] M. Abdallah et al., *Macromolecules* 52 (2019) 2446–2455, <https://doi.org/10.1021/acs.macromol.8b01729>.
- [50] H. Frisch et al., *Angew. Chem. Int. Ed.* 57 (2018) 2036–2045, <https://doi.org/10.1002/anie.201709991>.
- [51] L.A. Connal et al., *Adv. Funct. Mater.* 18 (2008) 3315–3322, <https://doi.org/10.1002/adfm.200800333>.
- [52] X. Qian et al., *Adv. Mater.* 30 (2018), <https://doi.org/10.1002/adma.201801103>.
- [53] M.K. McBride et al., *Adv. Mater.* 29 (2017) 1606509, <https://doi.org/10.1002/adma.201606509>.
- [54] Y. Li et al., *RSC Adv.* 7 (2017) 37248–37254, <https://doi.org/10.1039/c7ra06343a>.
- [55] P.K. Shah, J.W. Stansbury, C.N. Bowman, *Polym. Chem.* 8 (2017) 4339–4351, <https://doi.org/10.1039/C7PY00702G>.
- [56] B.T. Worrell et al., *Nat. Commun.* 9 (2018) 2804, <https://doi.org/10.1038/s41467-018-05300-7>.
- [57] X. Kuang et al., *Multifunct. Mater.* 3 (2020), <https://doi.org/10.1088/2399-7532/abbdc1.045001>.
- [58] U. Haldar et al., *ACS Appl. Mater. Interfaces* 7 (2015) 8779–8788, <https://doi.org/10.1021/acsmi.5b01272>.
- [59] C. Ding et al., *ACS Biomater. Sci. Eng.* 6 (2020) 3855–3867, <https://doi.org/10.1021/acsbmaterials.0c00588>.
- [60] P. Zhang et al., *RSC Adv.* 4 (2014) 47361–47367, <https://doi.org/10.1039/C4RA08189G>.
- [61] Z. Guo et al., *Soft Matter* 13 (2017) 7371–7380, <https://doi.org/10.1039/c7sm00916j>.
- [62] W. Denissen, J.M. Winne, F.E. Du Prez, *Chem. Sci.* 7 (2016) 30–38, <https://doi.org/10.1039/c5sc02223a>.
- [63] R.L. Snyder et al., *Macromolecules* 51 (2018) 389–397, <https://doi.org/10.1021/acs.macromol.7b02299>.
- [64] D. Zhang et al., *Macromol. Chem. Phys.* 221 (2020) 1–9, <https://doi.org/10.1002/macp.201900564>.
- [65] Q. Li et al., *J. Mater. Chem. A* 7 (2019) 18039–18049, <https://doi.org/10.1039/c9ta04073k>.
- [66] P. Taynton et al., *Adv. Mater.* 28 (2016) 2904–2909, <https://doi.org/10.1002/adma.201505245>.
- [67] W. Denissen et al., *Adv. Funct. Mater.* 25 (2015) 2451–2457, <https://doi.org/10.1002/adfm.201404553>.
- [68] P.R. Christensen et al., *Nat. Chem.* 11 (2019) 442–448, <https://doi.org/10.1038/s41557-019-0249-2>.
- [69] J.S.A. Ishibashi, J.A. Kalow, *ACS Macro Lett.* 7 (2018) 482–486, <https://doi.org/10.1021/acsmacrolett.8b00166>.
- [70] J. Huang et al., *Compos. Sci. Technol.* 168 (2018) 320–326, <https://doi.org/10.1016/j.compscitech.2018.10.017>.
- [71] P. Chakma et al., *ACS Macro Lett.* 8 (2019) 95–100, <https://doi.org/10.1021/acsmacrolett.8b00819>.
- [72] B. Hendriks et al., *ACS Macro Lett.* 6 (2017) 930–934, <https://doi.org/10.1021/acsmacrolett.7b00494>.
- [73] M. Röttger et al., *Science* 356 (2017) 62–65, <https://doi.org/10.1126/science.aah5281>.
- [74] W.A. Ogden, Z. Guan, *J. Am. Chem. Soc.* 140 (2018) 6217–6220, <https://doi.org/10.1021/jacs.8b03257>.
- [75] A. Ruiz De Luzuriaga et al., *Mater. Horizons* 3 (2016) 241–247, <https://doi.org/10.1039/c6mh00029k>.
- [76] M. Capelot et al., *J. Am. Chem. Soc.* 134 (2012) 7664–7667, <https://doi.org/10.1021/ja302894k>.
- [77] M. Capelot et al., *ACS Macro Lett.* 1 (2012) 789–792, <https://doi.org/10.1021/mz300239f>.
- [78] M. Delahaye, J.M. Winne, F.E. Du Prez, *J. Am. Chem. Soc.* 141 (2019) 15277–15287, <https://doi.org/10.1021/jacs.9b07269>.
- [79] C. He et al., *J. Am. Chem. Soc.* 141 (2019) 13753–13757, <https://doi.org/10.1021/jacs.9b06668>.
- [80] W.X. Liu et al., *J. Am. Chem. Soc.* 139 (2017) 8678–8684, <https://doi.org/10.1021/jacs.7b03967>.
- [81] Y. Yang et al., *J. Am. Chem. Soc.* 138 (2016) 2118–2121, <https://doi.org/10.1021/jacs.5b12531>.

- [82] Z. Wang et al., *Polymers* 10 (2018) 65, <https://doi.org/10.3390/polym10010065>.
- [83] J.P. Brutman, P.A. Delgado, M.A. Hillmyer, *ACS Macro Lett.* 3 (2014) 607–610, <https://doi.org/10.1021/mz500269w>.
- [84] F.I. Altuna, V. Pettarin, R.J.J. Williams, *Green Chem.* 15 (2013) 3360–3366, <https://doi.org/10.1039/c3gc41384e>.
- [85] J. Wu et al., *ACS Sustain. Chem. Eng.* 8 (2020) 6479–6487, <https://doi.org/10.1021/acssuschemeng.0c01047>.
- [86] X. Yang et al., *Mater. Des.* 186 (2020), <https://doi.org/10.1016/j.matdes.2019.108248>.
- [87] T. Liu et al., *Macromolecules* 50 (2017) 8588–8597, <https://doi.org/10.1021/acs.macromol.7b01889>.
- [88] S. Zhang et al., *Green Chem.* 20 (2018) 2995–3000, <https://doi.org/10.1039/c8gc01299g>.
- [89] L. Zhang, S.J. Rowan, *Macromolecules* 50 (2017) 5051–5060, <https://doi.org/10.1021/acs.macromol.7b01016>.
- [90] W. Zhao et al., *ACS Appl. Mater. Interfaces.* 11 (2019) 36090–36099, <https://doi.org/10.1021/acsami.9b11991>.
- [91] H. Ying, Y. Zhang, J. Cheng, *Nat. Commun.* 5 (2014) 3218, <https://doi.org/10.1038/ncomms4218>.
- [92] D.A. Bachmann, *Justus Liebig's Ann. Der Chem.* 218 (1883) 38–56, <https://doi.org/10.1002/jlac.18832180105>.
- [93] J.W. Hill, W.H. Carothers, *J. Am. Chem. Soc.* 57 (1935) 925–928, <https://doi.org/10.1021/ja01308a045>.
- [94] Q. Li et al., *Macromolecules* 53 (2020) 1474–1485, <https://doi.org/10.1021/acs.macromol.9b02386>.
- [95] S. Yu et al., *ACS Macro Lett.* 9 (2020) 1143–1148, <https://doi.org/10.1021/acsmacrolett.0c00527>.
- [96] P. Taynton et al., *Adv. Mater.* 26 (2014) 3938–3942, <https://doi.org/10.1002/adma.201400317>.
- [97] S. Dhers, G. Vantomme, L. Avérous, *Green Chem.* 21 (2019) 1596–1601, <https://doi.org/10.1039/c9gc00540d>.
- [98] S.K. Schoustra et al., *Chem. Sci.* 12 (2021) 293–302, <https://doi.org/10.1039/d0sc05458e>.
- [99] W. Denissen et al., *Nat. Commun.* 8 (2017) 14857, <https://doi.org/10.1038/ncomms14857>.
- [100] T. Stukenbroeker et al., *Polym. Chem.* 8 (2017) 6590–6593, <https://doi.org/10.1039/c7py01488k>.
- [101] J.J. Lessard et al., *Macromolecules* 52 (2019) 2105–2111, <https://doi.org/10.1021/acs.macromol.8b02477>.
- [102] Y. Spiesschaert et al., *Macromolecules* 53 (2020) 2485–2495, <https://doi.org/10.1021/acs.macromol.9b02526>.
- [103] M. Guerre et al., *J. Am. Chem. Soc.* 140 (2018) 13272–13284, <https://doi.org/10.1021/jacs.8b07094>.
- [104] W. Denissen et al., *Macromolecules* 51 (2018) 2054–2064, <https://doi.org/10.1021/acs.macromol.7b02407>.
- [105] C. He et al., *Angew. Chem. Int. Ed.* 59 (2020) 735–739, <https://doi.org/10.1002/anie.201912223>.
- [106] B.M. El-Zaatari, J.S.A. Ishibashi, J.A. Kalow, *Polym. Chem.* 11 (2020) 5339–5345, <https://doi.org/10.1039/d0py00233j>.
- [107] M.M. Obadia et al., *J. Am. Chem. Soc.* 137 (2015) 6078–6083, <https://doi.org/10.1021/jacs.5b02653>.
- [108] P. Chakma et al., *Macromolecules* 53 (2020) 1233–1244, <https://doi.org/10.1021/acs.macromol.0c00120>.
- [109] D. Van Ooteghem, R. Deveux, E.J. Goethals, *Chem. Inf.* 5 (1974). 10.1002/chin.197424261.
- [110] Z. Tang et al., *Green Chem.* 20 (2018) 5454–5458, <https://doi.org/10.1039/c8gc02932f>.
- [111] O.R. Cromwell, J. Chung, Z. Guan, *J. Am. Chem. Soc.* 137 (2015) 6492–6495, <https://doi.org/10.1021/jacs.5b03551>.
- [112] F. Caffy, R. Nicolay, *Polym. Chem.* 10 (2019) 3107–3115, <https://doi.org/10.1039/c9py00253g>.
- [113] A. Breuillac, A. Kassalias, R. Nicolay, *Macromolecules* 52 (2019) 7102–7113, <https://doi.org/10.1021/acs.macromol.9b01288>.
- [114] S. Delpierre et al., *Chem. Mater.* 31 (2019) 3736–3744, <https://doi.org/10.1021/acs.chemmater.9b00750>.
- [115] Y. Yang et al., *ACS Appl. Mater. Interfaces* 12 (2020) 33305–33314, <https://doi.org/10.1021/acsami.0c09712>.
- [116] C.A. Tretbar, J.A. Neal, Z. Guan, *J. Am. Chem. Soc.* 141 (2019) 16595–16599, <https://doi.org/10.1021/acsami.9b08876>.
- [117] S. Gao et al., *J. Mater. Chem. A* 7 (2019) 17498–17504, <https://doi.org/10.1039/c9ta04951g>.
- [118] I. Azcune, I. Odriozola, *Eur. Polym. J.* 84 (2016) 147–160, <https://doi.org/10.1016/j.eurpolymj.2016.09.023>.
- [119] S. Nevejangs et al., *Phys. Chem. Chem. Phys.* 18 (2016) 27577–27583, <https://doi.org/10.1039/c6cp04028d>.
- [120] A. Ruiz De Luzuriaga et al., *J. Mater. Chem. C* 4 (2016) 6220–6223, <https://doi.org/10.1039/c6tc02383e>.
- [121] P. Yan et al., *Angew. Chem. Int. Ed.* 59 (2020) 13371–13378, <https://doi.org/10.1002/anie.202004311>.
- [122] A. Tsuruoka et al., *Angew. Chem. Int. Ed.* 59 (2020) 4294–4298, <https://doi.org/10.1002/anie.201913430>.
- [123] F. Fan et al., *Angew. Chem. Int. Ed.* 57 (2018) 16426–16430, <https://doi.org/10.1002/anie.201810297>.
- [124] M. Chen et al., *ACS Macro Lett.* 8 (2019) 255–260, <https://doi.org/10.1021/acsmacrolett.9b00015>.
- [125] S. Wang et al., *Macromolecules* 53 (2020) 2919–2931, <https://doi.org/10.1021/acs.macromol.0c00036>.
- [126] Y. Chen et al., *Macromolecules* 52 (2019) 3805–3812, <https://doi.org/10.1021/acs.macromol.9b00419>.
- [127] Y. Liu et al., *ACS Macro Lett.* 8 (2019) 193–199, <https://doi.org/10.1021/acsmacrolett.9b00012>.
- [128] L. Li et al., *Macromolecules* 51 (2018) 5537–5546, <https://doi.org/10.1021/acs.macromol.8b00922>.
- [129] J.J. Cash et al., *Polym. Chem.* 9 (2018) 2011–2020, <https://doi.org/10.1039/c8py00123e>.
- [130] R. Zhang et al., *Macromolecules* 53 (2020) 5937–5949, <https://doi.org/10.1021/acs.macromol.0c00407>.
- [131] B. Krishnakumar et al., *Chem. Eng. J.* 385 (2020), <https://doi.org/10.1016/j.cej.2019.123820>.
- [132] N. Zheng et al., *Chem. Rev.* 121 (2021) 1716–1745, <https://doi.org/10.1021/acs.chemrev.0c00938>.
- [133] Y. Zhu et al., *ACS Appl. Mater. Interfaces* 12 (2020), <https://doi.org/10.1021/acsami.0c02722>.
- [134] C.J. Rhodes, *Sci. Prog.* 101 (2018) 207–260, <https://doi.org/10.3184/003685018X15294876706211>.
- [135] Y. Yang et al., *Prog. Mater. Sci.* (2020), <https://doi.org/10.1016/j.pmatsci.2020.100710>.
- [136] H. Memon et al., *Macromolecules* 53 (2020), <https://doi.org/10.1021/acs.macromol.9b02006>.
- [137] C. Hao et al., *Macromolecules* (2020), <https://doi.org/10.1021/acs.macromol.9b02243>.
- [138] X. Zhao, X.L. Wang, F. Tian, W.L. An, S. Xu, Y.Z. Wang, *Green Chem.* 21 (2019), <https://doi.org/10.1039/c9gc00685k>.
- [139] J.J. Lessard et al., *ACS Appl. Polym. Mater.* 2 (2020), <https://doi.org/10.1021/acsapm.0c00523>.
- [140] K. Jin, L. Li, J.M. Torkelson, *Adv. Mater.* 28 (2016), <https://doi.org/10.1002/adma.201600871>.
- [141] C. Taplan et al., *Mater. Horiz.* 7 (2020) 104–110, <https://doi.org/10.1039/C9MH01062A>.
- [142] B.B. Jing, C.M. Evans, *J. Am. Chem. Soc.* 141 (2019) 18932–18937, <https://doi.org/10.1021/jacs.9b09811>.
- [143] S. Boncel et al., *ACS Appl. Nano Mater.* 1 (2018) 6542–6555, <https://doi.org/10.1021/acsanm.8b01824>.
- [144] L. Yue et al., *Glob. Challenges* 3 (2019) 1800076, <https://doi.org/10.1002/gch2.201800076>.
- [145] L. Yue et al., *ACS Macro Lett.* 9 (2020) 836–842, <https://doi.org/10.1021/acsmacrolett.0c00299>.
- [146] Y. Yang et al., *Angew. Chem.* 131 (2019) 17635–17640, <https://doi.org/10.1002/ange.201911612>.
- [147] F. Schwarzl, A.J. Staverman, *J. Appl. Phys.* 23 (1952) 838–843, <https://doi.org/10.1063/1.1702316>.
- [148] S.P. Lyu et al., *Biomacromolecules* 8 (2007) 2301–2310, <https://doi.org/10.1021/bm070313n>.
- [149] K. Yu, A. Xin, Q. Wang, *J. Mech. Phys. Solids* 121 (2018) 409–431, <https://doi.org/10.1016/j.jmps.2018.08.007>.
- [150] A. Susa et al., *ACS Appl. Mater. Interfaces* 8 (2016) 34068–34079, <https://doi.org/10.1021/acsami.6b10433>.
- [151] E.B. Stukalin et al., *Macromolecules* 46 (2013) 7525–7541, <https://doi.org/10.1021/ma401111n>.
- [152] J. Tang et al., *J. Mater. Chem. A* 5 (2017), <https://doi.org/10.1039/c7ta06650c>.
- [153] L. Jiang et al., *ACS Appl. Polym. Mater.* 1 (2019) 3261–3268, <https://doi.org/10.1021/acsapm.9b00672>.
- [154] Z. Wang et al., *Macromolecules* 53 (2020) 956–964, <https://doi.org/10.1021/acs.macromol.9b02325>.

- [155] F. Vidal et al., *J. Am. Chem. Soc.* 141 (2019) 15963–15971, <https://doi.org/10.1021/jacs.9b07452>.
- [156] Y. Oh et al., *Chem. Mater.* 32 (2020), <https://doi.org/10.1021/acs.chemmater.0c01392>.
- [157] H. Liu et al., *Chem. Eng. J.* 368 (2019) 61–70, <https://doi.org/10.1016/j.cej.2019.02.177>.
- [158] C. Cui et al., *ACS Appl. Mater. Interfaces* 12 (2020) 47975–47983, <https://doi.org/10.1021/acsami.0c14189>.
- [159] Q. Zhao et al., *Sci. Adv.* 2 (2016) 1–8, <https://doi.org/10.1126/sciadv.1501297>.
- [160] N. Zheng et al., *Angew. Chem. Int. Ed.* 55 (2016) 11421–11425, <https://doi.org/10.1002/anie.201602847>.
- [161] W. Yuan et al., *ACS Macro Lett.* 9 (2020) 588–594, <https://doi.org/10.1021/acsmacrolett.0c00075>.
- [162] Y. Wu, Y. Wei, Y. Ji, *Polym. Chem.* 11 (2020) 5297–5320, <https://doi.org/10.1039/d0py00075b>.
- [163] D.W. Hanzon et al., *Soft Matter* 14 (2018) 951–960, <https://doi.org/10.1039/c7sm02110k>.
- [164] M.O. Saed, A. Gablier, E.M. Terentejv, *Adv. Funct. Mater.* 30 (2020) 1–8, <https://doi.org/10.1002/adfm.201906458>.
- [165] Y. Wu et al., *Angew. Chem. Int. Ed.* 59 (2020) 4778–4784, <https://doi.org/10.1002/anie.201915694>.
- [166] Q. Shi et al., *Mater. Horizons* 4 (2017) 598–607, <https://doi.org/10.1039/c7mh00043j>.
- [167] E. Rossegger et al., *Polym. Chem.* 12 (2021) 639–644, <https://doi.org/10.1039/d0py01520b>.
- [168] H. Gao et al., *ACS Appl. Mater. Interfaces* 13 (2021) 1581–1591, <https://doi.org/10.1021/acsami.0c19520>.
- [169] M. Chen et al., *Front. Chem.* 8 (2020) 1–6, <https://doi.org/10.3389/fchem.2020.00706>.
- [170] T. Wright et al., *Macromolecules* 52 (2019) 36–42, <https://doi.org/10.1021/acs.macromol.8b01898>.
- [171] T. Ube, K. Kawasaki, T. Ikeda, *Adv. Mater.* 28 (2016) 8212–8217, <https://doi.org/10.1002/adma.201602745>.
- [172] Z. Jiang et al., *Angew. Chem.* 132 (2020) 4955–4961, <https://doi.org/10.1002/ange.202000181>.
- [173] X. Lu et al., *Adv. Mater.* 29 (2017) 1–7, <https://doi.org/10.1002/adma.201606467>.
- [174] Z.C. Jiang et al., *Angew. Chem. Int. Ed.* 58 (2019) 5332–5337, <https://doi.org/10.1002/anie.201900470>.
- [175] G.B. Lyon et al., *Macromolecules* 49 (2016) 8905–8913, <https://doi.org/10.1021/acs.macromol.6b01281>.
- [176] S. Ji et al., *ACS Appl. Mater. Interfaces* 9 (2017) 33169–33175, <https://doi.org/10.1021/acsami.7b11188>.
- [177] M. Giebler et al., *Macromol. Rapid Commun.* 42 (2020) 2000466, <https://doi.org/10.1002/marc.202000466>.
- [178] Q. Chen et al., *Chem. Sci.* 8 (2016) 724–733, <https://doi.org/10.1039/C6SC02855A>.
- [179] H. Zheng et al., *Ind. Eng. Chem. Res.* 59 (2020) 21768–21778, <https://doi.org/10.1021/acs.iecr.0c04257>.
- [180] Z. Yang, Q. Wang, T. Wang, *ACS Appl. Mater. Interfaces* 8 (2016) 21691–21699, <https://doi.org/10.1021/acsami.6b07403>.
- [181] P. Yan et al., *J. Appl. Polym. Sci.* 135 (2018) 1–8, <https://doi.org/10.1002/app.45784>.
- [182] Y. Liu et al., *Compos. Sci. Technol.* 168 (2018) 214–223, <https://doi.org/10.1016/j.compscitech.2018.10.005>.
- [183] H. Zhang, H. Han, X. Xu, *Compos. Sci. Technol.* 158 (2018) 61–66, <https://doi.org/10.1016/j.compscitech.2018.02.003>.
- [184] G. Zhao et al., *Adv. Mater.* 31 (2019) 1–7, <https://doi.org/10.1002/adma.201900363>.
- [185] Z. Li et al., *J. Mater. Chem. A* 5 (2017) 6740–6746, <https://doi.org/10.1039/C7TA00458C>.
- [186] F. Lossada et al., *Biomacromolecules* 20 (2019) 1045–1055, <https://doi.org/10.1021/acs.biomac.8b01659>.
- [187] C. Xiong et al., *J. Mater. Chem. A* 8 (2020) 10898–10908, <https://doi.org/10.1039/d0ta03664a>.
- [188] F. Lossada et al., *ACS Macro Lett.* 9 (2020) 70–76, <https://doi.org/10.1021/acsmacrolett.9b00997>.
- [189] L. Yu et al., *ACS Appl. Polym. Mater.* 1 (2019) 2535–2542, <https://doi.org/10.1021/acsapm.9b00641>.
- [190] K. Yu et al., *Adv. Funct. Mater.* 26 (2016) 6098–6106, <https://doi.org/10.1002/adfm.201602056>.
- [191] H. Memon et al., *Compos. Sci. Technol.* 199 (2020), <https://doi.org/10.1016/j.compscitech.2020.108314> 108314.
- [192] Mallinda, (n.d.). www.Mallinda.com (accessed February 8, 2021).